A GRAVIMETRIC SURVEY OF THE SANTA CRUZ-AÑO NUEVO POINT CONTINENTAL SHELF AND ADJACENT COASTLINE

Clayton Henry Spikes

NAVAL POSTGRADUATE SCHOOL
Monterey, California

THESIS

A Gravimetric Survey
of
the Santa Cruz-Año Nuevo Point Continental Shelf
and Adjacent Coastline

by

Clayton Henry Spikes

Thesis Advisors: Robert S. Andrews
Joseph J. von Schwind

Approved for public release; distribution unlimited.

A Gravimetric Survey

of

the Santa Cruz-Año Nuevo Point Continental Shelf

and Adjacent Coastline

by

Clayton Henry Spikes
Lieutenant, United States Navy
B.S., United States Naval Academy, 1966

Submitted in partial fulfillment of the
requirements for the degree of

MASTER OF SCIENCE IN OCEANOGRAPHY

from the

NAVAL POSTGRADUATE SCHOOL
September 1973

ABSTRACT

Gravity data was collected from 82 seafloor and 41 land stations in a 334 sq km area between Santa Cruz and Año Nuevo Point, California.

The methods of data collection and reduction are discussed, with the introduction of a unique sequence pertaining to application of gravity data corrections. A complete Bouguer anomaly map is depicted and subsequently tied in with a previous survey of northern Monterey Bay. Isoline gradient analysis supports the concept that complete Bouguer anomaly profiles can be utilized to map granitic basement displacements.

Complete Bouguer anomaly cross-sections are compared with corresponding profiles of seismic, well core, sea surface gravity, and magnetic data. Excellent correlation is exhibited between these profiles and the Palo Colorado-San Gregorio fault zone. Faulting within the Monterey Bay fault zone can be traced from analysis of related profiles. Supporting evidence of the purported dip-slip and strike-slip motion along the Palo Colorado-San Gregorio fault zone is presented.

TABLE OF CONTENTS

LIST OF TABLES

LIST OF FIGURES

23. Comparison of CBA and seismic profiles for trackline C'C.

24. Geophysical tracklines for 23 kJ seismic profile data.

25. Comparison of CBA and seismic profiles for trackline FF'.

26. Comparison of CBA and seismic profiles for trackline GG'.

27. Comparison of CBA and seismic profiles for trackline HH'.

28. Geographical location of profiles for CBA comparison with well core data.

29. Comparison of CBA profile with profile of proposed basement depth from well core data along trackline DD'.

30. Comparison of CBA profile with profile of proposed basement depth from well core data along trackline EE'.

31. Comparison of sea surface and seafloor gravity data for trackline BB'.

32. Comparison of sea surface and seafloor gravity data for trackline CC'.

33. Comparison of magnetic data and the seismic profile for trackline BB'.

34. Comparison of magnetic data and the seismic profile for trackline CC'.

LIST OF SYMBOLS AND ABBREVIATIONS

ba - Daily Base Station Value for Underwater Gravimetry

bc_1 - Initial Bouguer Correction

bc_2 - Secondary Bouguer Correction

BC - Total Bouguer Correction

bm - Pier Benchmark Value for Land Gravimetry

CBA - Complete Bouguer Anomaly

CC - Curvature Correction

cf - Conversion Factor for Gravimeter G-08

cv - Control Box Counter Value

D - Drift Correction

ET - Earth Tide Correction

FAA - Free-Air Anomaly

FAC - Free-Air Correction

G - Universal Gravitational Constant

G_1 - Uncorrected Observed Gravity

H - Land Station Elevation

L - Latitude

M - Mass of the Earth

MFAA - Mass-Adjusted Free-Air Anomaly

MSL - Mean Sea Level

OG - Observed Gravity

R - Radius of the Earth

SBA - Simple Bouguer Anomaly

σ_r - Mean Density of Crustal Rock

σ_w - Density of Sea Water

TC - Terrain Correction

THG - Theoretical Gravity

z - Underwater Gravimeter Depth

z_t - Oceanic Tidal Height

ACKNOWLEDGEMENTS

The author wishes to express his sincere appreciation for the encouraging guidance and professional advice afforded by his advisors, Dr. Robert S. Andrews and Dr. Joseph J. von Schwind of the Naval Postgraduate School (NPS) Department of Oceanography. Because seafloor gravimetry is necessarily a two-man project, mention must be made of the invaluable assistance provided by LT Hap Woodson, USN, during all aspects of the survey. The strategic support of Captain Woodrow Reynolds and the entire crew of the R/V ACANIA made the continental shelf survey possible. Dr. Howard Oliver, Dr. S. L. Robbins, and Mr. Richard Farewell, from the U. S. Geological Survey (USGS), provided timely information and access to the land gravimeter. Mr. H. Gary Greene, USGS marine geologist, was extremely helpful in assisting in the analysis of seismic data and in making pertinent geologic publications available. ST1 Rick Desgrange and Mr. Dana Mayberry, the NPS Oceanography Department's electronics technicians, aided the author time and again in solving meter circuitry problems. Acknowledgement is made to Mr. Jack Mellor for his diving assistance and the loan of various necessary equipment. Material assistance from Mr. Yogi Parks and Mr. Joe Bighorse of LaCoste and Romberg, Inc. was essential in the maintenance of the underwater gravimeter. Special thanks must go to Mrs. W. Estes, NPS Oceanography Departmental secretary, for her help in acquiring important logistic support. Finally, the author must express his gratitude to Ms. Nunna Spikes for her continuous encouragement and patience throughout data collection and the subsequent writing of this report.

Partial funding for this project was provided by NPS Research Foundation from Office of Naval Research Resources.

I. INTRODUCTION

Today, earth scientists can obtain crustal information directly from well drillings (8-10 km) or indirectly through seismic reflection and refraction profiles, magnetic anomaly, heatflow, or electrical measurements, and gravity measurements. The latter method is the subject of this paper. The measured factor, the acceleration of gravity, results from the gravitational attraction between the mass of the earth and a test mass. Changes in crustal density result in variations in the earth's gravitational field. The unit of acceleration, 1 cm/sec^2 is called a gal (for Galileo) and it is possible to determine gravitational acceleration to within 0.01 mgal.

This research is based on the occupation of 82 underwater ocean stations and 41 land stations during the spring of 1973. The bottom gravity data was collected through utilization of the Naval Postgraduate School's research vessel R/V ACANIA (Fig. 1).

A. OBJECTIVES

The main objective of this study was to conduct a bottom gravity survey in a fault zone area and produce gravity anomaly charts that could be tied in with a previous shallow water survey (Cronyn, 1973) and various land surveys (Bouguer gravity maps of California by Bishop and Chapman, 1967). Sea surface gravimetry in this region would prove difficult, if not impossible. The stability of the seafloor and minimum distance between the test mass (gravimeter) and the density contrasts of the crustal material lent high credibility to the results obtained.

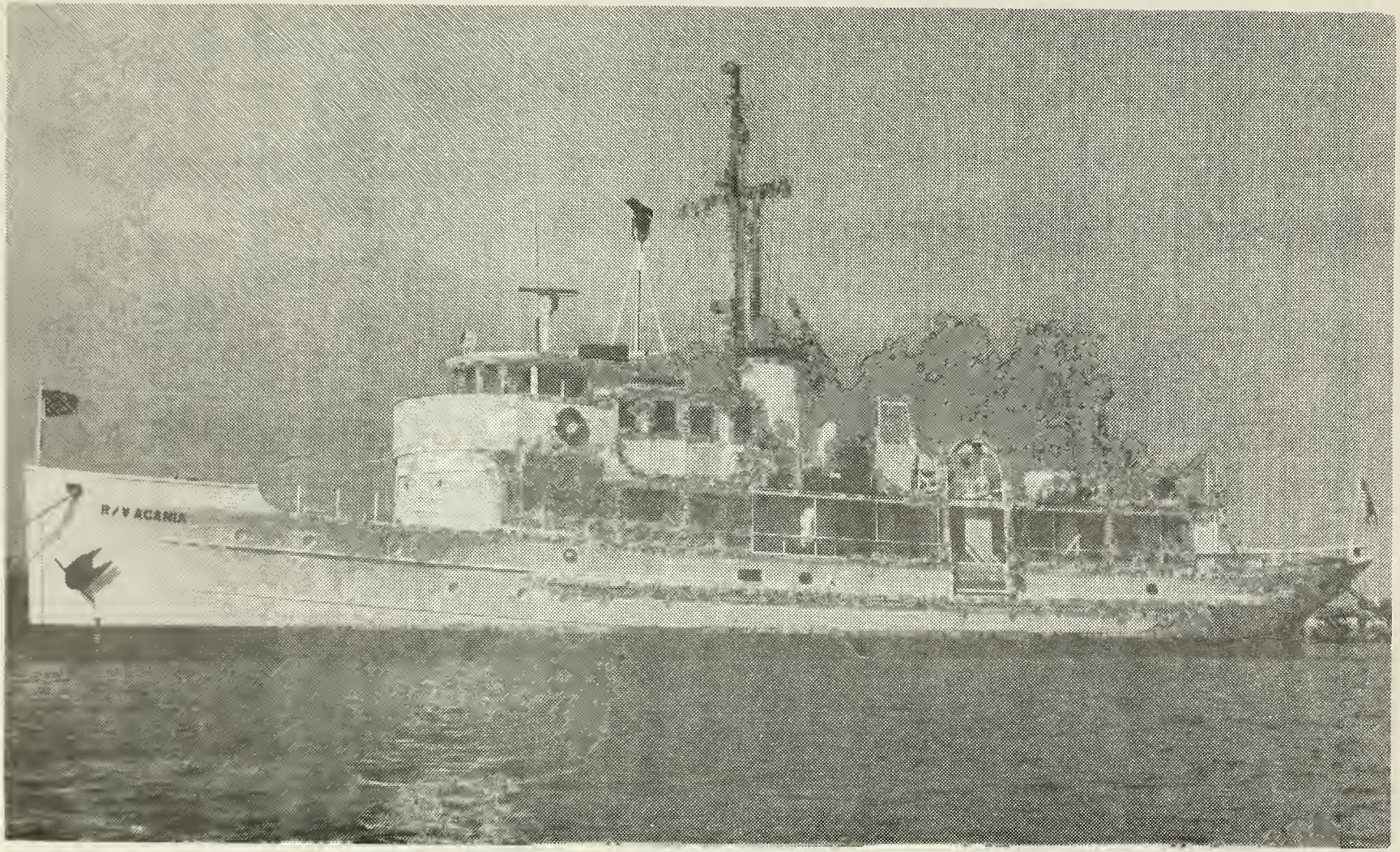

Figure 1. U. S. Naval Postgraduate School's Oceanographic R/V ACANIA.

No previous gravity anomaly charts of the survey area were available. The geological substructure of this part of Monterey Bay and adjoining continental shelf has hitherto been inferred from seismic profiling (Green, 1969 and 1970) and bottom samples (Martin, 1964). The present work was undertaken to verify, modify, and amplify the earlier geological analyses. It was hoped that the plotted gravity anomalies could aid in accurate delineation of the fault zones cutting through the area investigated. Thus, this research may assist scientists in making predictions of seismic activity.

This report will first discuss the physical and geological setting of the surveyed area, prior to the development of the problem of gravimetry itself. The experimental procedures are then discussed, followed by explanations of the numerous corrections necessarily applied in the reduction of the observed data. Finally, the gravity anomalies are presented in chart format, with accompanying analyses and interpretations.

B. SURVEY AREA DESCRIPTION

Santa Cruz on the northern edge of Monterey Bay, is located approximately 104 km south-southeast of San Francisco. The survey area extends up the coast from Santa Cruz to Año Nuevo Point and from the 50-fathom curve to approximately one mile inland (Fig. 2). The area covered is about 334 sq km. A gently sloping continental shelf is prevalent with small elevation gradients exhibited immediately along the seashore. An exception to this is the coastline between the town of Davenport and Año Nuevo Point were cliffs are evident at the water's edge.

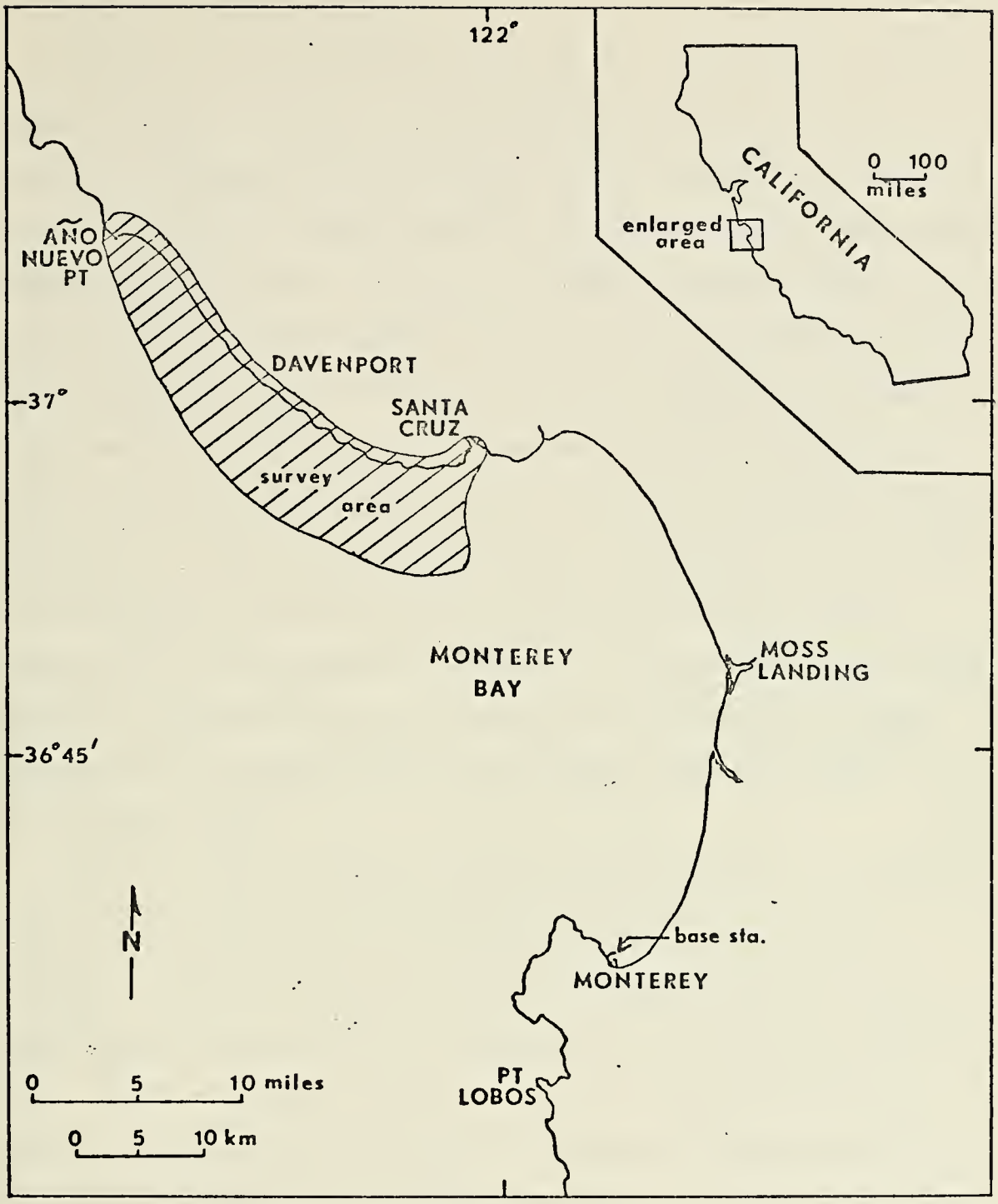

Figure 2. Survey Area Location

C. LOCAL GEOLOGICAL DESCRIPTION

One of the most seismically active regions in North America, the San Andreas fault zone, lies just 24 km northeast of the surveyed area (Fig. 3). It probably represents part of a transform fault along which the Pacific and North American plates are slipping relative to each other. Scientists consider the entire coastal area west of the San Andreas to be geologically active. The region between the San Andreas fault zone and the Sur-Nacimiento fault zone to the southwest encompasses the Salinian block (Reed, 1933), which consists of continental crust dominated by granitic rocks, flanked on either side by oceanic crust of the Franciscan assemblage. North of Monterey Bay, faults in the Salinian block usually trend northwest-southeast and tend to offset the Cretaceous granitic basement rocks and overlying Tertiary strata (Jennings and Burnett, 1961). Offshore, the granitic basement of the Salinian block imparts a rigid block-faulting structural style to the overlying sediments (Hoskins and Griffiths, 1971).

The narrow Palo Colorado-San Gregorio fault zone (about 3 km wide) appears to come ashore at Año Nuevo Point and ties in with the San Gregorio fault. Here the Miocene Monterey Formation appears to have been thrust to the southwest over the Pleistocene marine terrace deposits with a dip-slip component of about 3 m (Fig. 4). Four miles to the south, at Greyhound Rock, the Santa Cruz Mudstone and terrace deposits are vertically offset by 6 m at three separate but closely spaced faults (Griggs, 1973). Also, the terrace deposits on the sea cliffs where the San Gregorio fault goes out to sea are offset 2 to 3 m (Clark, 1970). Offshore, the Palo Colorado-San Gregorio fault zone juxtaposes the Pliocene Purisma Formation and the upper Miocene Santa Cruz Mudstone.

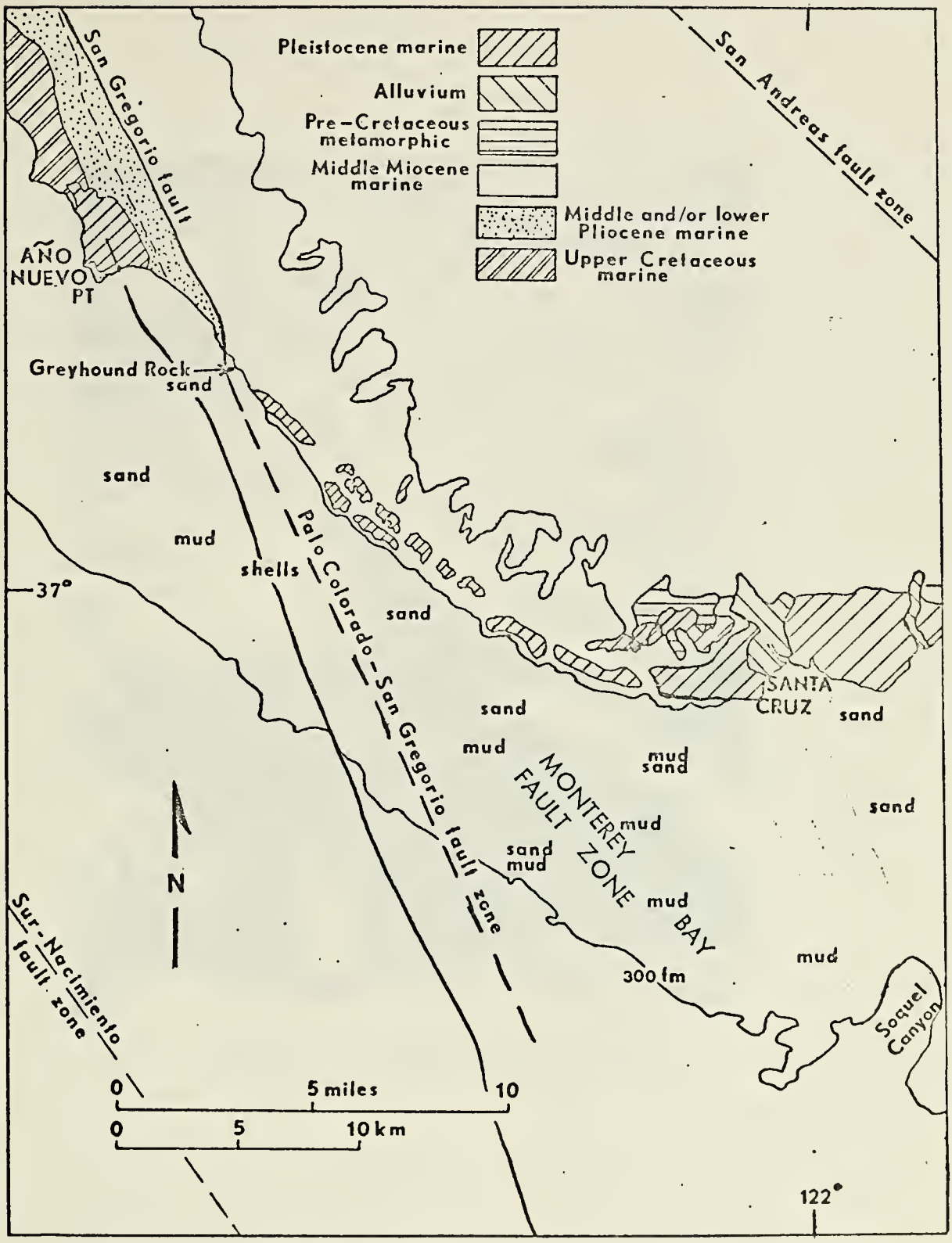

Figure 3. Regional Geology of the Survey Area
(After Bishop and Chapman, 1967)

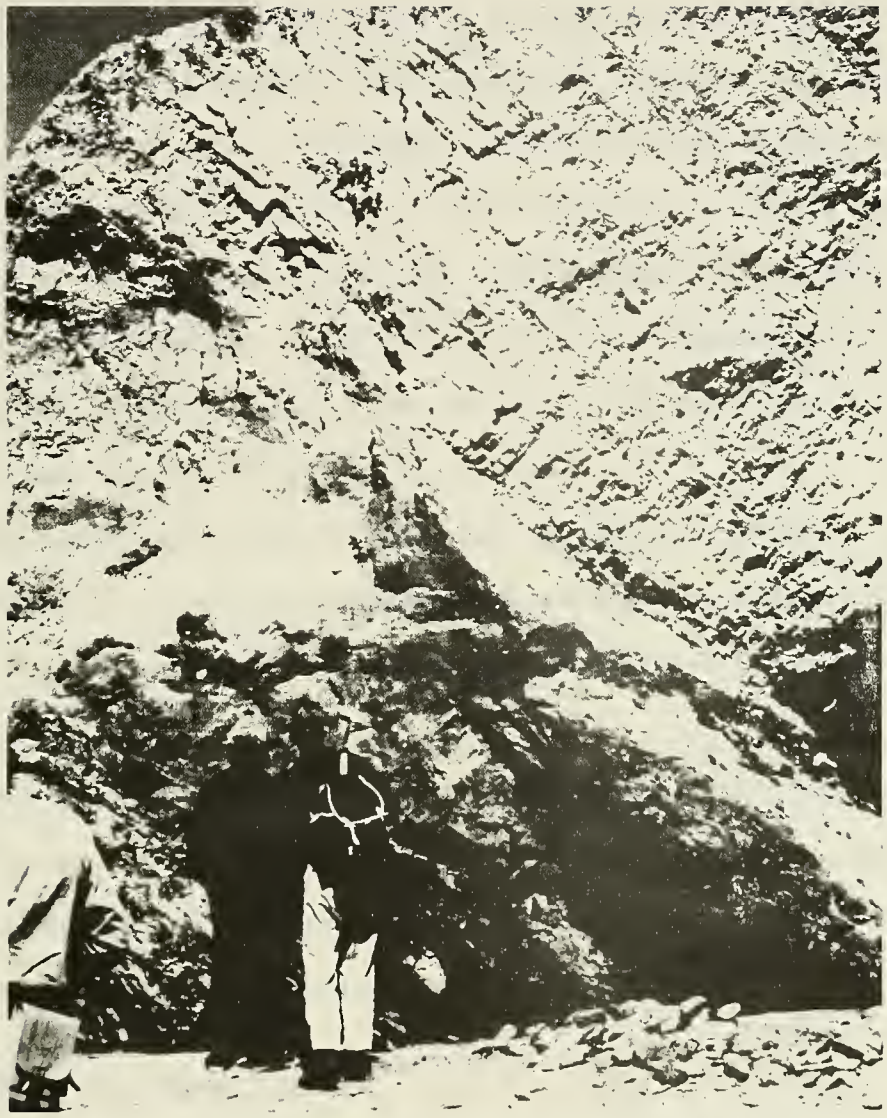

Figure 4. Recent Fault Exposed in Sea Cliff at Año Nuevo Point. (After Clark, 1970)

Fault plane solutions for five earthquakes since 1969 show nearly vertical fault planes and right-lateral strike-slip motion 6 m or less from the seafloor (Green et al., 1973).

The Monterey Bay fault zone (10-15 km wide) also exhibits fault planes that are nearly vertical with right-lateral strike-slip displacement occurring on the northwest-southeast trending faults. Again the fault offsets often extend to within 6 m of the seafloor, generally displacing late Pliocene strata, some displacing Pleistocene deposits, and in a few cases, Holocene deposits. Thus they can be termed "geologically young." Most of these faults are downthrown on the landward side and are accompanied by drag folding (Green et al., 1973).

On the continental shelf itself, the uppermost sediment is predominately sand with green mud in increasing evidence as Soquel Canyon is approached at the southeastern end of the survey area (Bishop and Chapman, 1967).

Visible proof of crustal motion in this region, historial accounts of earthquakes dating back to 1836, and the lack of reliable information as to the offshore geological substructure make this area very interesting to oceanographers, seismologists, and geologists.

D. PREVIOUS AREA INVESTIGATION

Past geological and geophysical investigations of the area have been primarily reconnaissance studies (Shepard and Emery, 1941; Shepard, 1948; Martin, 1964; Curray, 1965, 1966; Rusnak, 1966; Martin and Emery, 1967; Hoskins and Griffiths, 1971; and Silver et al., 1971). The research was concerned with the general regional structure and major faulting as related to the more extensive investigations of the central California

shelf. Martin (1964) utilized bathymetry and bottom samples as a basis for a geologic map of Monterey Bay but did not describe the area north of Santa Cruz. The land geology of the region has been thoroughly mapped by no less than 14 different persons starting with Johnson (1855), and most recently by Brabb (1970). The onland faults have been studied by Fairborn (1963), Sieck (1964), Durham (1965), Burford (1971), and Gilbert (1971).

Clark (1970), and Evans and Lajoie (1971) have studied the northern end of the San Gregorio fault at Año Nuevo Point. Hoskins and Griffiths (1971) suggested that faults across the Santa Cruz-Año Nuevo Point continental shelf did not affect rocks above a buried erosional unconformity of late Miocene age. Weber and Tinsley (1971) have also added insight as to the geological structure of the faults traversing Año Nuevo Point.

Jennings and Burnett (1961) and Jennings and Strand (1958) respectively, compiled the San Francisco and Santa Cruz geological maps for the California Division of Mines and Geology. Bouguer gravity anomalies are plotted on the Santa Cruz sheet but those for the San Francisco sheet have not at the time of this writing, been published.

Bolt, Lomnitz, and McEvilly (1968) postulated that the earthquakes occurring in the vicinity of Monterey and Santa Cruz in the 1800's and early 1900's may well have occurred in the two fault zones that cross the survey area covered in this report. Griggs (1973) has chronologically compiled the earthquake history of this region from 1836 to 1971. Most recently Greene et al., (1973) have depicted the crustal structure of the area in detail, paying close attention to the offshore faults in the Santa Cruz-Año Nuevo Point sector.

E. BOTTOM GRAVIMETRY

The measurement of gravity in the water covered regions of the earth is a difficult task. Gravity surveys at sea have been carried out from diving bells (Frowe, 1947), submarines (Meinesz, 1958), surface ships (Graf, 1958), and using a gravimeter enclosed within a waterproof pressure chamber able to withstand many atmospheres of pressure at depth. Meter functions are remotely controlled from the attending surface ship through a number of separate electrical conductors located in an insulated, armored, oceanographic cable. A specialized winch with numerous slip-rings must be employed.

Bottom topography plays an important role in bottom gravimetry in that the meter leveling system can operate only within a slope range of 15°. The most important difference between bottom and sea surface surveys is the necessity of maintaining the research vessel above the meter and lowering enough cable so that the gravimeter will not be tipped over or dragged by the cable while the mass is in the unclamped mode. This could result in damage to the delicate precision spring suspension system and render the meter inoperable. Concurrently, navigation and accuracy of station plotting is an additional inherent problem of sea gravimetry. Table I is a summary of the major differences between land and oceanic gravity surveys.

	LAND GRAVIMETRY	OCEANIC GRAVIMETRY
SURROUNDING MEDIUM	AIR: NEGLIGIBLE DENSITY	SEAWATER: ASSUME DENSITY OF 1.027 gm/cc (complicates Bouguer and terrain corrections)
OCEAN TIDES	NO EFFECT	MUST BE APPLIED TO FREE-AIR AND BOUGUER CORRECTIONS
DEPTH OF OVER-LYING WATER COL-UMN	NOT APPLICABLE	MUST BE APPLIED TO FREE-AIR AND BOUGUER CORRECTIONS
BOUGUER CORRECTION	ONE-STEP CORRECTION (remove excess underlying crust)	TWO-STEP CORRECTION (remove overlying water attraction, then fill in ocean with an infinite crustal slab)

Table I. Major Differences Between Land and Oceanic Gravimetry.

II. SURVEY EQUIPMENT

The first instrument used to measure gravity was a torsion balance (Cavendish, 1791); the pendulum was widely employed from about 1900 to the middle 1930's, and since then the gravimeter has been used almost exclusively. Because geophysical surveys are usually concerned with differences in gravity from one area to another, and not absolute values, there is limited need for an instrument that measures gravity directly. The gravimeter measures small variations in gravity, usually to a precision of about 0.01 mgal.

A. LAND GRAVIMETER

A LaCoste and Romberg Model G-08 geodetic land gravimeter (Fig. 5) provided by the U. S. Geological Survey (USGS) at Menlo Park, California, was used to conduct the coastal survey. Its characteristics and features are listed in Table 2. Figure 6 shows a simplified diagram of the meter's essential operating mechanisms. The zero-length spring exhibits a linear relationship between its elongations and compressions and increases and decreases in gravity itself (LaCoste, 1934). Rotation of the measuring screw brings the light beam to the equilibrium position by physically changing the location of the upper connection of the zero-length spring. Minimum meter drift is maintained by a thermister-transistor heater control system.

B. UNDERWATER GRAVIMETER

A LaCoste and Romberg Model H6G underwater gravimeter was used for the continental shelf portion of the survey. It was provided by the

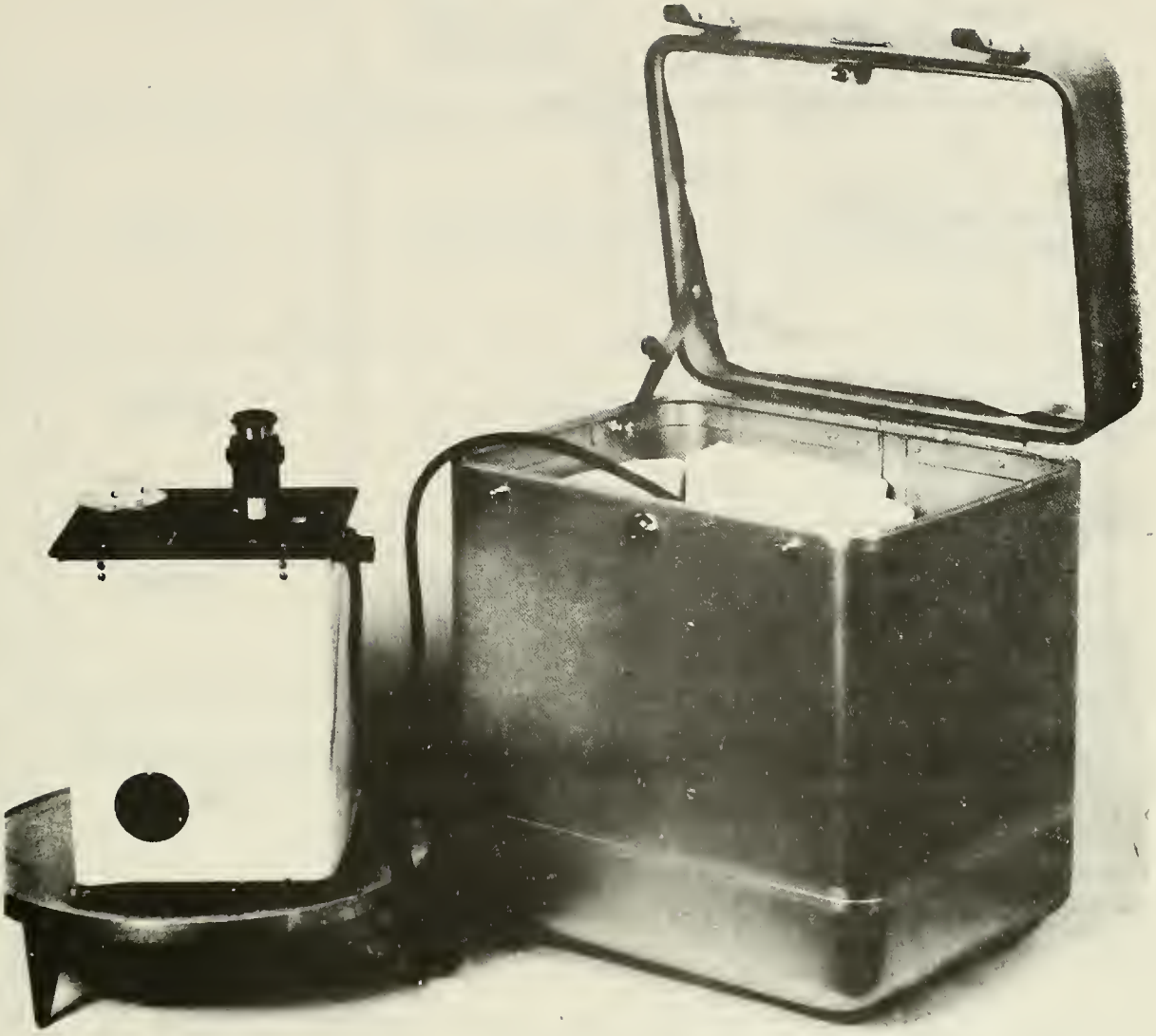

Figure 5. LaCoste and Romberg Model G-08 Geodetic Land Gravimeter.

	MODEL G-08 GEODETIC LAND GRAVIMETER	MODEL H6G UNDERWATER GRAVIMETER
SIZE	6 1/2 in X 5 3/4 in X 8 1/2 in	39 in triangular base, 29 in height
WEIGHT	20 lb, including battery and carrying case	350 lb plus additional weight to increase sink rate
RANGE	worldwide (7000 mgal)	worldwide (7000 mgal)
OPTIMUM/REALISTIC ACCURACY	$\pm$ 0.01/$\pm$ 0.04 mgal	$\pm$ 0.02/$\pm$ 0.10 mgal
POWER SOURCE	battery	115 vac, 60 Hz
LEVELING SYSTEM	manual micrometer screws	automatic servo motors
DRIFT	less than 0.5 mgal/month	less than 1.0 mgal/month

Table II. Land And Underwater Gravimeter Characteristics.

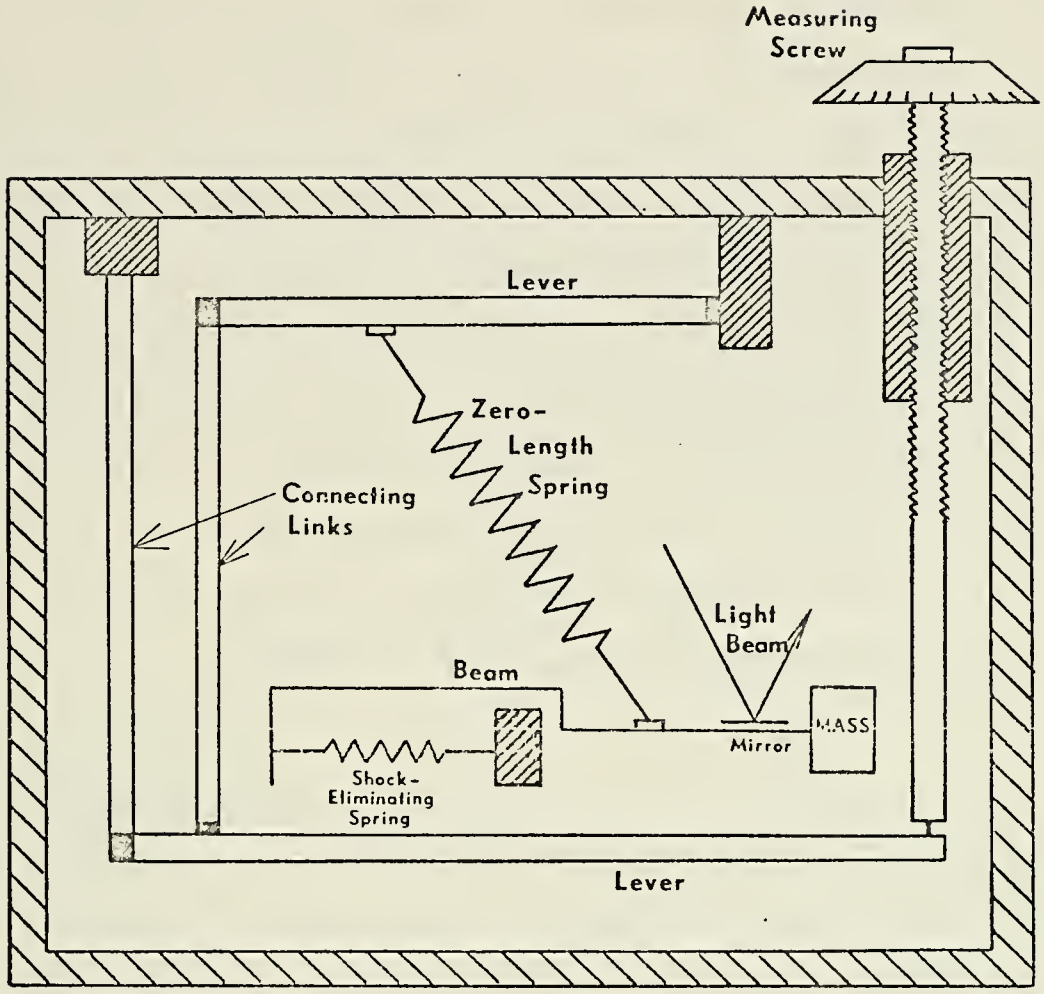

Figure 6. Simplified Diagram of the LaCoste and Romberg Gravimeter (after LaCoste, 1967).

Naval Oceanographic Office, Washington, D. C.. The underwater gravimeter is essentially a land meter mounted within a shell of two thick aluminum hemispheres. Its features, compared with those of the land gravimeter, are listed in Table 2. Again, internal temperature of the meter is maintained by a thermister-transistor circuit within the outer sphere. Clamping and unclamping of the gravimeter beam or weight, the meter leveling system, and the measuring screw operation are all remotely controlled through a multi-conductor cable terminating at the control box on the research vessel. Figure 7 shows the complete underwater unit with the electrical termination located directly atop the pressure shell and the oceanographic armored cable protruding through the top of the termination housing. In Figure 8 the top hemisphere has been removed and the meter itself is visible, along with the leveling mechanisms and various other electrical components.

1. Auxiliary Equipment

Figure 9 shows a simplified diagram of the components of the auxiliary equipment. Primary power is provided by a gasoline engine which drives a hydraulic pump which in turn drives the cable winch and the A-frame through a double set of two-way control valves. The hinged A-frame, which provides a clear passage for the gravimeter over the ship's side, is shown in its fully-extended position with the meter ready for lowering in Figure 10.

The permanent electrical termination of the cable is routed inside the hollow winch shaft and out through a slip-ring assembly which is connected via a cannon plug to the control box. The basic electrical power source is that of the shipboard 115 vac electrical system which is connected through an isolation transformer and a kepco rectifier to the control box.

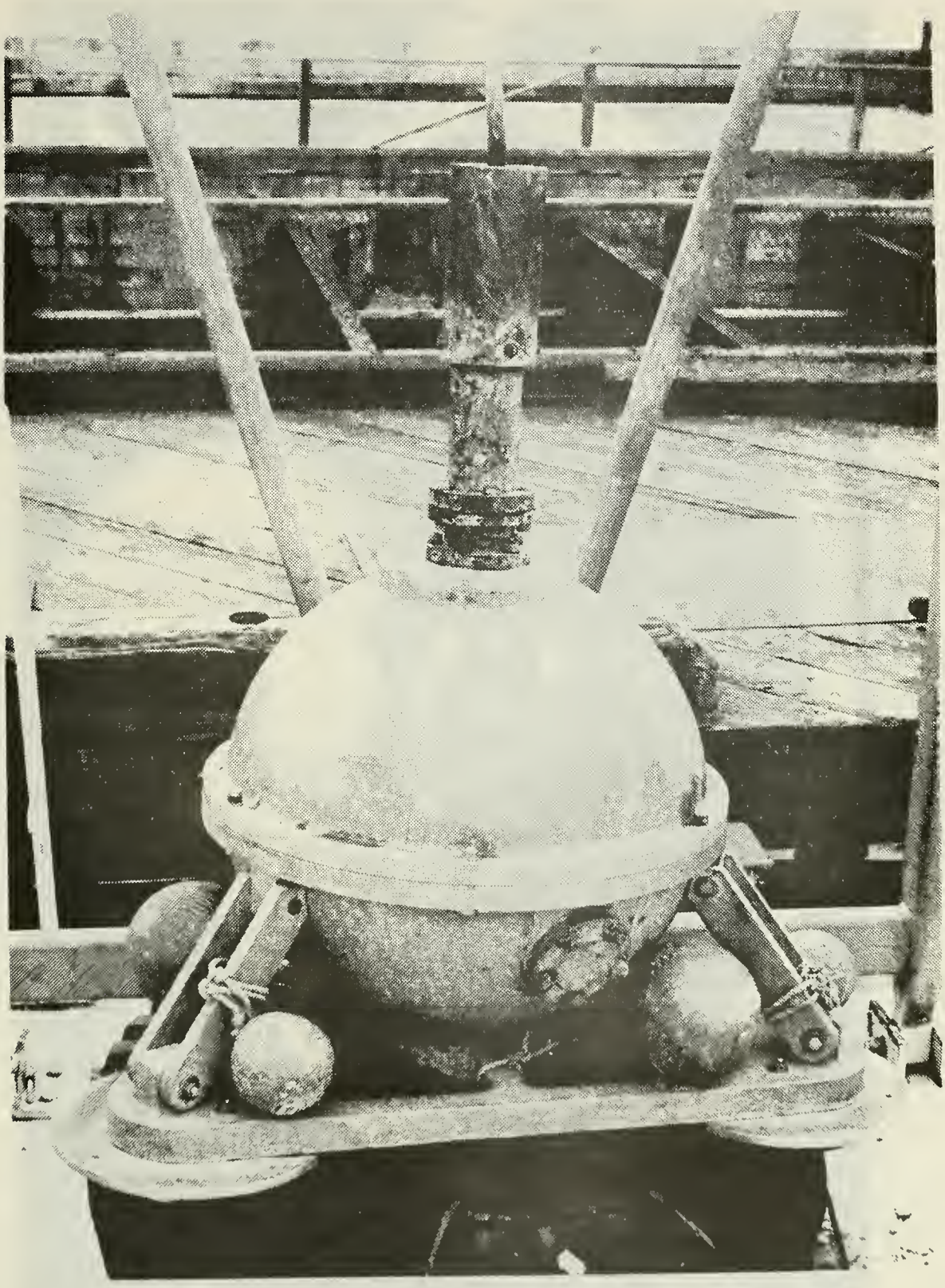

Figure 7. Model H6G Gravimeter Ready for Use.

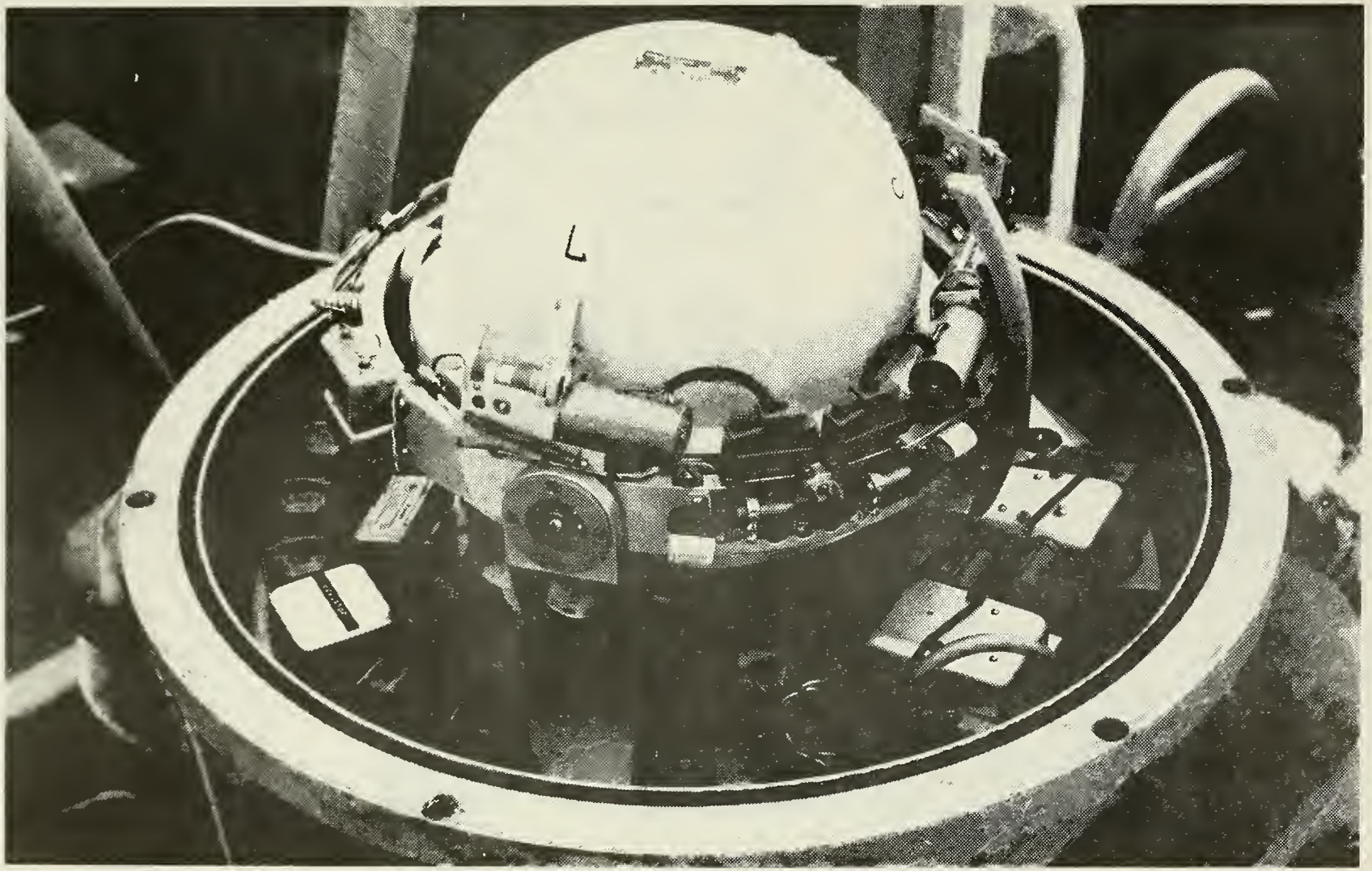

Figure 8. Internal View of the Model H6G Gravimeter.

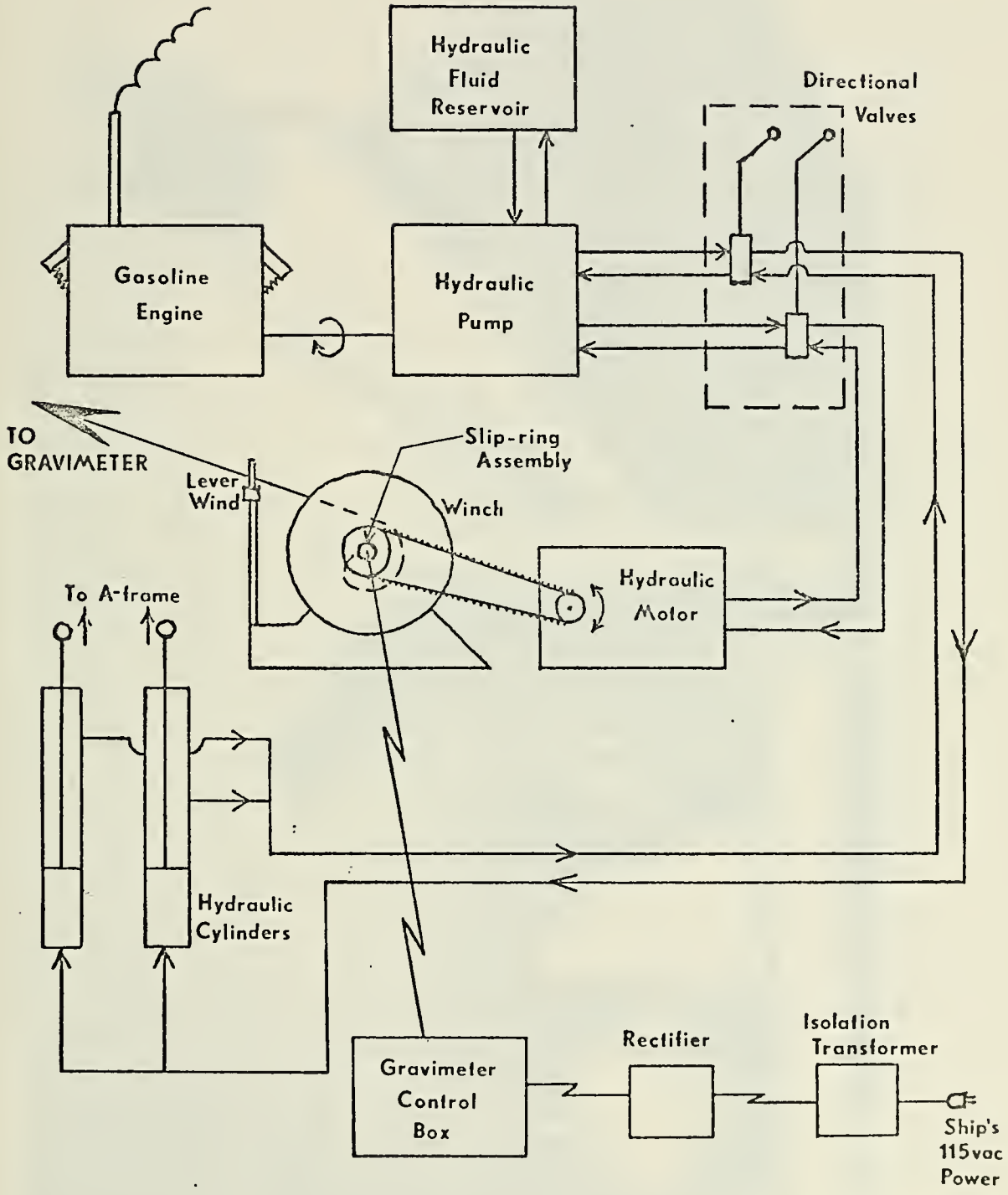

Figure 9 . Schematic Diagram of the Auxiliary Equipment.

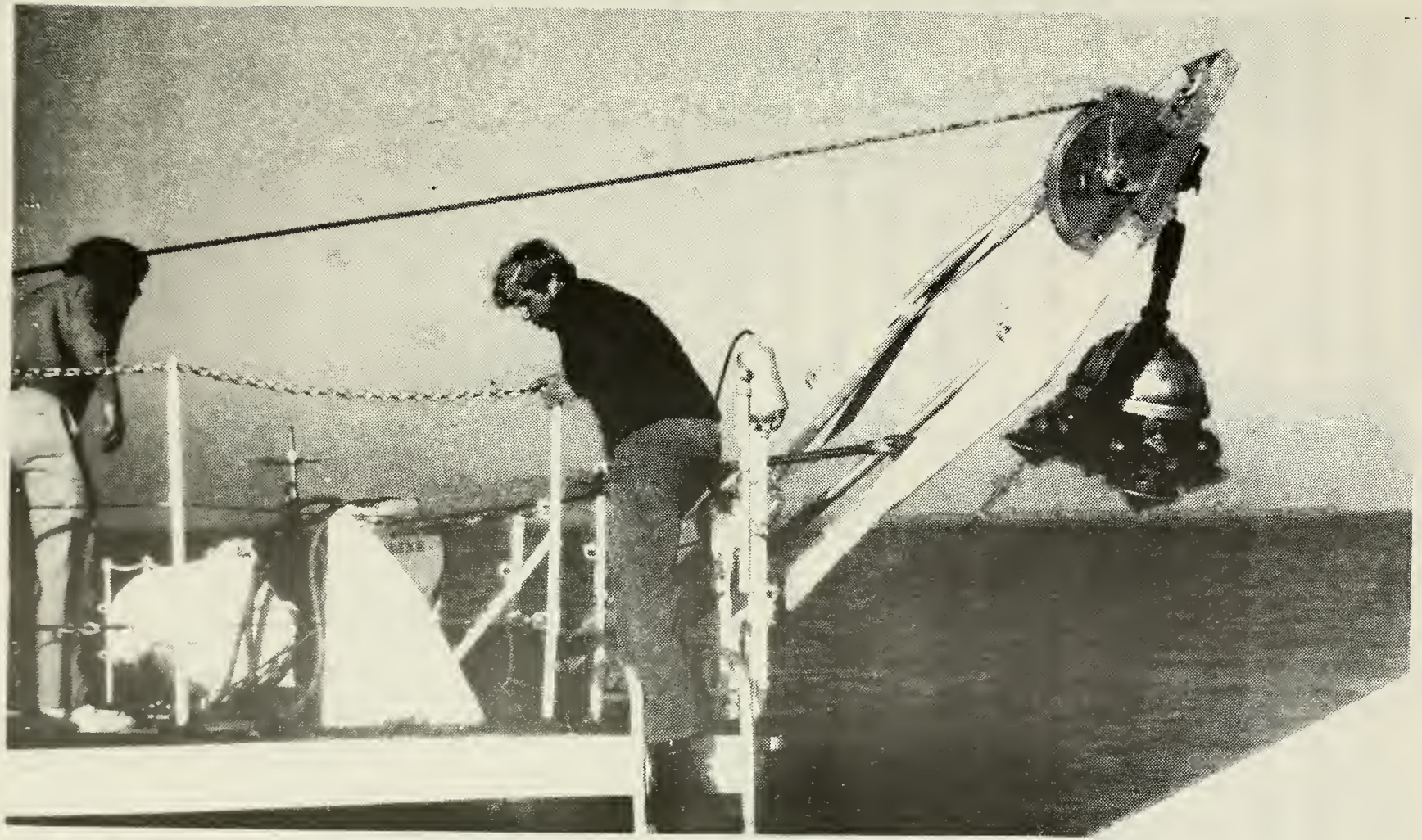

Figure 10. Author And Co-Worker With Gravimeter Ready For Lowering Onboard R/V ACANIA.

2. Shipboard Installation

The 33 m oceanographic research vessel R/V ACANIA was the platform from which the underwater survey was conducted. Its shallow draft of 3 m made it possible to take measurements in waters where larger ships, employing sea surface gravimeters, would dare not venture.

The 4 tons of equipment was distributed about the after end of the upper deck, with the A-frame, its supporting plate, and the gravity meter located on the starboard side so that the person at the control box inside the dry lab could observe the raising and lowering of the meter (Fig. 11). The horizontal A-frame supporting plate was held in place with four 1/2-inch (1.27 m) bolts through the upper-level deck. The other equipment was affixed to the deck with lag bolts. Additionally, the reel frame was welded to the outboard fishplate via four solid steel bars. A modified hand brake for the real drum was installed as an added safety feature.

Figure 11. Auxiliary Equipment Installed Aboard the R/V ACANIA.

III. SURVEY PROCEDURES

A. CALIBRATION OF GRAVIMETERS

The land gravimeter used in the coastal survey features hardened micrometer screws and lever systems upon which the calibration factors depend. For this reason the calibration factors do not change perceptibly with time, eliminating the need for frequent checking. Nevertheless, after obtaining the meter at the USGS, a calibration run was made from the USGS headquarters in Menlo Park (USGS 1 JD) to Skeggs Point (USGS B-388). This route encompasses 5 benchmarks and a range of 137.20 mgal (Chapman, 1966). Subsequent reduction of the observed data on the IBM 360 computer at the Naval Postgraduate School yielded a difference of 137.13 mgal over the calibration range.

Initial calibration of the underwater meter was carried out by LaCoste and Romberg technicians in Houston prior to shipment to Monterey. The excellent stable calibration characteristics previously mentioned for the land gravimeter are also inherent in the underwater model. Preceeding the author's survey, an additional calibration check was effected between the Woolard Airport Base WA-84 Station at the Monterey County Airport and benchmark WH-29 at the end of the U. S. Coast Guard pier, Monterey Harbor (stations designated by Woollard and Rose, 1963). Slight modification to the readings due to recent construction at the airport station led to the estimation that the observed gravity difference between the airport and the pier stations was within 0.1 mgal of the value of 22.5 mgal as recorded by Brooks (1973).

B. COASTAL SURVEY

A total of 41 shoreline stations were occupied during the survey. It was felt that a high station density along the shoreline would aid in the analysis of the data obtained from the offshore survey. A fairly constant horizontal range variation between stations was sought. Ultimate station selection was based on the accessibility of the USGS topographic map positions where elevation was recorded. Thirty stations were fixed at street or farm road intersections where the elevation was recorded, two were located at the maximum elevation of sea cliffs, and two were located at bridges where State Highway 1 crosses over creeks. An attempt was made to occupy as many USGS monumented benchmarks as possible. Of the seven benchmarks plotted on the maps, only three were found. The remaining four stations were located at the best estimated position of the plotted benchmarks, using surrounding topographical features and man-made structures indicated on the maps as references. The unoccupied benchmarks had most likely been destroyed by construction or were concealed by thick vegetation.

It is estimated that the position accuracy of the coastal stations was at least twice as good as that of the underwater stations. Figure 12 shows the plotted locations of the 41 land stations (letters) and Table 3 gives pertinent station location information.

The first and last gravity readings each day were taken at the pier benchmark (WH-29). Observed meter drift was negligible throughout the coastal survey.

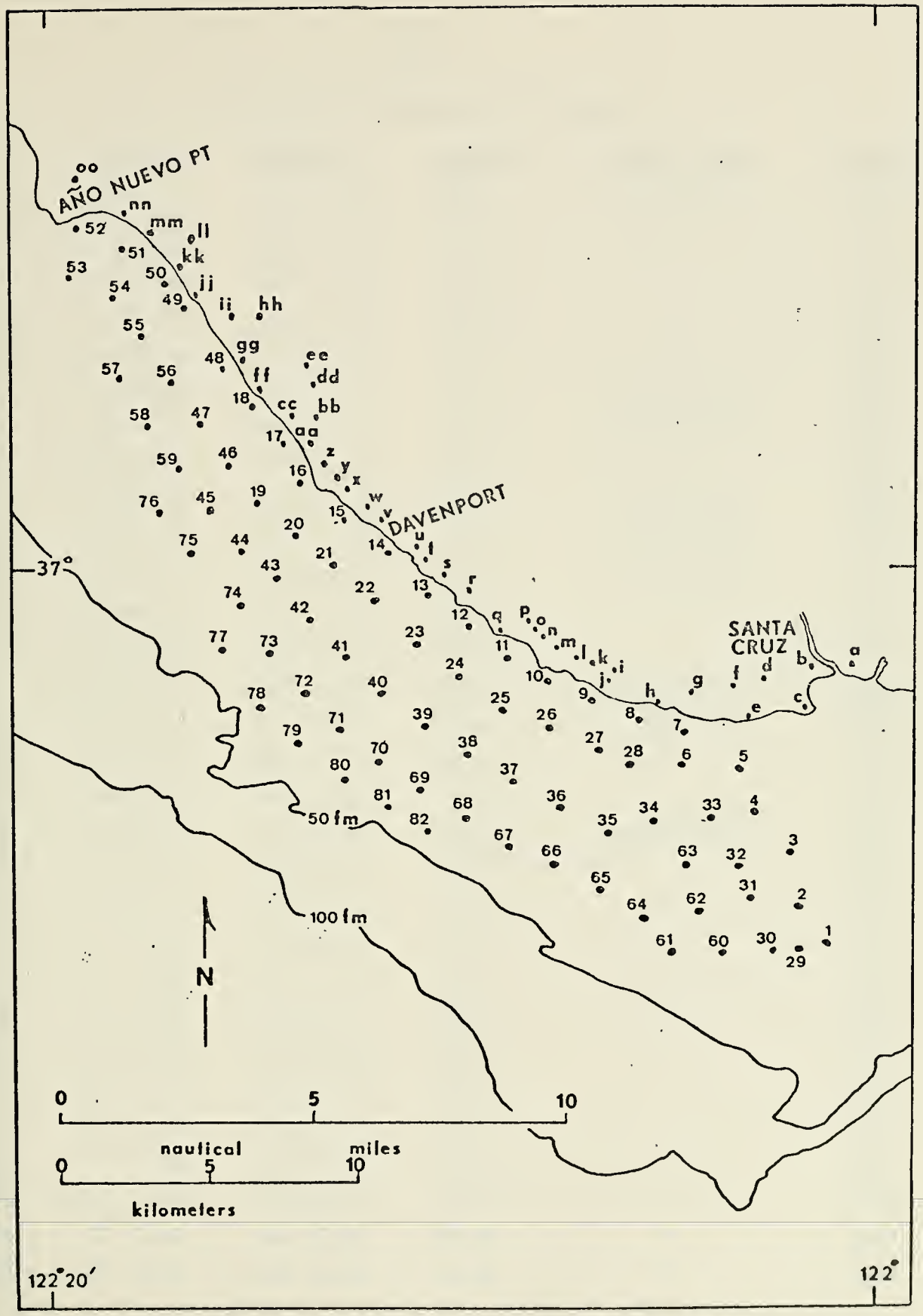

Figure 12. Land and Sea Station Locations

TABLE III

LAND STATION LOCATION INFORMATION

STA	LAT (N)	LONG (W)	ELEV (M)	DATE OCCUPIED	HOUR (PST)
A	36 58.03	122 0.50	14.33	16 APR 1973	1400
B	36 57.87	122 1.57	3.96	"	1415
C	36 57.08	122 1.57	9.75	"	1432
D	36 57.70	122 2.45	17.68	"	1448
E	36 56.98	122 3.05	13.72	"	1503
F	36 57.58	122 3.33	22.86	17 APR 1973	1328
G	36 57.47	122 4.15	18.90	16 APR 1973	1525
H	36 57.28	122 5.35	18.29	"	1544
I	36 57.85	122 6.23	35.97	17 APR 1973	1348
J	36 57.75	122 6.48	21.03	16 APR 1973	1612
K	36 58.00	122 6.62	20.12	17 APR 1973	1357
L	36 58.20	122 7.13	22.25	"	1407
M	36 58.38	122 7.62	25.30	"	1449
N	36 58.72	122 8.08	29.57	16 APR 1973	1630
O	36 58.83	122 8.30	25.91	17 APR 1973	1440
P	36 58.97	122 8.55	32.92	"	1434
Q	36 58.82	122 8.95	18.90	"	1425
R	36 59.47	122 9.75	31.09	18 APR 1973	1328
S	36 59.77	122 10.28	29.87	"	1334
T	37 0.07	122 10.75	22.56	"	1341
U	37 0.42	122 11.08	34.14	"	1348
V	37 0.98	122 12.03	30.48	"	1400
W	37 1.32	122 12.37	31.39	"	1405
X	37 1.50	122 12.60	19.81	"	1409
Y	37 1.72	122 12.88	25.60	"	1415
Z	37 1.82	122 13.03	28.65	"	1422
AA	37 2.33	122 13.53	14.02	"	1455
BB	37 2.62	122 13.42	3.66	"	1443
CC	37 2.65	122 13.85	37.19	"	1502
DD	37 3.25	122 13.43	12.19	"	1431

TABLE III (CONTINUED)

STA	LAT (N)	LONG (W)	ELEV (M)	DATE OCCUPIED	HOUR (PST)
EE	37 3.62	122 13.43	33.22	23 APR 1973	1403
FF	37 3.47	122 14.67	56.69	18 APR 1973	1509
GG	37 4.23	122 15.40	64.01	"	1519
HH	37 5.03	122 15.70	109.42	23 APR 1973	1415
II	37 5.08	122 16.00	43.89	"	1422
JJ	37 5.25	122 16.33	36.58	"	1426
KK	37 5.87	122 16.67	3.66	"	1439
LL	37 6.53	122 16.33	8.53	"	1451
MM	37 6.65	122 17.72	32.31	"	1508
NN	37 6.83	122 18.05	29.87	"	1513
OO	37 7.42	122 18.87	35.36	"	1530

C. CONTINENTAL SHELF SURVEY

The underwater survey encompassed a total of 82 sea stations.

1. Station Selection

Station locations were selected so as to cover the maximum amount of continental shelf in the survey area in the time available. A relatively constant spacing of approximately 2 km was maintained between stations. A grid of 100 stations was initially planned, but due to repeated equipment problems, rough seas, and limited ship availability, only the 82 stations were eventually occupied. However, a good representative areal density was maintained and coupled with the extensive coastal survey, resulted in a reasonably large area being covered. The stations were numbered consecutively according to time of occupation (Fig. 12). The total 123 stations within the 334 sq km area yielded a station density of approximately one station per sq km, which was better than initially intended. Table 4 lists the underwater station location information.

Stations at the eastern edge of the survey area were located as close as possible to the western edge of the shallow water area investigated by Cronyn (1972). It was felt this would simplify matters when attempting to tie in his gravity anomaly isolines and this author's. In fact, two of Cronyn's stations were reoccupied for the purpose of comparison.

2. Navigation

During this investigation, navigation was by visual bearings to prominent landmarks which were already accurately plotted on USGS maps. Generally, three bearings were taken at each station along with radar ranges to the coastline. Usually the estimated radius of accuracy of

TABLE IV

SEA STATION LOCATION INFORMATION

STA	LAT (N)	LONG (W)	DEPTH (M)	DATE OCCUPIED	HOUR (PDT)
1	36 52.60	122 0.97	58.52	5 FEB 1973	1340
2	36 53.32	122 1.68	55.08	"	1500
3	36 54.38	122 1.68	42.37	"	1515
4	36 55.13	122 2.68	39.59	"	1540
5	36 55.93	122 3.83	33.95	"	1552
6	36 55.90	122 5.20	42.86	7 FEB 1973	0845
7	36 56.75	122 4.58	18.32	"	0900
8	36 56.67	122 5.83	32.55	"	0913
9	36 57.23	122 6.87	28.77	"	0925
10	36 57.58	122 7.95	26.27	"	0940
11	36 58.13	122 8.97	22.56	"	0950
12	36 58.92	122 10.00	16.95	"	1005
13	36 59.50	122 10.83	15.91	"	1020
14	37 0.20	122 11.65	17.83	"	1030
15	37 0.90	122 12.72	15.42	"	1050
16	37 1.55	122 13.58	17.40	"	1105
17	37 2.42	122 14.17	21.12	"	1130
18	37 3.17	122 14.97	24.45	"	1145
19	37 1.52	122 14.73	36.49	"	1220
20	37 0.65	122 14.08	44.44	"	1300
21	37 0.05	122 13.08	42.09	"	1315
22	36 59.37	122 12.17	34.69	"	1335
23	36 58.70	122 11.28	37.83	"	1350
24	36 58.05	122 10.33	37.46	"	1405
25	36 57.47	122 9.35	41.67	"	1415
26	36 56.80	122 8.43	49.59	"	1430
27	36 56.33	122 7.33	48.07	"	1443
28	36 55.75	122 6.32	47.55	"	1500
29	36 52.37	122 1.47	64.31	16 FEB 1973	0825
30	36 52.33	122 2.17	70.38	"	0845

TABLE IV (CONTINUED)

STA	LAT (N)	LONG (W)	DEPTH (M)	DATE OCCUPIED	HOUR (PDT)
31	36 53.58	122 2.50	55.84	16 FEB 1973	1015
32	36 54.13	122 3.07	57.06	"	1035
33	36 54.92	122 3.88	47.09	"	1135
34	36 55.00	122 5.27	48.65	"	1220
35	36 54.75	122 6.42	62.39	"	1258
36	36 55.20	122 7.67	65.56	"	1325
37	36 55.80	122 8.50	61.17	"	1342
38	36 56.42	122 9.55	64.01	22 MAY 1973	0935
39	36 57.05	122 10.50	62.30	"	0953
40	36 57.67	122 11.47	60.41	"	1005
41	36 58.38	122 12.42	58.22	"	1020
42	36 59.07	122 13.33	56.51	"	1030
43	36 59.82	122 14.42	56.94	"	1050
44	37 0.42	122 15.23	55.69	"	1103
45	37 1.33	122 15.93	52.58	"	1115
46	37 2.28	122 15.45	39.11	"	1130
47	37 3.05	122 16.20	35.66	"	1143
48	37 3.97	122 15.75	19.87	"	1200
49	37 5.05	122 16.50	15.67	"	1215
50	37 5.62	122 17.05	16.61	"	1228
51	37 6.30	122 17.97	17.19	"	1245
52	37 6.73	122 19.03	12.34	"	1300
53	37 5.82	122 19.28	28.35	"	1315
54	37 5.45	122 18.28	30.21	"	1330
55	37 4.80	122 17.57	30.51	"	1343
56	37 3.90	122 16.92	36.64	"	1355
57	37 3.83	122 18.13	48.65	"	1410
58	37 2.97	122 17.38	50.20	"	1425
59	37 2.13	122 16.65	53.98	"	1435
60	36 52.47	122 3.37	84.67	23 MAY 1973	0835
61	36 52.55	122 4.60	90.25	"	0845
62	36 53.25	122 4.17	81.81	"	0900

TABLE IV (CONTINUED)

STA	LAT (N)	LONG (W)	DEPTH (M)	DATE OCCUPIED	HOUR (PDT)
63	36 53.13	122 4.42	78.24	23 MAY 1973	0915
64	36 53.33	122 5.38	90.40	"	0930
65	36 53.73	122 6.42	83.67	"	0945
66	36 54.30	122 7.50	78.06	"	1000
67	36 54.75	122 8.50	76.81	"	1010
68	36 55.40	122 9.08	77.15	"	1025
69	36 56.00	122 10.63	75.23	"	1040
70	36 56.65	122 11.63	73.55	"	1055
71	36 57.33	122 12.58	71.81	"	1110
72	36 58.00	122 13.50	70.87	"	1125
73	36 58.70	122 14.50	69.62	"	1140
74	36 59.45	122 15.40	68.70	"	1155
75	37 0.32	122 16.30	65.56	"	1245
76	37 1.17	122 17.05	64.31	"	1300
77	36 58.40	122 15.65	86.50	"	1325
78	36 57.57	122 14.58	86.20	"	1340
79	36 56.97	122 13.70	86.81	"	1355
80	36 56.28	122 12.70	86.84	"	1405
81	36 55.50	122 11.67	89.52	"	1420
82	36 54.97	122 10.67	90.40	"	1435

each fix was small enough to be ultimately neglected during data reduction. A north-south plotting error of 0.2 km would result in only a 0.14 mgal difference in the value for theoretical gravity. Navigational and plotting procedures were carried out by two members of the ship's crew immediately upon lowering the gravimeter towards the seafloor. The ship's geographical position was kept approximately identical with that of the meter by heading the ship into the wind or prevailing swell prior to meter lowering and by maneuvering with the ship's engines thereafter. Sometimes cable had to be payed out to preclude the possibility of putting sufficient tension on it so as to drag or overturn the meter while it was on the bottom.

3. Measurements

Each day survey operations began with a measurement taken at the base station; ACANIA's two buoy harbor mooring next to WH-29, at the seaward end of the USCG pier. The absolute gravity measurement at WH-29 was referenced to the counter readings obtained during several pier station occupations so that a formula could be employed to relate the daily base station readings with the known gravity value at WH-29. Upon reaching the desired location, the meter was lowered as fast as practicable to the seafloor. The meter lowering rate was usually a little over 5 cm/sec. Bottom arrival was indicated when the depth counter units ceased increasing. This value was recorded along with the fathometer reading. High speed leveling was initiated and flood and tilt checks made (meter leakage never occur and repositioning of the meter due to excessive bottom slope, was never necessary). After coarse leveling was completed the mass was unclamped. While fine leveling adjustments continued automatically, the beam position and gravity counter switches were manipulated

to null the beam position galvanometer needle. Hysteresis problems were avoided by always approaching the ultimate counter reading from low to high values. After obtaining and recording the correct counter value the mass was clamped by switching to the "deck" mode on the control box, the meter was raised and two-blocked, and the ACANIA was headed for the next assigned station.

Under calm sea conditions and in intermediate depths (15 to 60 m) four stations could be occupied per hour. Shallow stations took longer because of galvanometer needle oscillations induced by the sea and swell. Deep stations proved to be time-consuming due to the large cable length required.

4. Meteorological Efforts

It is felt there is a high reliability factor in the station plots since all survey operations took place during daylight hours. Although fog often prevails in the area during the spring months, no visibility problems were encountered throughout the survey.

At wind speeds of 15 knots and greater more meter cable had to be let out. Even with constant maneuvering, the ACANIA could not be held in one spot. This problem resulted in a slight deterioration in position accuracy. The inevitable pitching and rolling often made operations more difficult and lengthy than predicted. On two separate occasions work had to be suspended due to high seas and/or strong swell.

IV. DATA REDUCTION

In order to be useful to the geophysicist, observed gravity data must be corrected for station elevation, mass differences, the influence of nearby topography, and latitude. In general, all gravity values are reduced to a datum plane, which for this investigation will be taken as mean sea level (MSL). Due to the fact that absolute gravity values are rarely plotted on maps and charts, it is only necessary that anomalies be consistent as to the chosen datum.

Much of the theory of the reduction of gravity data applies to both land and underwater surveys; but there are some important differences between the two. These will be explained in this section. Most of the actual numerical calculations were carried out on the Naval Postgraduate School's IBM-360 computer, programmed in Fortran langauge.

A. OBSERVED GRAVITY

As previously mentioned, a tie-in between WH-29 and ACANIA's harbor mooring was necessary to effect a working base station from which observed underwater gravity values could be derived through gravity difference calculations. The counter units recorded from the control box must be modified through a conversion factor in order to yield true milligal values. The conversion table provided by the manufacturers (LaCoste and Romberg, 1970) gives a single conversion factor of 1.03985 due to the fact that all counter values fell between 3300 and 3400 counter units.

The absolute reference of 979891.7 mgal for WH-29 was correlated with the author's daily base readings (ba) taken at ACANIA's mooring. These values varied between 3323.67 and 3323.76 counter units. This variation

was due principally to earth and ocean tides and the difficulty involved in reading the meter scale during high sea and swell conditions. Therefore, the initial uncorrected observed gravity (G_1) for the seafloor stations can be computed from the formula:

$$G_1 = 979891.7 + (cv - ba)(1.03985) \text{ mgal}, \quad (1)$$

where cv is the control box counter value recorded at each station. The first half of each day's readings were referred to the morning pier reading and the afternoon readings were referenced to the evening counter value measured at WH-29.

For land stations the equation is:

$$G_1 = 979891.7 + (cv - bm)(cf) \text{ mgal}, \quad (2)$$

where bm is the pier benchmark reading taken with the land gravimeter. For the coast survey, the base station readings varied between 3405.47 and 3405.67. Linear modification of the recorded counter values from the land meter was carried out through interpolation of conversion factors (cf in equation (2)) peculiar to meter G-08. All the calculations were done by computer using the Fortran program supplied by USGS.

1. Earth Tide Correction

The first correction that must be applied to G_1, the earth tide correction (ET), is a result of the same forces that cause oceanic tides: the moon and the sun. Because the earth is not an infinitely rigid body, its inherent elasticity enables crustal deformations to occur due to the sun's and moon's gravitational attractive forces. These effects can vary the earth's radius as much as 30 cm in a few hours; yielding a net change of 0.1 mgal in gravity. Therefore, this correction can not usually be neglected in the determination of gravity anomalies. Again, a USGS computer program was utilized to carry out the necessary calculations

for both land and sea stations, the input parameters being the geographical coordinates of the station.

2. Instrument Drift Correction

Readings were taken each day prior to sea survey operations and again upon returning to ACANIA's mooring. After removal of earth and ocean tidal variations, meter drift rate should be calculable between the times of base station occupation. Linearity in drift rate was not observed as the small amount of drift noted during the four months when operations were carried out was as much a positive factor as it was negative. Thus, meter drift was assumed to be negligible and was not considered in computing observed gravity.

Drift for the land gravimeter was also assumed to be zero due to the characteristic calibration features inherent in the meter itself and the excellent correlation between previous USGS calibration runs and those of the author.

3. Earth Curvature Correction

The curvature correction (CC) is needed to compensate for the assumption of an infinite flat plate made in the ensuing Bouguer correction. Since terrain corrections were carried out to distances of 160 km from each station the flat earth assumption would ultimately result in significant errors. The USGS formula used was:

$$CC = -1.376 \times 10^{-4}(z-z_t) + 3.049 \times 10^{-9}(z-z_t)^2 - 1.110 \times 10^{-17}(z-z_t)^3, \quad (3)$$

where z is gravimeter depth and z_t tidal height, both in meters. Curvature corrections for the sea stations varied from -0.02 mgal at a 12 m depth to -0.13 mgal at 90 m. Corrections for land stations were made from the equation:

$$CC = 1.376 \times 10^{-4}H - 3.049 \times 10^{-9}H^2 + 1.110 \times 10^{-17}H^3 \text{ mgal}, \quad (4)$$

where H is station elevation in meters above MSL. A maximum correction of 0.16 mgal corresponded to a 110 m elevation.

It is now possible to calculate the observed corrected gravity (OG) from the equation:

$$OG = G_1 + ET + D + CC, \tag{5}$$

where D is the meter drift (taken as zero in this work).

B. THEORETICAL GRAVITY

For the purpose of geophysical surveys, a reference ellipsoid has been adopted for use in calculation of the theoretical gravity (THG). This is the value of gravity expected if the earth were an ellipsoid of revolution fitted as closely as possible to MSL.

Numerous variations in the equation for theoretical gravity as given by the International Gravity Formula have been derived. The equation and coefficents used by the author were those based on the formula of Heiskanen and Vening Meinesz (1958):

$$THG = 978049.0(1 + 0.0052884 \sin^2 L - 0.0000059 \sin^2 2L) \text{ mgal}, \tag{6}$$

where L is the latitude. From differentiation of equation (6) one obtains an average south-to-north increase (in the Northern Hemisphere) in THG of 0.81 mgal/km. This variation is due to both the decrease of the centripetal acceleration, due to the earth's diurnal rotation, from the equator to the poles and to the difference between the polar and equatorial radii. This variation in gravity with latitude constitutes the so-called "latitude correction."

C. ADDITIONAL GRAVITY CORRECTIONS

Four additional modifications have to be made to the underwater gravity data so as to obtain a complete Bouguer anomaly (CBA). In order of increasing difficulty they are: the free-air correction, the initial

and secondary Bouguer corrections, and the terrain correction. The most logical sequence for understanding the physical significance of each of the applied corrections is that prescribed by Andrews (1973), which is followed henceforth.

1. Initial Bouguer Correction

This step essentially removes the gravitational effect of the water above the meter, a problem peculiar to underwater gravimetry. An infinite "Bouguer plate" of water is assumed to lie over the meter, with properties of density σ_w and thickness $|z|$. The equation relating these parameters to the correction (bc_1) is:

$$bc_1 = 2\pi\sigma_w Gz \tag{7}$$

where G is the universal gravitational constant (6.670×10^{-8} $cm^3/g\text{-}sec^2$). This correction will be positive because the water above the occupied station exerts an upward attraction on the gravimeter. Given a water density of $\sigma_w = 1.027$ g/cm^3 (this value is used throughout this paper) and measuring the depth z in meters, equation (7) becomes:

$$bc_1 = 0.04304z \quad \text{mgal.} \tag{8}$$

As previously stated, this correction does not apply to land stations as the surrounding medium is air of negligible density.

2. Free-Air Correction

Next, the gravity station must be repositioned to the approximated reference ellipsoid, that is MSL. If a gravity station were located exactly at MSL, this correction would not be required, but in this survey all stations were either below or above MSL. At MSL the free-air gravity gradient is 0.3083 mgal/m (Heiskanen, 1967). The general formula for the free-air correction (FAC) for underwater

stations is:

$$FAC = -2GM(z - z_t)/R^3 , \qquad (9)$$

where M is the earth's mass (5.97×10^{27} g), and R the earth's mean radius (6.371×10^{6} m)(MacDonald, 1966). Equation (9) reduces then to the form:

$$FAC = -0.3083(z - z_t) \text{ mgal}, \qquad (10)$$

where z and z_t are measured in meters.

Since station depth and tide level are the only variable parameters in equation (10) it is clear that the accuracy with which they are measured is critical. A transducer inside the bottom of the gravimeter sphere measures differences between surface and seafloor pressure. These differences are indicated by a counter in the control box which is related to depth by calibration tables provided by the meter manufacturer.

The tidal heights were computed using the average between local stations at Santa Cruz and Año Nuevo Island, related to San Francisco, the reference station for both. Since all tide tables use mean lower low water (MLLW) for their datum plane, it was necessary to determine the vertical distance between MLLW and MSL. This difference was found to be 0.884 m (Coast and Geodetic Survey chart 5403).

For underwater gravity stations, the FAC derived from equation (10) is negative since the meter is always below MSL. However, this does not hold true for land measurements, for which the following equation is used:

$$FAC = 0.3083H \text{ mgal}, \qquad (11)$$

where H is the station elevation in meters. In this case the meter is always above MSL and hence the FAC is positive.

3. Secondary Bouguer Correction

This correction involves filling in the region between the reference spheroid (MSL) and the station elevation with rock of appropriate density. In this way seafloor gravity observations can be correlated with land observations. The formula for this correction (bc_2) for a seafloor station is:

$$bc_2 = 2\pi \sigma_r G(z - z_t), \tag{12}$$

where σ_r is the mean density of crustal rock in the Bouguer plate (Dobrin, 1960). Numerical substitution for G, and using a value of $2.67\ g/cm^3$ for σ_r (a value to be used throughout this paper) yields:

$$bc_2 = 0.1119(z - z_t) \quad mgal, \tag{13}$$

where z and z_t are again measured in meters. This correction fills the space from the actual station depth to MSL with a uniform infinite plate of mean crustal density. For underwater stations, bc_2 is a positive correction as mass is being added below the reference ellipsoid.

For land stations the following equation is given:

$$bc_2 = - 0.1119H \quad mgal, \tag{14}$$

where again H is station elevation in meters. This correction will be negative because we are effectively removing the material between MSL and the station elevation.

Combining the initial and secondary Bouguer corrections yields the complete Bouguer correction (BC). For the underwater stations the combination of equations (8) and (13) gives:

$$BC = 0.04304z + 0.1119(z - z_t) \quad mgal. \tag{15}$$

For the land stations equation (14) is the complete Bouguer correction. Figure 13 schematically portrays the procedures for application of the free-air and Bouguer adjustments.

4. Terrain Correction

By far the most tedious part of gravity data reduction is that of calculating the terrain correction (TC). The Bouguer correction assumes that the topography surrounding the station is that of an infinite flat plate. The terrain correction evaluates the error in the Bouguer correction due to undulations of the terrain about the plane through the station. For land stations the Bouguer correction overestimates the gravitational attraction of the mass below station elevation because it ignores voids in this space. For underwater stations, the attraction is underestimated since the Bouguer plate only extends down to the original station depth, neglecting any voids below. The importance connected with this portion of the terrain correction in the author's survey area can be considered a direct function of the close proximity of large-scale bathymetric features. These include the Monterey Submarine Canyon and deep Pacific Ocean abyssal plains to the south and southwest, respectively. Therefore, the corrected gravity value obtained through application of the Bouguer correction will in actuality be too low (too much was subtracted for the land stations and too little was added for the seafloor stations). Furthermore, the upward component of the gravitational attraction of the mass above the plane through the station, which tends to lower observed gravity, is ignored in the Bouguer correction. Again, it can be seen that this is an important factor in reduction of the author's data due to the proximity of the Diablo, Santa Lucia, and Santa Cruz Mountain Ranges. In summary then, topographic elevations above and depressions

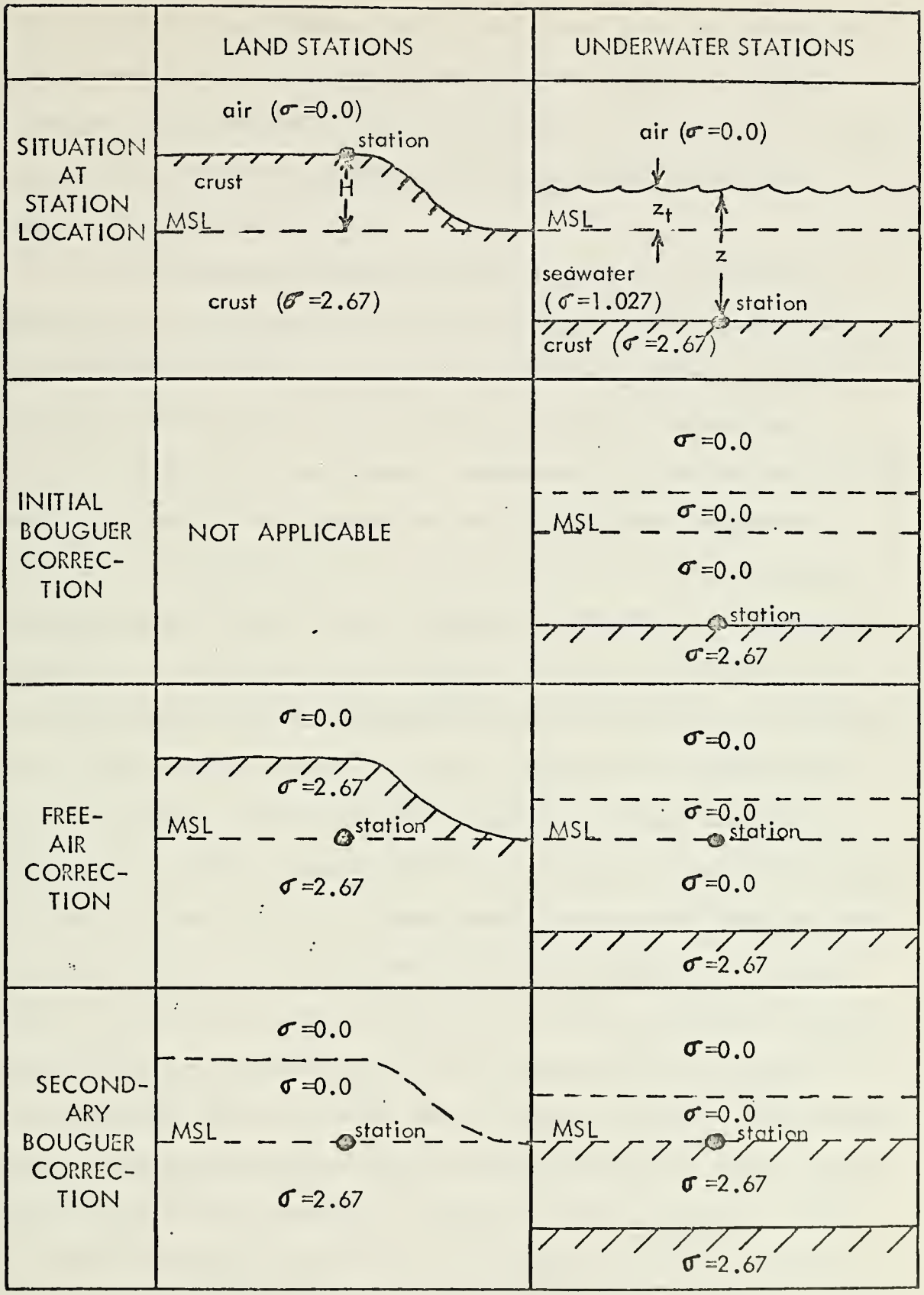

Figure 13. Schematic Representation of Free-Air and Bouguer Corrections for Land and Underwater Stations. (Densities in gm/cm^3)

below station location both act in the same sense, i.e., to reduce the gravity reading, and the gravity values modified only by the Bouguer correction will always be too low. Corrections for the effect of terrain elevation variations with respect to the plane through the gravity station will always be positive.

The topographic attraction is most conveniently estimated by dividing the area around the station into segments. The terrain effect for any segment is then a function of the difference, whether positive or negative, between the station elevation (or depth) and the mean elevation (or depth) of the segment. Segmentation of the area surrounding each station was effected through the use of transparent templates (graticules) made up by the author. Three different maps were employed, requiring three separately scaled templates (1:24,000; 1:210,668; and 1:820,000). Each template, when centered on a station, divides the surrounding terrain into compartments formed by radial lines through the station, intersecting concentric circles centered at the template axis. The lettered areas between concentric circles are "zones" which are sectioned into numbered "compartments" by the radial lines passing through the station. Zone A, with two compartments, has an outer radius of only 2 m, while Zone O, the most distant, has 28 compartments and an inner radius of 98.9 km and an outer radius of 166.7 km. After positioning the template over the desired station, the average elevation (or depth) of each compartment above (or below) MSL is visually estimated. The absolute numerical difference between station elevation and each of these compartmental values is then tabulated. With these values appropriate tables are entered to give the additional vertical gravitational attraction at the station for the compartments. Each compartmental correction is then

summed to give the zonal corrections which in turn are totalled to give the entire terrain correction for the station in question. There are 199 compartmental corrections to tally for each station.

The terrain correction tables used for this survey were based on those of Hayford and Bowie (1912). Bullard (1936) modified the Hayford-Bowie tables by enlarging the more distant compartments and reducing the compartments in the zones near the station. This eliminated some of the labor involved in use of the tables. In turn, the USGS modified Swick's (1942) work which was based on Bullard's tables. These then are the tables actually used in this research. A crustal density of 2.67 g/cm^3 was assumed and a 0.615 multiplication constant was applied to oceanic compartments in which the average bottom depth was greater than that of the station. This proportionality factor was derived from the equation:

$$\frac{\sigma_r - \sigma_w}{\sigma_r} = \frac{2.67 - 1.027}{2.67} = 0.615 \ . \qquad (16)$$

Computation of the corrections necessary for the land stations is relatively straightforward. However, care must be taken when averaging depths in the oceanic compartments. Use of the 0.615 factor for the entire compartmental column from land station elevation to seafloor fails to take into account the existence of air between the station and MSL. Since the average vertical distance from land station elevation to MSL was small in comparison to the overall compartmental depths, simple multiplication of the tabular values by 0.615 proved to be sufficiently accurate for all oceanic segments when calculating land station terrain corrections.

Precise calculation of terrain corrections for underwater stations requires a two-step procedure. Because seawater surrounds the station instead of air, and because some of the nearby topography is above MSL due to the close proximity of the coastline, it again becomes necessary to apply a weighting factor to the terrain correction tables.

Step one involves filling in the voids below station depth with rock of density 2.67 g/cm^3 (area 1, Fig. 14). Since water of density 1.027 g/cm^3 already fills these areas, the factor of 0.615 must be applied to the tabular values extracted for each ocean compartment with a bottom depth greater than that of the station itself.

The next step entails removing the effect of the crustal rock lying above the meter (areas 2 and 3, Fig. 14). This is done in two operations since the rock in area 2 is immersed in seawater, while that in area 3 is surrounded by air. First, the total correction for areas 2 and 3 is calculated assuming an average crustal density of 2.67 g/cm^3. As usual, this part is added to the observed gravity, as it represents mass removed from above the meter location. Figure 14 illustrates that at this point too much mass has in fact been removed since in area 2 a fraction of the terrain effect of the rock is counteracted by the overlying seawater. Therefore, part two involves computation of the effect for area 2 assuming a density for seawater of 1.027 g/cm^3. The total terrain correction for area 2 must be multiplied by the factor 0.385 derived from the equation:

$$\frac{\sigma_w}{\sigma_r} = \frac{1.027}{2.67} = 0.385 \ . \qquad (17)$$

This second part of the correction should be subtracted from the observed gravity, as water of depth z (area 2) is added above the meter.

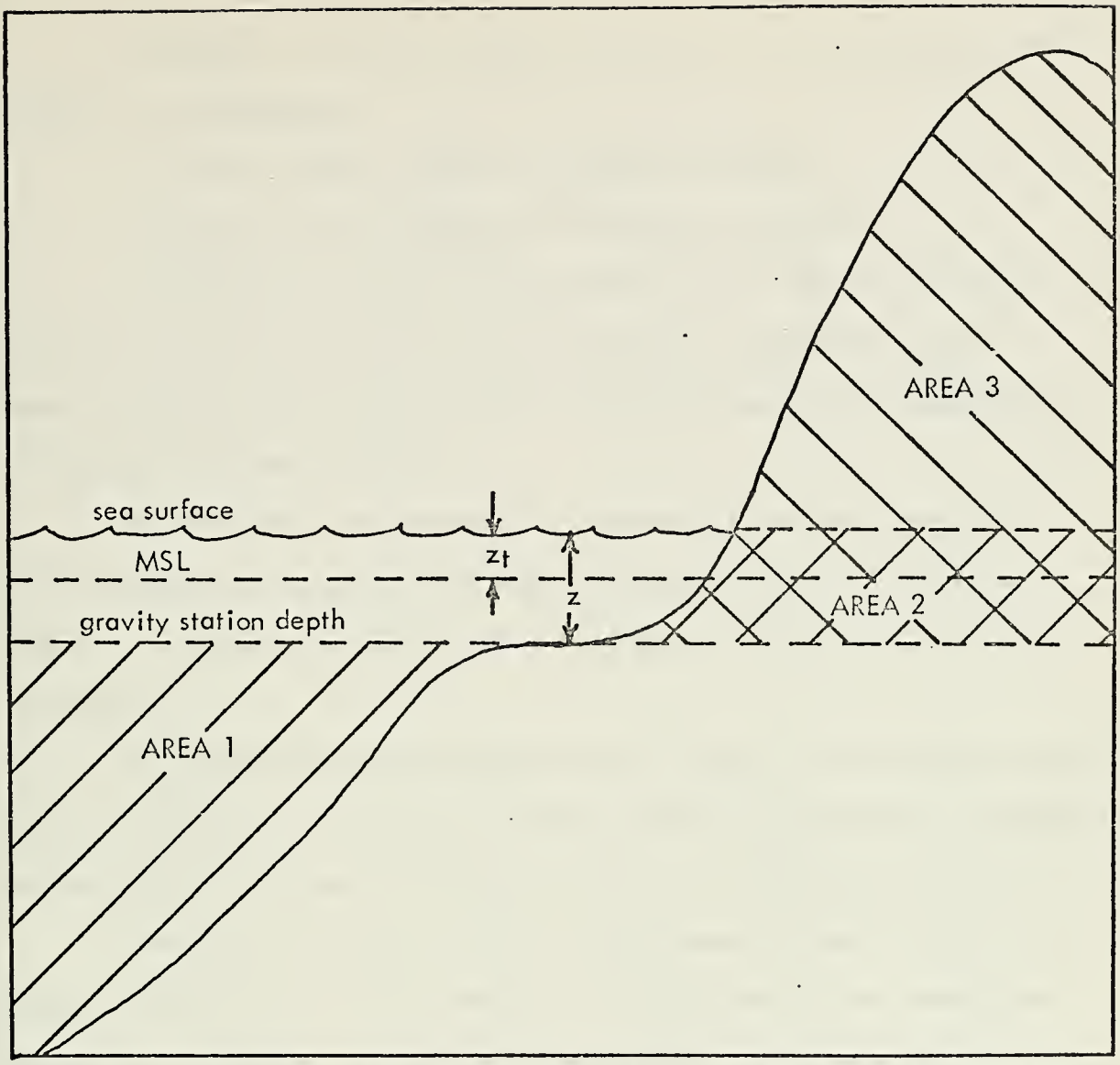

Figure 14. Schematic Diagram Showing Areas Involved in Terrain Corrections.

In summary, the total terrain correction for each seafloor station involves the following:

(1) fill in area 1 with rock instead of water,

(2) fill in area 2 with water instead of rock, and

(3) remove the effect of the crustal rock above MSL in area 3.

In practice, the station depths (z) were small in comparison to the elevations of the terrestrial features (area 3); hence, the contribution of equation (17) was negligible.

The possible error involved in calculating terrain corrections is estimated to be approximately $\pm$ 0.02 mgal/zone which could ultimately result in a maximum possible error of $\pm$ 0.35 mgal for the entire station correction.

The maximum terrain correction was 6.53 mgal for Station LL located almost 2 km inland at the base of a steep-sided valley, while the minimum correction was 2.36 mgal for Station A located in downtown Santa Cruz.

Sea-surface gravimetry usually yields massive banks of data compared to the relatively small amounts of bottom gravity data available. Correlation of the two is often a valuable tool to the geophysicist. With this in mind it is probably more realistic to first calculate the terrain correction for the bottom data prior to computation of the mass-adjusted free-air anomaly (to be discussed in the next section). This procedural alteration is proposed by Andrews (1973), based on the concept of downward continuation (Peters, 1949; Trejo, 1954) which asserts that the terrain correction for bottom gravimetry is greater than that for sea-surface gravimetry at a finite distance above the same location.

Tables V and VI list observed and theoretical gravity and associated corrections for all land and sea stations.

TABLE V

LAND STATION GRAVITY CORRECTIONS

STA	OG	THG	FAC	BC	IC
A	979932.361	979914.168	4.42	-1.60	2.36
B	979936.046	979913.908	1.22	-0.44	2.44
C	979931.104	979912.781	3.01	-1.09	2.40
D	979937.426	979913.734	5.46	-1.98	2.51
E	979936.400	979912.695	4.23	-1.54	2.48
F	979939.683	979913.561	7.06	-2.56	2.69
G	979940.708	979913.388	5.83	-2.11	2.56
H	979938.447	979913.128	5.64	-2.04	2.62
I	979936.632	979913.908	11.10	-4.02	3.09
J	979937.991	979913.821	6.50	-2.35	2.87
K	979940.429	979914.168	6.21	-2.25	2.96
L	979940.512	979914.427	6.87	-2.49	3.00
M	979941.127	979914.687	7.81	-2.83	3.07
N	979942.253	979915.207	9.12	-3.31	3.44
O	979942.178	979915.381	8.00	-2.90	3.41
P	979938.578	979915.554	10.16	-3.68	3.49
Q	979938.478	979915.294	5.84	-2.14	3.03
R	979929.145	979916.247	9.60	-3.48	3.32
S	979925.263	979916.681	9.22	-3.34	3.30
T	979925.093	979917.114	6.96	-2.52	3.22
U	979922.690	979917.634	10.53	-3.82	3.23
V	979923.274	979918.414	9.41	-3.41	3.28
W	979923.666	979918.934	9.69	-3.51	3.29
X	979926.149	979919.194	6.11	-2.22	3.58
Y	979924.997	979919.541	7.90	-2.87	3.36
Z	979924.172	979919.628	8.84	-3.21	3.31
AA	979927.280	979920.408	4.33	-1.57	3.37
BB	979931.855	979920.842	1.13	-0.41	3.98
CC	979922.574	979920.842	11.48	-4.16	3.28
DD	979933.188	979921.709	3.76	-1.36	4.67

TABLE V (CONTINUED)

STA	OG	THG	FAC	BC	IC
EE	979931.048	979922.229	10.25	-3.72	4.64
FF	979919.272	979922.056	17.50	-6.34	3.56
GG	979920.592	979923.096	19.75	-7.16	3.28
HH	979914.996	979924.224	33.77	-12.24	3.31
II	979929.490	979924.397	13.55	- 4.91	3.60
JJ	979931.570	979924.658	11.29	- 4.09	4.03
KK	979942.380	979925.525	1.13	- 0.41	4.18
LL	979943.360	979926.480	2.63	- 0.96	6.53
MM	979941.140	979926.653	9.97	- 3.61	3.92
NN	979941.880	979926.913	9.22	- 3.34	3.35
OO	979944.210	979927.781	10.91	- 3.96	3.16

TABLE VI

SEA STATION GRAVITY CORRECTIONS

STA	OG	THG	FAC	BC	TC
1	979921.206	979906.287	-18.00	9.04	2.50
2	979920.940	979907.412	-17.11	8.57	2.48
3	979924.698	979908.884	-13.26	6.64	2.42
4	979928.702	979910.010	-12.40	6.20	2.39
5	979936.730	979911.136	-10.68	5.33	2.48
6	979934.257	979911.136	-13.33	6.68	2.56
7	979941.903	979912.348	- 5.75	2.87	2.51
8	979931.622	979912.175	-10.12	5.07	2.52
9	979936.948	979913.041	- 8.94	4.48	2.89
10	979939.242	979913.561	- 8.16	4.08	2.96
11	979941.807	979914.341	- 7.00	3.51	3.01
12	979935.515	979915.467	- 5.25	2.63	3.31
13	979927.607	979916.334	- 4.90	2.46	3.29
14	979928.914	979917.287	- 5.48	2.76	3.26
15	979928.608	979918.327	- 4.72	2.37	3.31
16	979928.615	979919.281	- 5.31	2.68	3.31
17	979928.470	979920.495	- 6.44	3.25	3.45
18	979933.715	979921.622	- 7.46	3.76	3.45
19	979932.408	979919.194	-11.16	5.61	3.19
20	979930.066	979917.981	-13.61	6.85	3.13
21	979928.409	979917.114	-12.89	6.48	3.21
22	979928.640	979916.074	-10.61	5.34	3.25
23	979930.676	979915.121	-11.59	5.83	3.28
24	979934.276	979914.254	-11.49	5.77	3.29
25	979934.330	979913.388	-12.79	6.43	2.99
26	979929.529	979912.435	-15.25	7.66	2.97
27	979930.261	979911.742	-14.80	7.44	2.95
28	979930.191	979910.876	-14.66	7.36	2.57
29	979912.739	979906.027	-19.57	9.86	2.58

TABLE VI (CONTINUED)

STA	OG	THG	FAC	BC	TC
30	979914.150	979905.940	-21.44	10.81	2.62
31	979922.410	979907.758	-16.99	8.57	2.47
32	979925.929	979908.538	-17.39	8.76	2.48
33	979929.792	979909.663	-14.43	7.26	2.37
34	979929.720	979909.837	-15.00	7.53	2.59
35	979923.180	979909.490	-19.34	9.70	3.14
36	979923.620	979910.096	-20.41	10.22	3.11
37	979924.130	979910.962	-19.10	9.56	3.41
38	979927.870	979911.829	-20.00	10.01	3.42
39	979928.700	979912.781	-19.45	9.73	3.42
40	979930.480	979913.648	-18.86	9.43	3.46
41	979931.210	979914.687	-18.16	9.10	3.41
42	979933.400	979915.641	-17.62	8.82	3.44
43	979935.650	979916.767	-17.73	8.88	3.36
44	979933.150	979917.634	-17.33	8.86	3.38
45	979930.610	979918.934	-16.35	8.19	3.37
46	979934.100	979920.321	-12.17	6.10	3.20
47	979934.680	979921.449	-11.09	5.56	3.28
48	979941.260	979922.749	- 6.19	3.10	3.44
49	979941.260	979924.311	- 4.87	2.44	3.43
50	979945.540	979925.178	- 5.15	2.58	3.48
51	979948.890	979926.133	- 5.30	2.66	3.43
52	979950.720	979925.699	- 3.78	1.90	3.20
53	979946.710	979925.439	- 8.71	4.38	2.96
54	979943.590	979924.918	- 9.27	4.66	3.10
55	979936.830	979923.964	- 9.35	4.71	3.08
56	979933.910	979922.663	-11.23	5.65	3.18
57	979929.020	979922.576	-14.93	7.50	3.01
58	979928.190	979921.275	-15.40	7.74	3.09
59	979927.260	979920.148	-16.56	8.33	3.18
60	979921.210	979906.114	-26.40	13.22	2.79
61	979921.000	979906.287	-28.12	14.08	2.88

TABLE VI (CONTINUED)

STA	OG	THG	FAC	BC	TC
62	979923.130	979907.326	-25.52	12.77	2.77
63	979921.620	979907.152	-24.41	12.21	2.66
64	979918.460	979907.326	-28.15	14.10	2.85
65	979918.910	979908.018	-26.06	13.05	3.26
66	979919.120	979908.797	-24.32	12.18	3.33
67	979919.950	979909.490	-23.93	11.98	3.31
68	979921.000	979910.356	-24.02	12.03	3.52
69	979924.960	979911.222	-23.42	11.73	3.65
70	979930.590	979912.175	-22.89	11.47	3.66
71	979935.390	979913.215	-22.33	11.19	3.59
72	979936.640	979914.168	-22.02	11.03	3.52
73	979933.730	979915.121	-21.61	10.83	3.50
74	979931.700	979916.247	-21.31	10.68	3.49
75	979929.100	979917.461	-20.28	10.17	3.44
76	979925.970	979918.674	-19.88	9.97	3.34
77	979932.410	979914.687	-26.69	13.40	3.60
78	979932.520	979913.474	-26.56	13.34	3.75
79	979932.940	979912.608	-26.74	13.43	3.77
80	979934.610	979911.655	-26.73	13.43	3.89
81	979931.750	979910.529	-27.55	13.85	3.78
82	979923.990	979909.750	-27.81	13.97	3.79

D. GRAVITY ANOMALIES

The difference between observed corrected gravity and theoretical gravity is an anomaly. When isolines are drawn to the gravity anomaly values plotted at their corresponding stations, analysis may reveal local and regional trends, which reflect geological substructure and density variations. Four different types of gravity anomalies were calculated for this survey.

1. Free-Air Anomaly

The vertical gradient of gravity can be approximated as the basic cause for gravity differences between adjacent stations. To a close approximation the vertical gradient is linear and is independent of latitude (see Equations 10 and 11). Application of the free-air correction (FAC) (previously derived) results in the corresponding first-order anomaly known as the free-air anomaly (FAA). It is called "free-air" because the theoretical anomaly is computed as if the gravity measurement were made at MSL but without taking into account the attraction of the crustal material (or seawater) between the actual topographic elevation at the station and MSL; that is, as if the gravimeter were suspended free in the air. This anomaly is given by the equation:

$$FAA = OG + FAC - THG. \tag{18}$$

The FAC is always negative for bottom stations and positive for land stations above MSL.

2. Simple Bouguer Anomaly

When the Bouguer correction is applied to the free-air anomaly, the simple Bouguer anomaly (SBA) results. The SBA is of little use in areas of prominently rugged terrain, but where uniform topography prevails

(e.g., Gulf of Mexico continental shelf) this anomaly can be utilized for gravity survey correlations and interpretations. The simple Bouguer anomaly is calculated as if the material under the station was of infinite horizontal extent. It is given by the expression:

$$SBA = OG + FAC + BC - THG, \tag{19}$$

or:

$$SBA = FAA + BC. \tag{20}$$

For land stations BC ($BC = bc_2$, Equation 14) is negative; for seafloor stations BC (Equation 15) is positive.

3. Complete Bouguer Anomaly

Upon application of the terrain correction (TC) to the simple Bouguer anomaly the complete Bouguer anomaly (CBA) results. This anomaly is usually used to make composite maps and charts of isolines to tie in separately surveyed areas. The plotted CBA isolines should reveal lateral crustal density variations and near-surface structural non-conformities, as well as variations in the depth to the Mohorovicic discontinuity. Due to the relatively small area involved in this survey, changes in MOHO depth were considered to be insignificant. This product of gravity data reduction is given by:

$$CBA = OG + FAC + BC + TC - THG, \tag{21}$$

or:

$$CBA = SBA + TC. \tag{22}$$

4. Mass-Adjusted Free-Air Anomaly

In order to be able to correlate bottom gravity measurements with sea-surface values, the mass-adjusted free-air anomaly (MFAA) is

introduced. Three steps are required:

(1) remove the upward attraction of the overlying seawater (bc_1),

(2) adjust the gravity as determined from the meter from its bottom value to that on the reference ellipsoid (FAC), and

(3) fill the ocean (now air below the meter repositioned at the reference ellipsoid) with seawater using the following mass-adjusted free-air correction:

$$MFAC = 2\pi \sigma_w G(z - z_t). \tag{23}$$

Numerical substitution for G and σ_w yields:

$$MFAC = 0.04304(z - z_t) \quad mgal, \tag{24}$$

Where z and z_t are measured in meters. This correction will be positive as the underlying mass of water will increase the downward gravitational attraction when the meter is relocated at MSL. Thus, the MFAA is given by:

$$MFAA = OG + bc_1 + FAC + MFAC - THG. \tag{25}$$

As previously mentioned for underwater stations, bc_1 is positive and the FAC is negative. Obviously, this anomaly is peculiar to bottom gravimetry and has no terrestrial counterpart.

In summary then, the forementioned corrections will have the signs:

	LAND STATIONS	UNDERWATER STATIONS
BC	-	+
FAC	+	-
TC	+	+

Gravity anomalies for both land and sea stations surveyed are tabulated in Tables VII and VIII.

TABLE VII

LAND STATION GRAVITY ANOMALIES

STA	FAA	SBA	CBA
A	22.61	21.01	23.37
B	23.36	22.92	25.36
C	21.33	20.24	22.64
D	29.15	27.17	29.68
E	27.94	26.40	28.88
F	33.18	30.62	33.31
G	33.15	31.04	33.60
H	30.96	28.92	31.54
I	33.82	29.80	32.89
J	30.66	28.31	31.18
K	32.47	30.22	33.18
L	32.95	30.46	33.46
M	34.25	31.42	34.49
N	36.17	32.86	36.30
O	34.79	31.89	35.30
P	33.18	29.50	32.99
Q	29.02	26.90	29.93
R	22.49	19.01	22.33
S	17.80	14.46	17.76
T	14.94	12.42	15.64
U	15.59	11.77	15.00
V	14.27	10.86	14.14
W	14.42	10.91	14.20
X	13.07	10.85	14.43
Y	13.36	10.49	13.85
Z	13.39	10.18	13.49
AA	11.20	9.63	13.00
BB	12.14	11.73	15.71
CC	13.21	9.05	12.33

TABLE VII (CONTINUED)

STA	FAA	SBA	CBA
DD	15.24	13.88	18.55
EE	19.07	15.35	19.99
FF	14.71	8.37	11.93
GG	17.25	10.09	13.37
HH	24.54	12.30	15.61
II	18.70	13.79	17.39
JJ	18.25	14.16	18.19
KK	17.99	17.58	21.76
LL	19.53	18.57	25.10
MM	24.50	20.89	24.81
NN	24.23	20.89	24.24
OO	27.39	23.43	26.59

TABLE VIII

SEA STATION GRAVITY ANOMALIES

STA	FAA	MFAA	SBA	CBA
1	-3.08	1.9	5.96	8.46
2	-3.58	1.2	4.99	7.47
3	2.55	6.2	9.19	11.61
4	6.29	9.7	12.49	14.88
5	14.92	17.9	20.25	22.73
6	9.79	13.5	16.47	19.03
7	23.81	25.4	26.68	29.19
8	9.33	12.1	14.40	16.92
9	14.97	17.5	19.45	22.34
10	17.53	19.8	21.61	24.57
11	20.47	22.4	23.98	26.99
12	14.80	16.3	17.43	20.74
13	6.37	7.7	8.83	12.12
14	6.14	7.7	8.90	12.16
15	5.56	6.9	7.93	11.24
16	4.02	5.5	6.70	10.01
17	1.53	3.3	4.78	8.23
18	4.63	6.7	8.39	11.84
19	2.06	5.2	7.67	10.86
20	-1.53	2.3	5.32	8.45
21	-1.59	2.0	4.89	8.10
22	1.96	4.9	7.30	10.55
23	3.97	7.2	9.80	13.08
24	8.54	11.8	14.31	17.60
25	8.15	11.7	14.58	17.57
26	1.85	6.1	9.51	12.48
27	3.72	7.9	11.16	14.11
28	4.66	8.8	12.02	14.59
29	-12.86	-7.4	-3.00	-0.42

TABLE VIII (CONTINUED)

STA	FAA	MFAA	SBA	CBA
30	-13.23	-7.2	-2.42	0.20
31	-2.34	2.4	6.23	8.70
32	-0.00	4.9	8.76	11.24
33	5.70	9.7	12.96	15.33
34	4.88	9.1	12.41	15.00
35	-5.74	-0.4	3.96	7.10
36	-6.98	-1.3	3.24	6.35
37	-6.03	-0.7	3.53	6.94
38	-4.05	1.5	5.96	9.38
39	-3.62	1.8	6.11	9.53
40	-2.11	3.1	7.32	10.78
41	-1.73	3.3	7.37	10.78
42	0.06	4.9	8.88	12.32
43	1.07	6.0	9.95	13.31
44	-1.89	2.9	6.79	10.17
45	-4.75	-0.2	3.44	6.81
46	1.55	4.9	7.65	10.85
47	2.09	5.2	7.65	10.93
48	12.29	14.0	15.39	18.83
49	12.05	13.4	14.49	17.92
50	15.19	16.6	17.77	21.25
51	17.44	18.9	20.10	23.53
52	21.22	22.3	23.12	26.32
53	12.52	15.0	16.90	19.86
54	9.36	12.0	14.02	17.12
55	3.47	6.1	8.18	11.26
56	-0.04	3.1	5.61	8.79
57	-8.55	-4.4	-1.05	1.96
58	-8.55	-4.2	-0.81	2.28
59	-9.52	-4.9	-1.19	1.99
60	-11.43	-4.1	1.79	4.58
61	-13.54	-5.7	0.54	3.42

TABLE VIII (CONTINUED)

STA	FAA	MFAA	SBA	CBA
62	-9.83	-2.8	2.94	5.71
63	-10.05	-3.3	2.16	4.82
64	-17.15	-9.3	-3.05	-0.20
65	-15.29	-8.1	-2.24	1.02
66	-14.11	-7.4	-1.93	1.40
67	-13.58	-6.9	-1.60	1.71
68	-13.49	-6.8	-1.46	2.06
69	-9.79	-3.3	1.94	5.59
70	-4.58	1.8	6.89	10.55
71	-0.26	5.9	10.93	14.52
72	0.35	6.5	11.38	14.90
73	-3.10	2.9	7.73	11.23
74	-5.95	-0.0	4.73	8.22
75	-8.73	-3.1	1.44	4.88
76	-12.67	-7.1	-2.70	0.64
77	-9.09	-1.6	4.31	7.91
78	-7.64	-0.2	5.70	9.45
79	-6.53	0.9	6.90	10.67
80	-3.90	3.6	9.53	13.42
81	-6.46	1.2	7.39	11.17
82	-13.70	-5.9	0.27	4.06

V. DATA PRESENTATION AND DISCUSSION

A. GENERAL

The computed values of the complete Bouguer anomalies for both land and sea stations were plotted at their respective positions on a composite large-scale USGS chart. Isolines were drawn by hand utilizing a 2-mgal spacing. The final result shown in this report exhibits the most logical fit between the data and previous knowledge of the regional and local substructure.

Inaccessability to precise basement depth data in the survey area precluded prediction of an accurate regional trend. Superficial examination based on a speculative basement depth prediction indicates no significant linear regional trend. Thus, no attempt was made to develop two-dimensional profile models of the area.

The values calculated for the mass-adjusted free-air anomalies for all the underwater stations were also plotted on the same charts used for CBA analysis. Isolines were manually drafted, again at 2-mgal intervals. Both isoline charts were tied in with the previous gravity survey values for northern Monterey Bay calculated by Cronyn (1973).

B. ERROR ANALYSIS

Table IX lists what the author believes to be the maximum possible errors inherent in calculation of the complete Bouguer anomaly. It is felt that ultimate CBA values are accurate to approximately $\pm$ 1.0 mgal for the sea stations, about five times more accurate than results from

INITIAL ERROR SOURCE	DATA REDUCTION STEP	ERROR IN COASTAL SURVEY	ERROR IN CONTINENTAL SHELF SURVEY
GRAVIMETER ACCURACY	OBSERVED GRAVITY	± 0.04	± 0.10
OPERATOR READING ACCURACY	OBSERVED GRAVITY	± 0.01	± 0.10
NAVIGATION	THEORETICAL GRAVITY	± 0.05	± 0.20
ELEVATION/ DEPTH CALCULATIONS	FREE-AIR AND BOUGUER CORRECTIONS	± 0.10	± 0.20
ELEVATION/ DEPTH CALCULATIONS	TERRAIN CORRECTION	± 0.35	± 0.35
TOTAL	COMPLETE BOUGUER ANOMALY	± 0.55	± 0.95

TABLE IX. Possible Errors in Complete Bouguer Anomaly Calculation (Values in milligals)

sea surface gravimetry. As expected, it was possible to compute the CBA for the land stations with far greater accuracy. It is estimated that they are accurate to within $\pm$ 0.55 mgal.

C. COMPLETE BOUGUER ANOMALY DISTRIBUTION

Although plotted gravity anomalies reflect, among other things, variations in depth to the Mohorovicic discontinuity, it is believed that the small areal extent of the survey excludes the possibility of the existence of large slopes at the MOHO. Therefore, the assumption is made that the CBA reflects crustal deformations and general depth to the granitic basement.

Figure 15 is a small-scale plot of the CBA isoline distribution for the survey area. The gravity high in the center of the area lies well within the Palo Colorado-San Gregorio fault zone. The high may be interpreted as an area of shallower depth to the basement complex Santa Lucia granite with respect to the surrounding portion of the continental shelf as will be shown later by seismic reflection profiles.

The anomalous low centered off Davenport is situated on the eastern side of the fault zone and probably signifies a down-thrust portion of the zone, that is, the granitic basement is deeper there than in the surrounding areas.

Northward, the large isoline gradients again reflect the presence of the Palo Colorado-San Gregorio fault zone extending into Año Nuevo Point. The fact that the isolines do not run parallel to the direction of the suggested fault zone at first seems misleading. However, reports of gravity investigations inland near Año Nuevo Point indicate similar CBA isoline trends (J. C. Clark, USGS, oral commun., 1973).

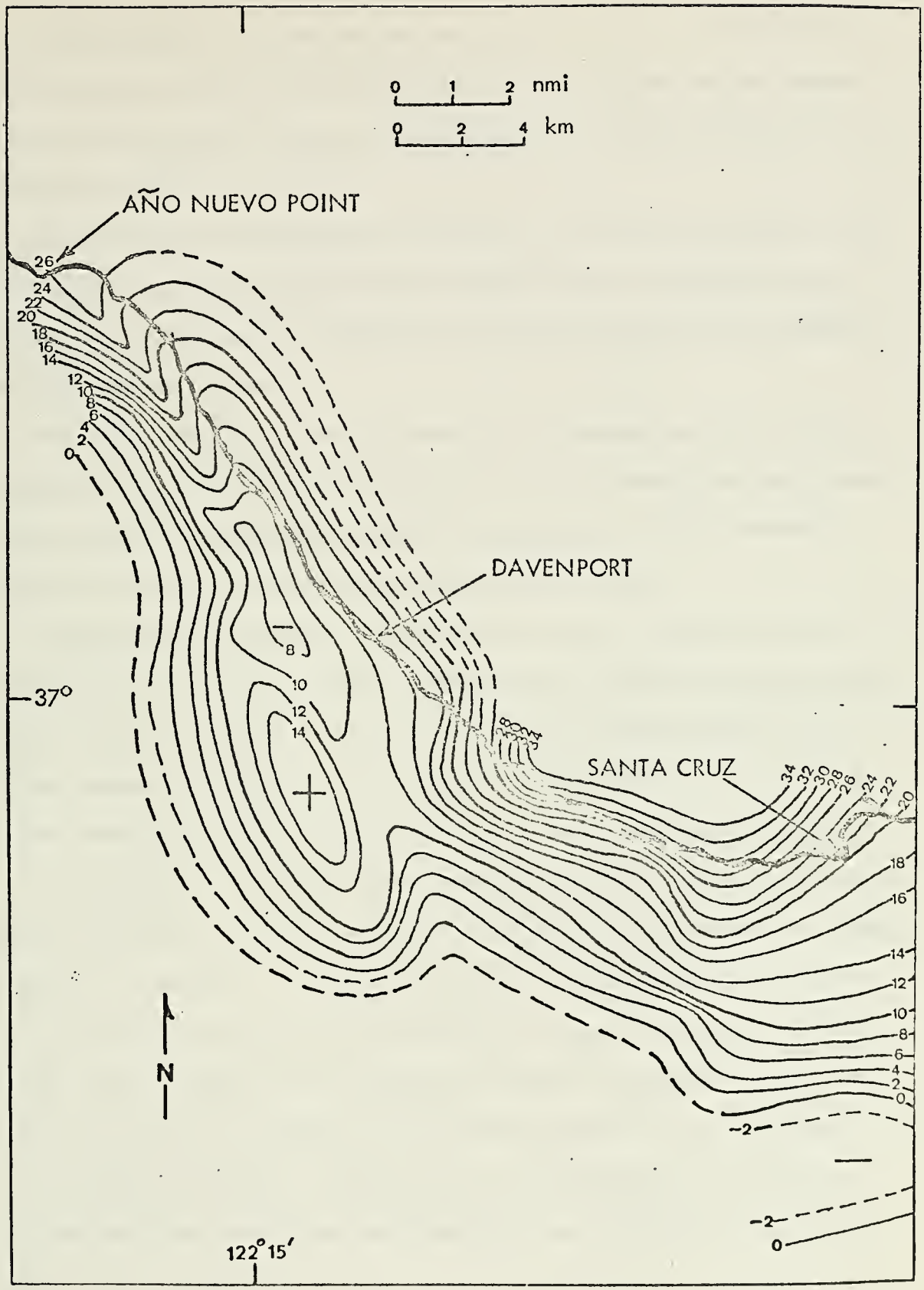

Figure 15. CBA Distribution for the Continental Shelf and Adjacent Coastline Between Santa Cruz and Año Nuevo Point. (Values in milligals)

The trending of the onshore isoline characteristics is based entirely on the author's data but the high station density of the coastal survey portion of this report lends much credibility to the CBA distribution on land (Fig. 15).

The intensive curvature of the isolines to the north and south of the centralized gravity high may support considerations of dip-slip fault motion (and also possible strike-slip movement) along the Palo Colorado-San Gregorio fault zone.

The tight gradient of the isolines in the southeastern part of the survey area is in excellent correlation with the Monterey Bay fault zone (Greene, 1973) where seismic profiling has indicated faults extending up to the base of the thin Holocene depositional layer.

The large positive CBA values near Santa Cruz coincide with the outcropping of the granitic basement complex north of Natural Bridges State Beach. Also in evidence is the north-northeast, south-southwest slope of the basement offshore. The isolines, the trend of which is confirmed by the Santa Cruz outcrop, are perpendicular to the proposed downslope.

A tie-in with the Bouguer Gravity Map of California was only possible in the land region near Santa Cruz as the Santa Cruz sheet does not extend beyond 37° N latitude. The general location of individual CBA isolines of the Santa Cruz sheet agreed well with the coastal and shelf stations of the author. However, once offshore the small extensions of the isolines on the Santa Cruz sheet do not conform exactly to the curvature of the author's isolines. Undoubtedly, this disagreement results from the previous land data being extrapolated to an extent beyond the shoreline.

D. MASS-ADJUSTED FREE-AIR ANOMALY DISTRIBUTION

Figure 16 depicts the mass-adjusted free-air anomaly chart for the Santa Cruz-Año Nuevo Point continental shelf. As expected, the general isoline trends run in the same directions as those of the CBA chart with the exception of the disappearance of the low previously encountered in the CBA distribution. This is undoubtedly due to the additional numerical modifications involved in the calculation of the three-step mass-adjusted free-air anomaly introduced earlier as equation (25).

The isolines terminate at the shoreline because there is no criteria for calculation of the MFAA at land stations. The MFAA plot is presented in this report solely for the purpose of possible correlation in the future, with sea surface gravity data.

E. NORTHERN MONTEREY BAY TIE-IN

Utilizing a pantograph to effect a 1/8th reduction in scale, composite charts were drawn using this author's data along with that of Cronyn's (1973) northern Monterey Bay survey.

1. Complete Bouguer Anomaly

Figure 17 portrays the composite CBA distribution resulting from connection of the northern Monterey Bay gravity values with those computed by the author. Isoline tie-ins were easily accomplished for the greater magnitude CBA values (10 through 25 mgal) in the northern part of Cronyn's area. At the extreme southeastern edge of the author's area correlation was not precise, although the anomalous trend was easily maintained and the extension of the author's isoline values to the east was readily carried out.

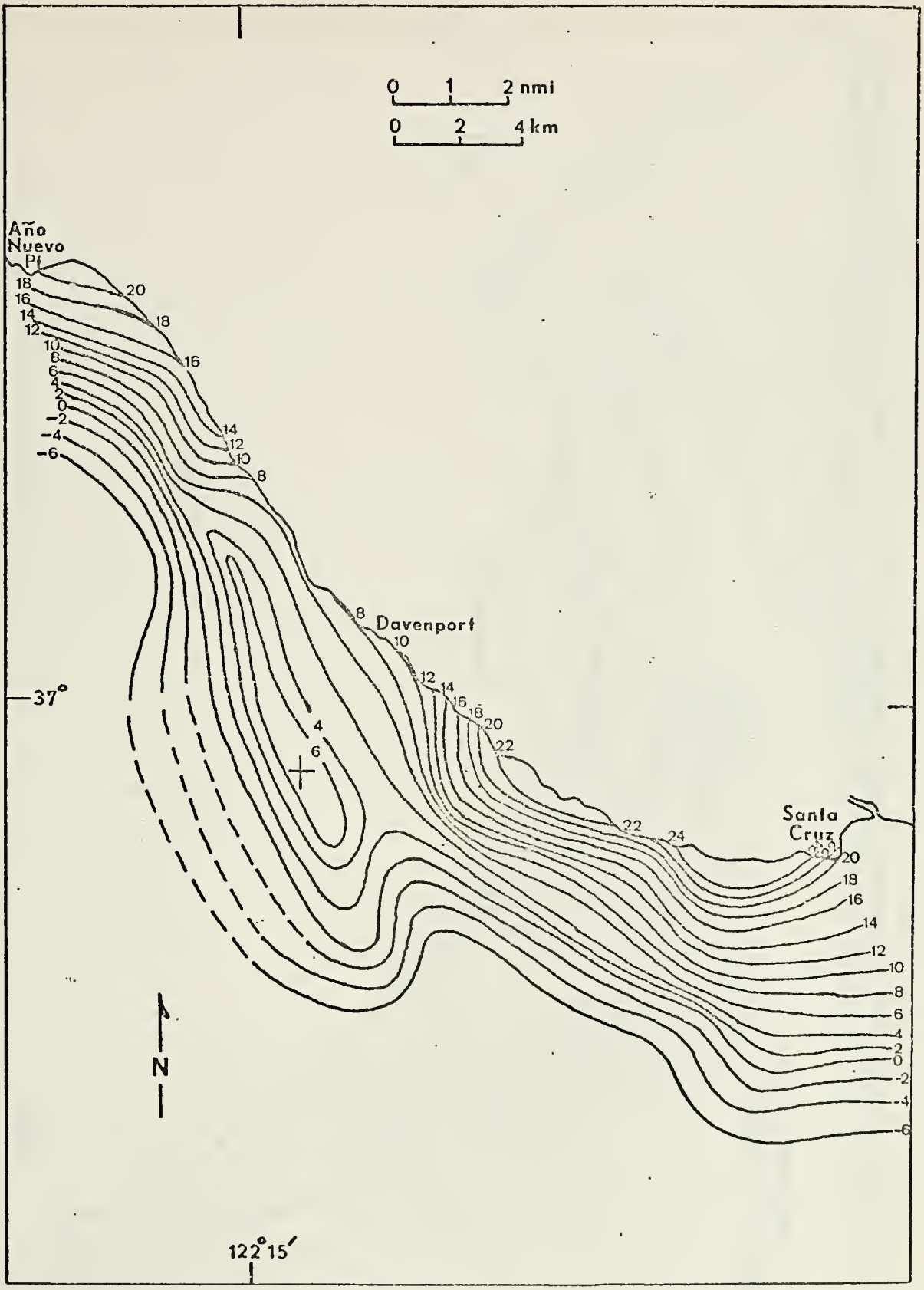

Figure 16. MFAA Distribution for the Continental Shelf Between Santa Cruz and Año Nuevo Point. (Values in milligals)

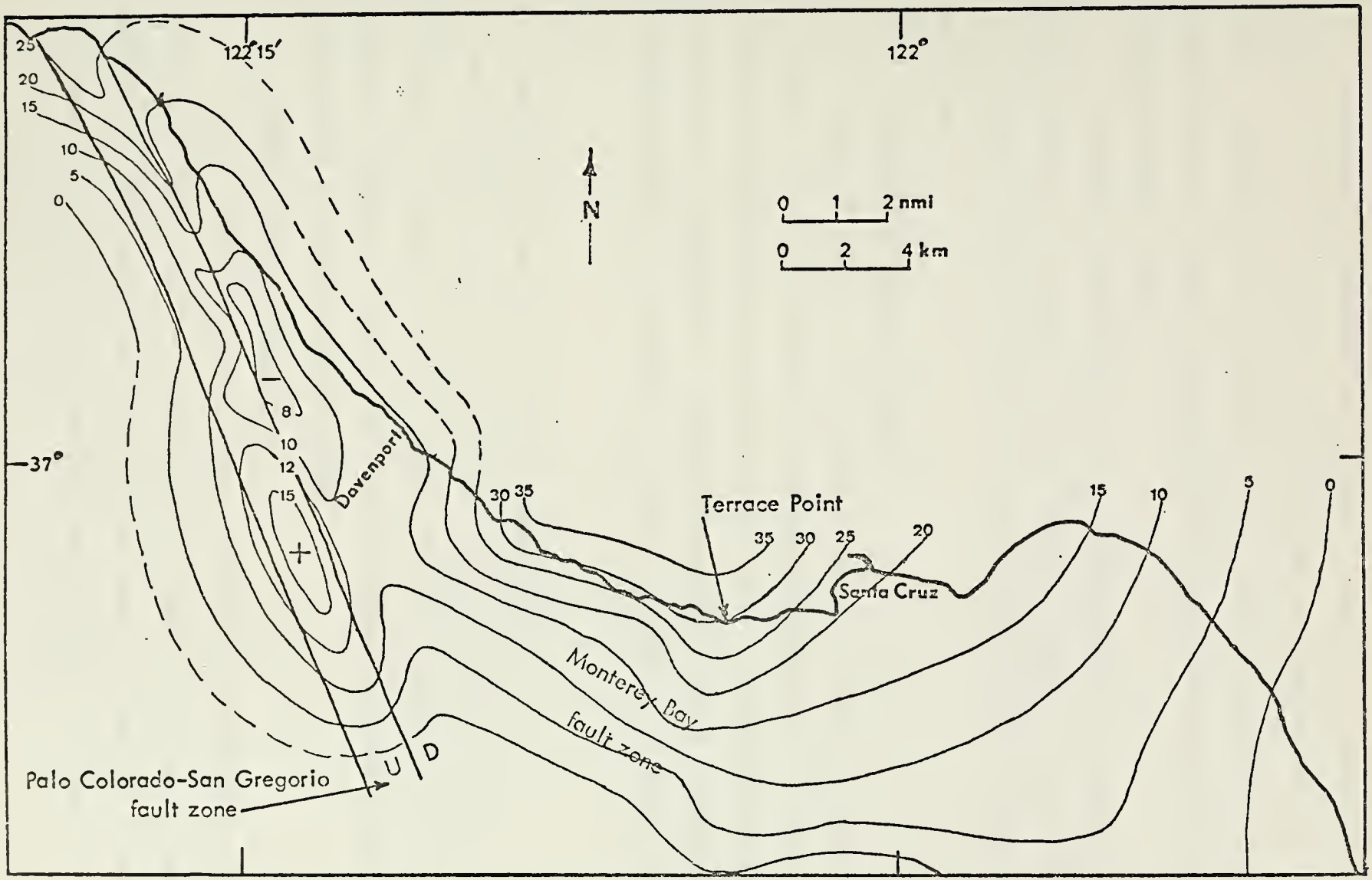

Figure 17. Composite CBA Chart of Extended Northern Monterey Bay Area. (Monterey Bay Contours after Cronyn, 1973.) (Values in milligals)

The gravity low sited approximately 10 km south of Santa Cruz (Fig. 15) is substantiated in Cronyn's analysis and appears to be an area of downdropping of the basement complex. This coincides with faulting that extends to the base of the Holocene deposits within the Monterey Bay fault zone (Greene, 1973).

The abrupt north-northwest, south-southeast trend of all but the 10-mgal isoline to the south of Terrace Point is probably indicative of the previously postulated strike-slip features within the Monterey Bay fault zone.

2. Mass-Adjusted Free-Air Anomaly

Figure 18 represents the overall mass-adjusted free-air anomaly distribution for northern Monterey Bay extending northwestward on the continental shelf through the author's survey area. Tie-in with Cronyn's data was easily accomplished. This composite chart has been produced for the express purpose of comparison with and addition to, sea surface gravity data.

F. CROSS-SECTION ANALYSES OF GEOLOGIC SUBSTRUCTURE

Data relating to subsurface structure, other than that obtained from gravimetry, is included in this section. Comparative analyses of this sort do much to minimize the speculative nature of crustal interpretations produced from reduced gravity data alone.

1. 160 kJ Seismic Profile Data

Figure 19 depicts the tracklines over which USNS BARTLETT (T-AGOR 13) made runs employing a 160 kJ seismic sparker system. Continuous seismic profiles were obtained by this relatively low-resolution system. These were compared with the profiles obtained from the author's CBA isoline

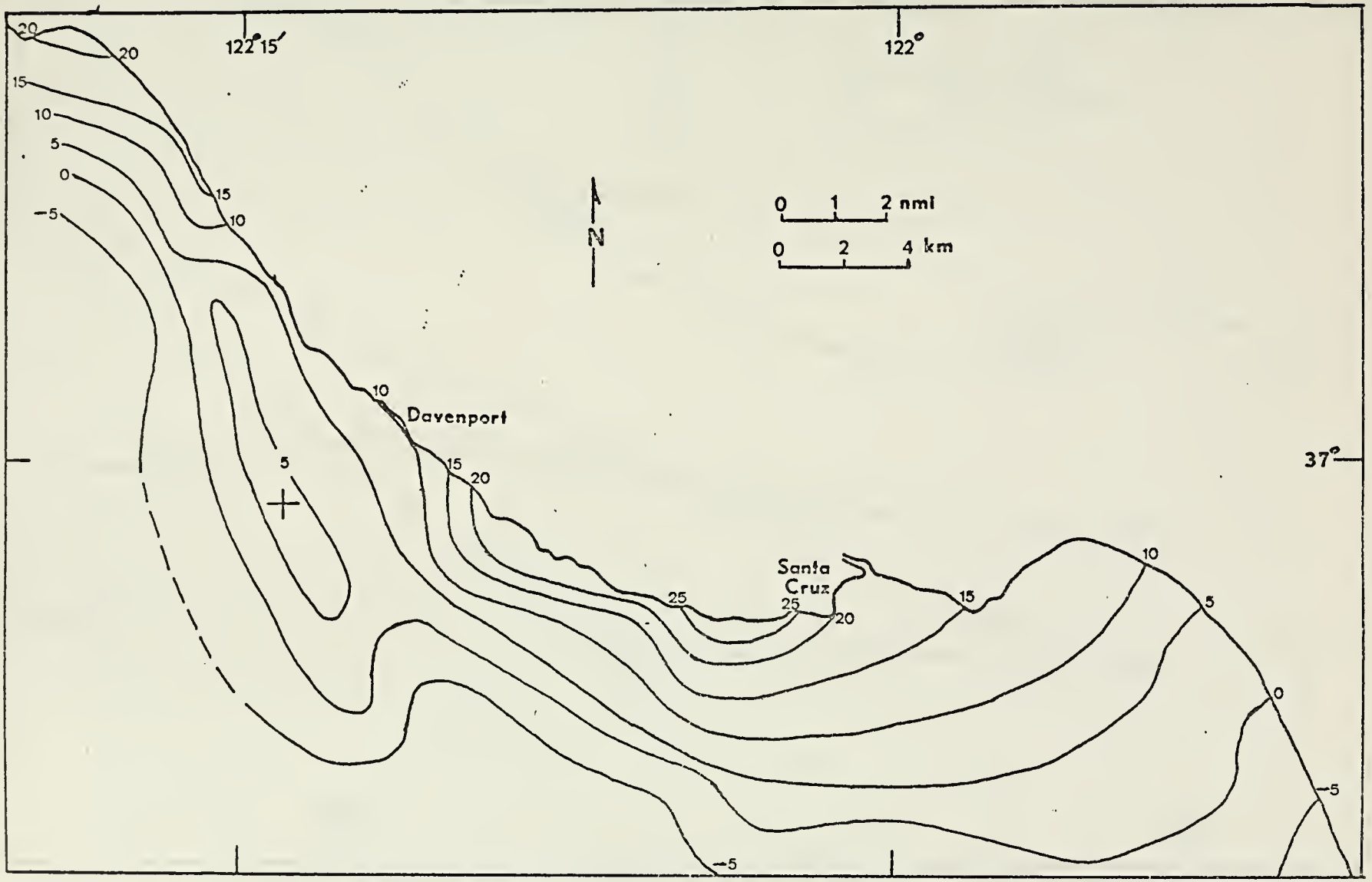

Figure 18. Composite MFAA Chart of Extended Northern Monterey Bay Area. (Monterey Bay contours after Cronyn, 1973.) (Values in milligals)

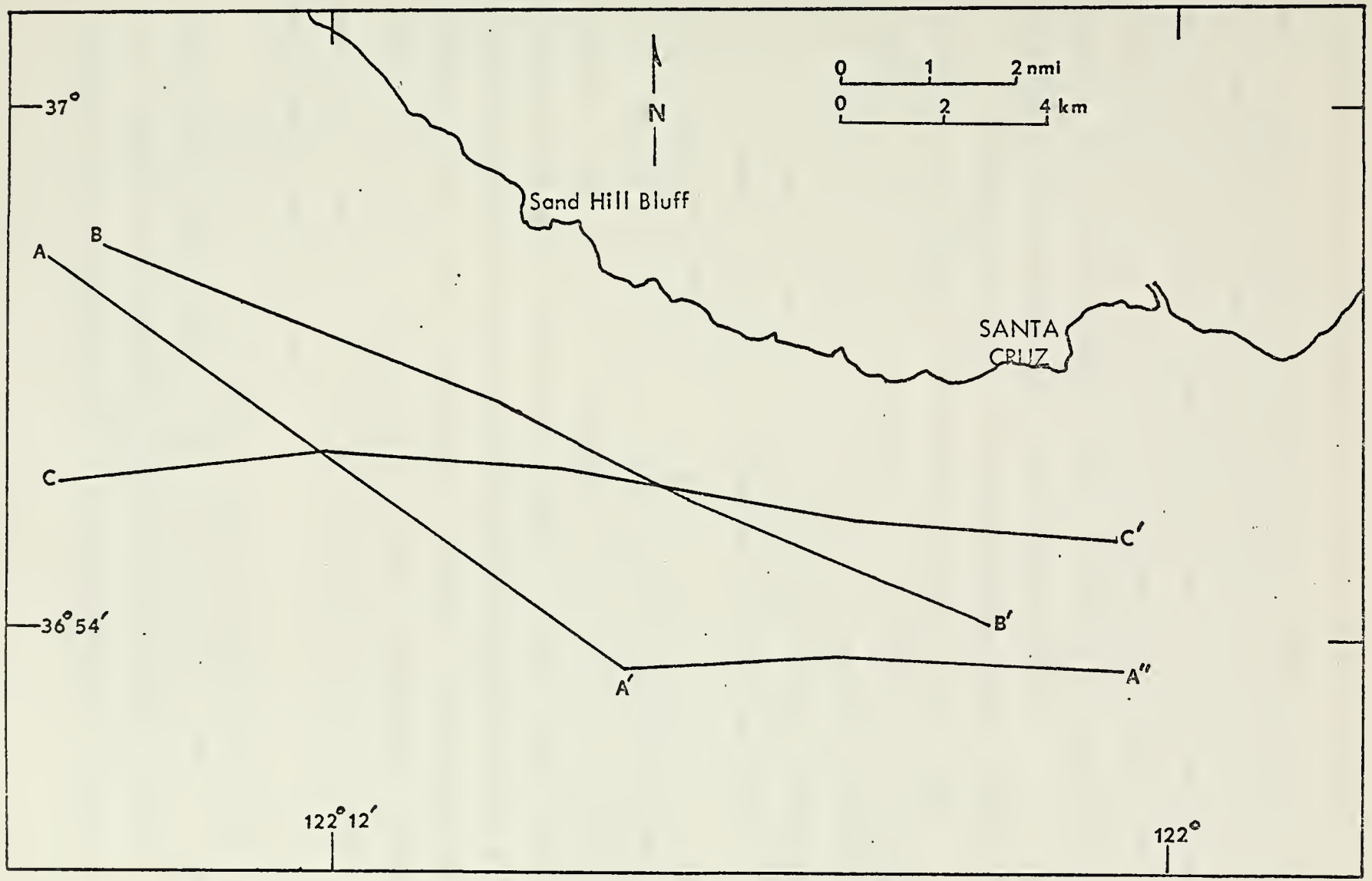

Figure 19. Geophysical Tracklines for 160 kJ Seismic Profile Data.

chart (Fig. 15). The measurement units for the seismic profiles are one-way sound pulse travel time in milliseconds. This is more realistic than conversion of the ordinate values to depths since to do so would require the inferrence of a density structure so as to calculate appropriate sound velocities. This would only degrade the accuracy of the profile. The postulated basement depths are sketched in dashed lines since they have been deduced solely from seismic profiles.

On trackline A'A (Fig. 20) the discontinuity shown at Station 80 corresponds to the Palo Colorado-San Gregorio fault zone, with a probable dip-slip component of about 430 m. The seismic data, in agreement with the fault map of Greene (1973), indicates this fault zone extends to within a few meters of the sea floor. The maximum CBA value of 14 mgal at Station 80 probably signifies the minimum depth to the dense granitic basement rock due to faulting.

The two vertical lines at Station 81 indicate probable basement faulting as interpreted from the seismic profile. The radical change in the CBA profile agrees with the seismic data, in which a 3 mgal/km gradient is exhibited in the fault zone area. The general downward trend of the proposed granitic basement in the seismic profile is to some extent paralleled in the decreasing CBA values to the west of Station 80. Also, the lower depth to basement to the east of Station 80 is reflected in the corresponding lower CBA values.

Trackline A"A (Fig. 21) shows excellent agreement between proposed granitic basement depth and the plotted CBA values. The two bulges in the otherwise smooth CBA trend coincide with the basement faulting interpreted from the seismic profile. No major faulting is apparent in

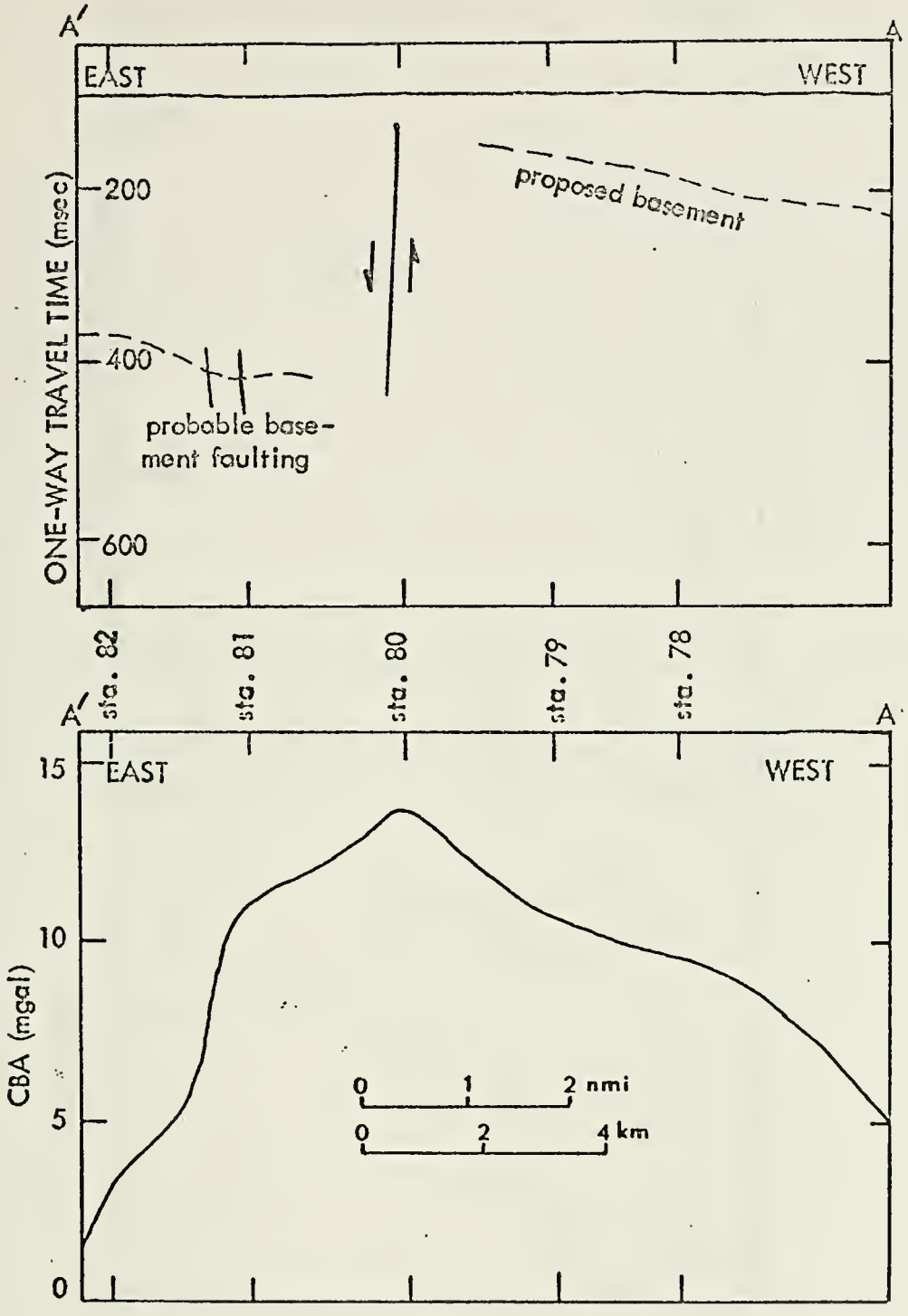

Figure 20. Comparison of CBA and Seismic Profiles for Trackline A'A. (Upper profile interpretation by R. S. Andrews, NPS, oral commun., 1973)

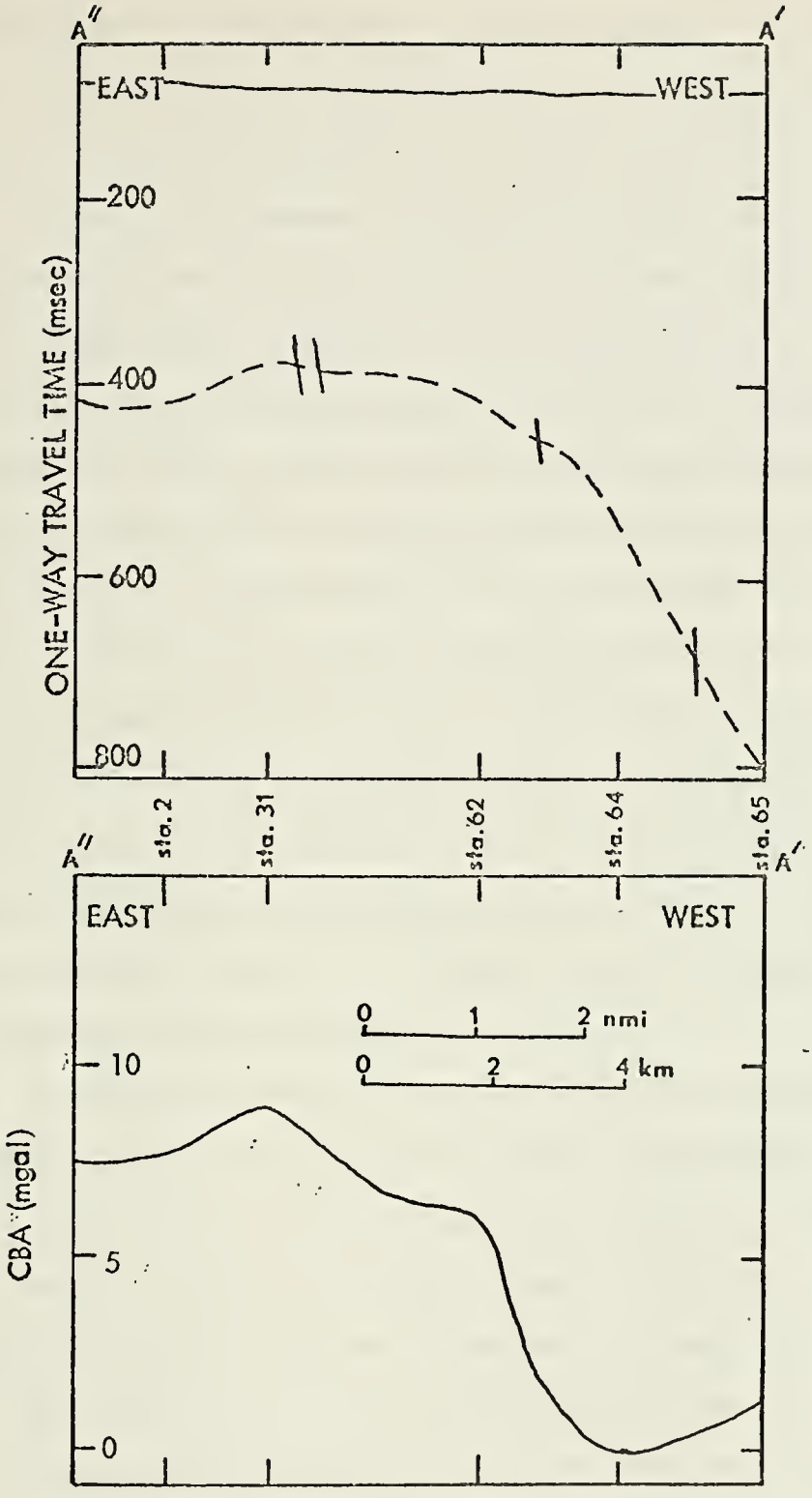

Figure 21. Comparison of CBA and Seismic Profiles for Trackline A"A'. (Upper profile interpretation by H. G. Greene, USGS, oral commun., 1973)

the seismic data but the decrease in basement depth from west to east agrees with the northward trending slope of the basement from south of Santa Cruz to the previously mentioned onshore granitic outcropping.

Figure 22 corresponds to track B'B in Figure 19. The prominent correlative feature in these drawings is again the Palo Colorado-San Gregorio fault zone at Station 71. The probable area of dip-slip motion agrees well with the maximum change in CBA values. The upthrown side of the fault zone shows a gravity high which most likely corresponds to the granitic basement being at a shallower depth than in the surrounding area. This in itself is a manifestation of the local seismic activity. The small irregularity in the seismic profile near Station 37 is probably a part of the Monterey Bay fault zone. No correlative feature is seen in the CBA profile. This is undoubtedly due to the depth of the basement in this area; that is, the change in gravity due to the faulting was filtered out by the Plio-Pleistocene crustal structure above it. It is possible to interpret the small deviation in basement profile at Station 34 as being in coincidence with the CBA high for that area.

Trackline C'C (Fig. 23) displays excellent correlation between the seismic profile data and the CBA vertical cross-section. First, the general trend and slope of the basement follows that of the CBA profile very closely. The Palo Colorado-San Gregorio fault zone corresponds to the high CBA gradient just west of Station 69. Again, the increase in the CBA further west agrees with the uplifted side of the fault zone, bringing denser basement granite closer to the crustal surface. The maximum CBA value of 21 mgal, at Station 5, is just to the south of Santa Cruz where the shallow basement is known to be sloping upwards to the north. This is also accurately depicted on the seismic profile to the east of Station 6.

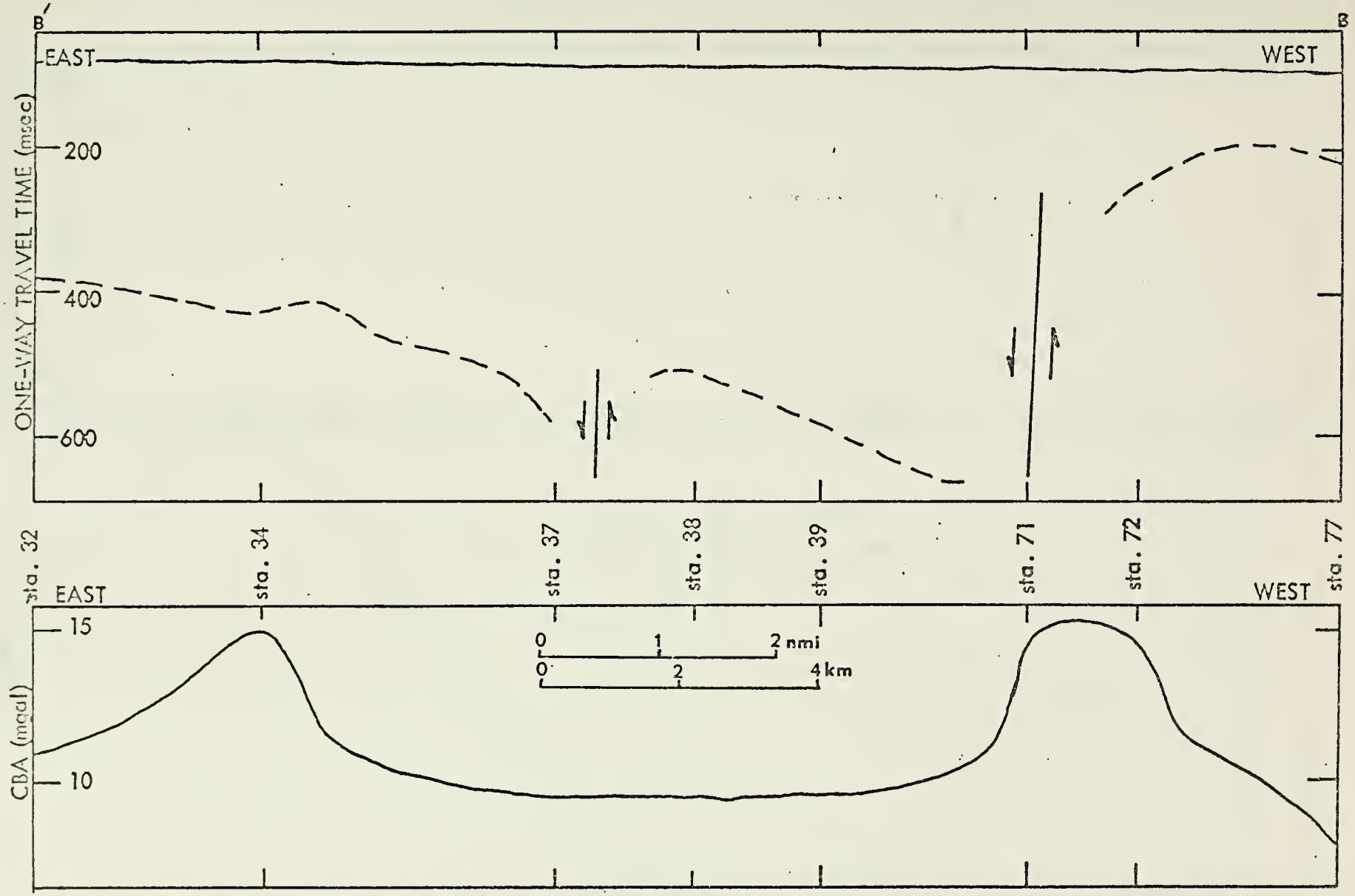

Figure 22. Comparison of CBA and Seismic Profiles for Trackline B'B. (Upper profile interpretation by H. G. Greene, USGS, oral commun., 1973)

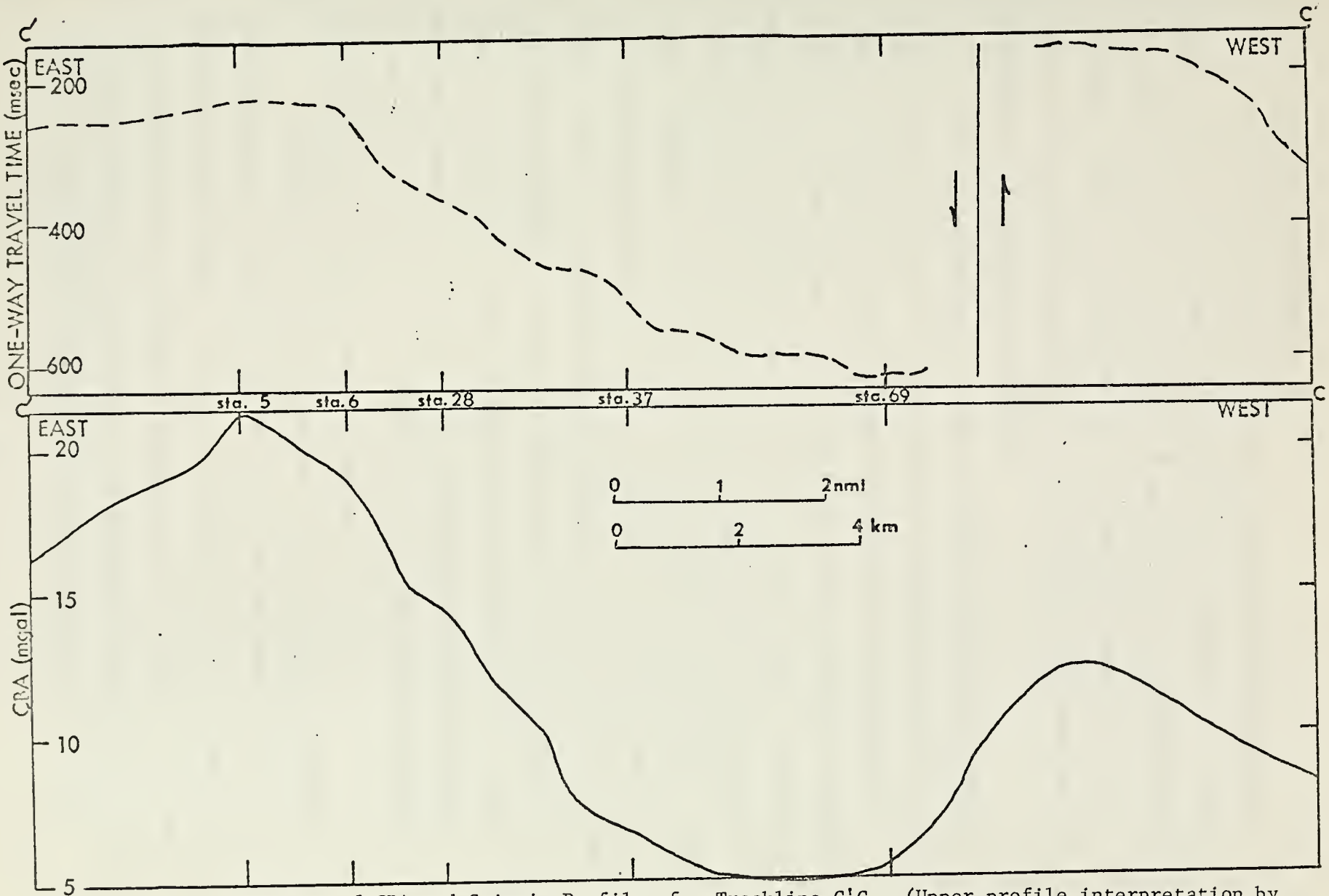

Figure 23. Comparison of CBA and Seismic Profiles for Trackline C'C. (Upper profile interpretation by H. G. Greene, USGS, oral commun., 1973).

2. 23 kJ Seismic Profile Data

Figure 24 shows segments of three different tracklines obtained from a seismic survey using a 23 kJ sparker system (Greene et al., 1973). This system resulted in about 1500 m of penetration with approximately 5 m resolution. Since the tracklines cross the author's survey area, comparison can be made between Greene's seismic profile interpretations and the author's corresponding CBA profiles.

The fault extending up to the sea floor in the bottom drawing of Figure 25 is at the eastern edge of the Palo Colorado-San Gregorio fault zone. The upper figure shows good correlation with the gravimetry as there is an abrupt change in the overall CBA trend at the fault location. Higher values of CBA and abnormal gradients coincide with it. The small subsurface fault depicted on the seismic profile at the northeast end of line FF' exhibits no characteristic modifications in the CBA trend. This could be due to the fact that it is of small extent (Fig. 24) and, as can be seen in the seismic profile reproduction, does not appear to alter the granitic basement (continuous solid line in Fig. 25). Thus, the lack of any dip-slip motion precludes the movement of any of the basement rock closer to the surface where a break in the CBA trend might be noticeable. Further, it is observed that the CBA profile parallels the seismically determined granitic basement.

Trackline GG' (Fig. 26) does not traverse the Palo Colorado-San Gregorio fault zone but does cut across the northwestern end of the Monterey Bay fault zone. Due to the intermediate-resolution characteristics of the sparker used, the granitic basement was not decypherable. However, the steep gradients of the CBA values (5 mgal/km) correspond with the high density of faults running through the area. As seen from the seismic

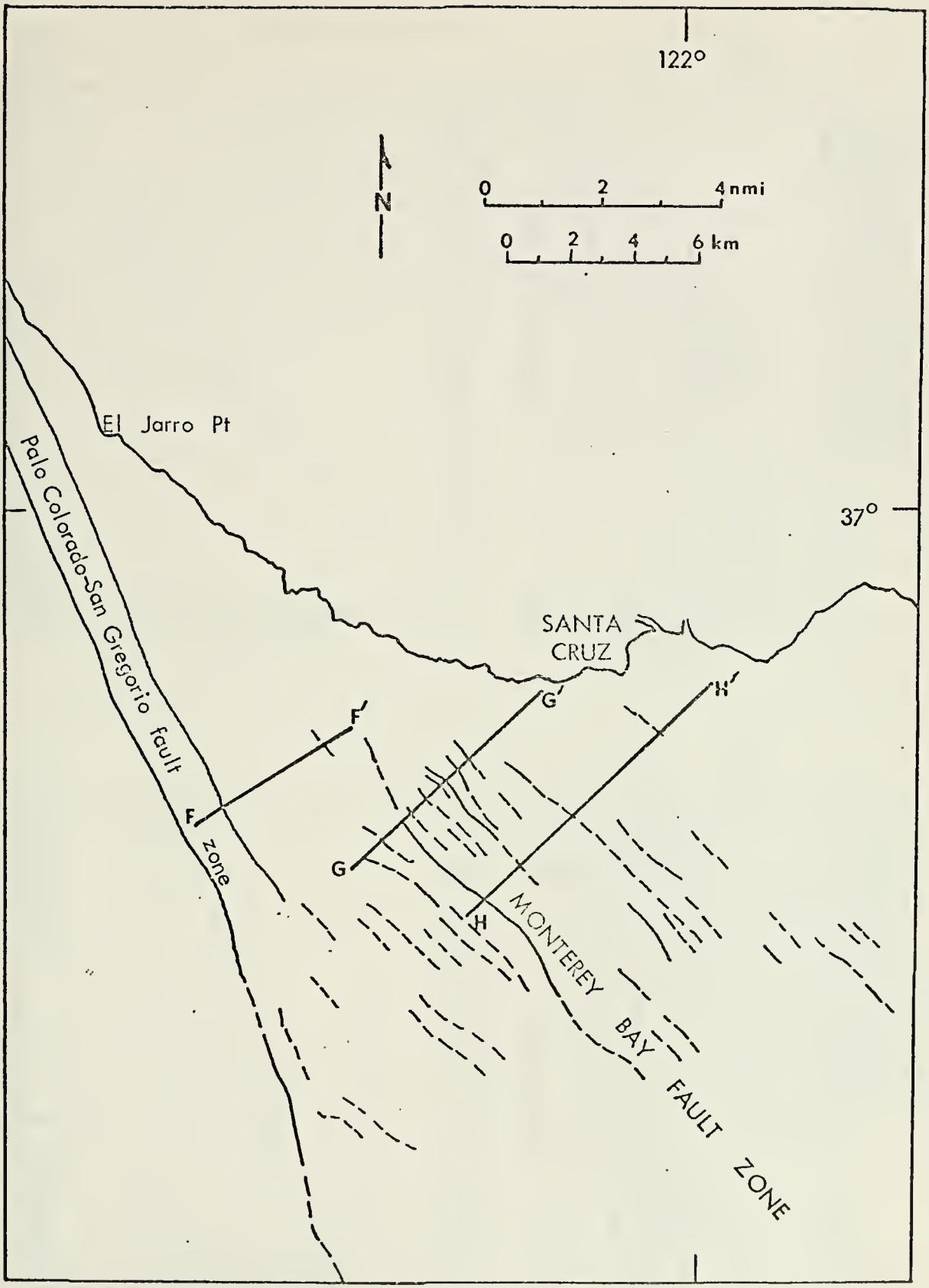

Figure 24. Geophysical Tracklines for 23 kJ Seismic Profile Data. (Fault zones after Greene et al., 1973.)

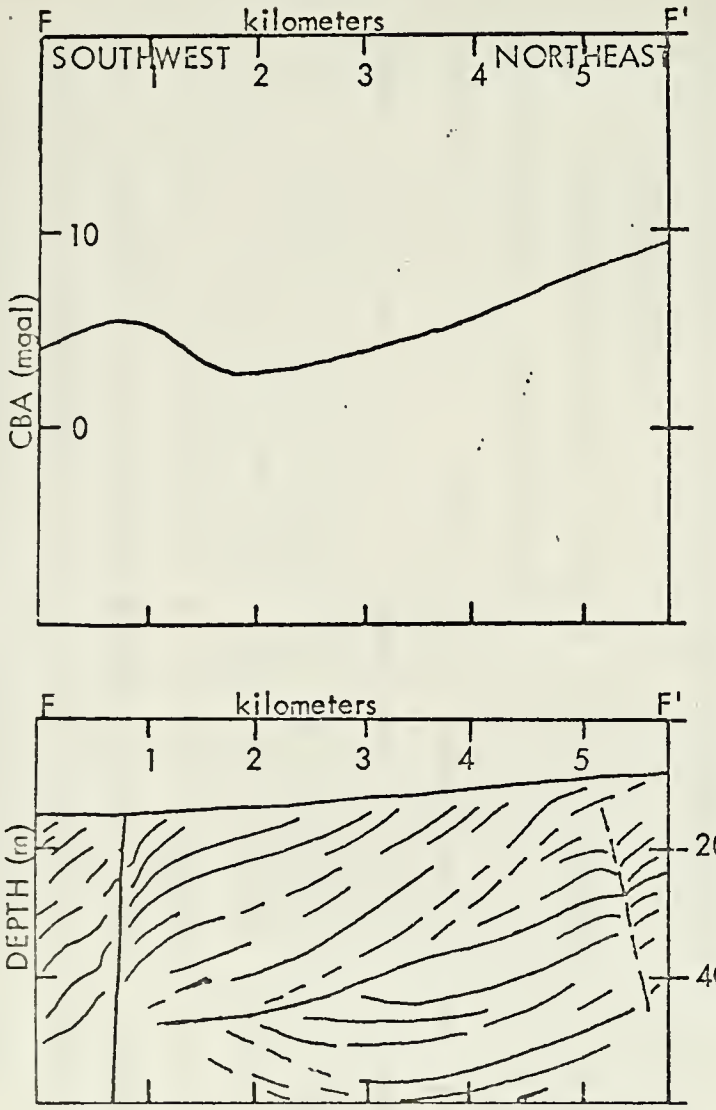

Figure 25. Comparison of CBA and Seismic Profiles for Trackline FF'. (Lower profile after Greene et al., 1973.)

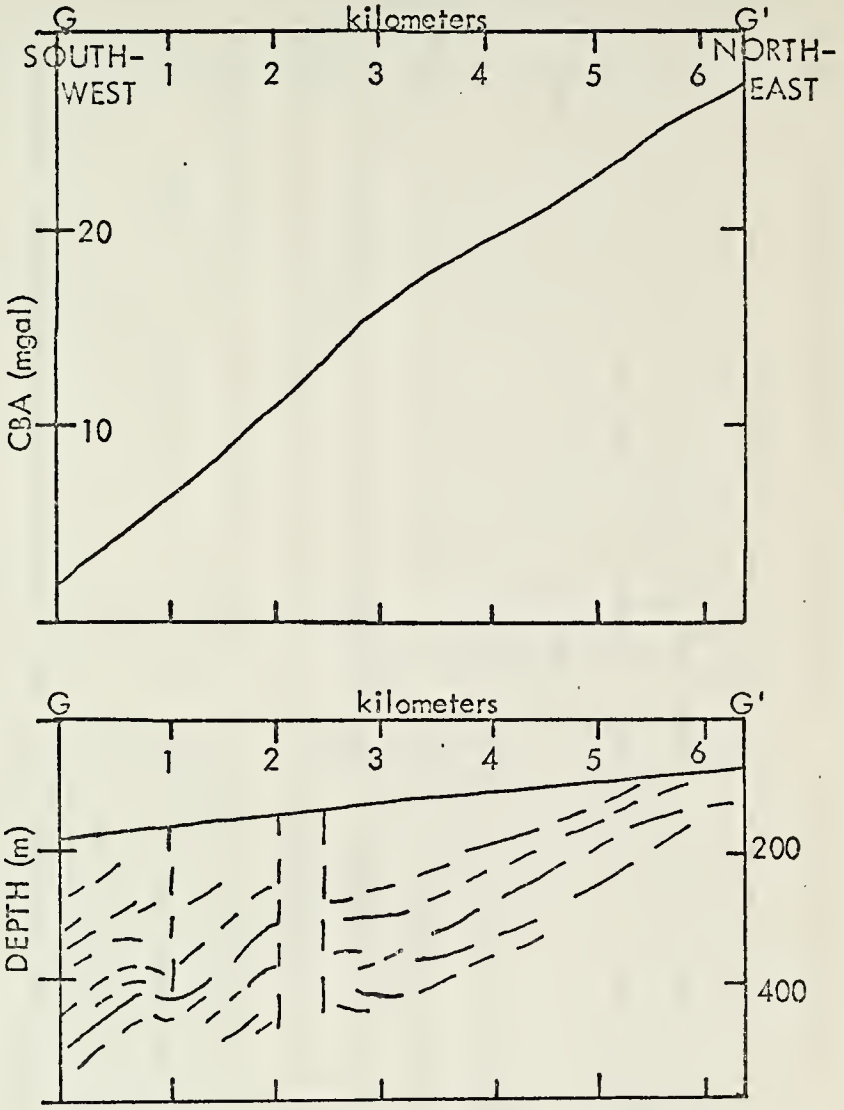

Figure 26. Comparison of CBA and Seismic Profiles for Trackline GG' (Lower profile after Greene et al., 1973.)

profile, the three separate faults appear to displace some Holocene deposits at the seafloor but probably do not reach the crustal surface itself. The overall trend of the strata shown in the seismic profile lends credence to the assumption that the general basement slope is on the order of the inclination exhibited by the CBA cross-section.

Trackline HH' (Fig. 27), as shown, extends to within 1 km of land to the east of Santa Cruz (Fig. 24). In fact, the high CBA values and rather horizontal structural characteristics indicated in the seismic profile for the northeastern 5 km of the track correspond to the northward trending upslope of the granitic basement from south of Santa Cruz (Cronyn, 1973). Again, the CBA gradient correlates well with the one fault zone depicted on the seismic profile. That no abrupt increase in CBA value is evident is probably due to the fact that the fault does not reach up to depths shallower than that of Pliocene age. Also, the general trend of the CBA profile parallels the predominate slope of the subsurface strata, which in turn probably reflects the general basement slope.

3. Well Core Data

Ross and Brabb (1973) have tied in known well depths to basement rock and derived a map showing depths to the granitic basement for most of the Monterey Bay area. Although highly speculative in nature, it nevertheless gives a starting point in attempting to portray the true basement depths. Line EE' (Fig. 28) connects two drill sites and extends westward into the oceanic portion of the author's survey area. Line DD' was picked so as to cross perpendicular to EE' and intersect one of the test wells. The Humble Oil and Refining Company test well reached granitic basement rock at approximately 228 m below MSL, while at the Monterey Bay Oil Company site the basement lies at slightly greater than 1620 m.

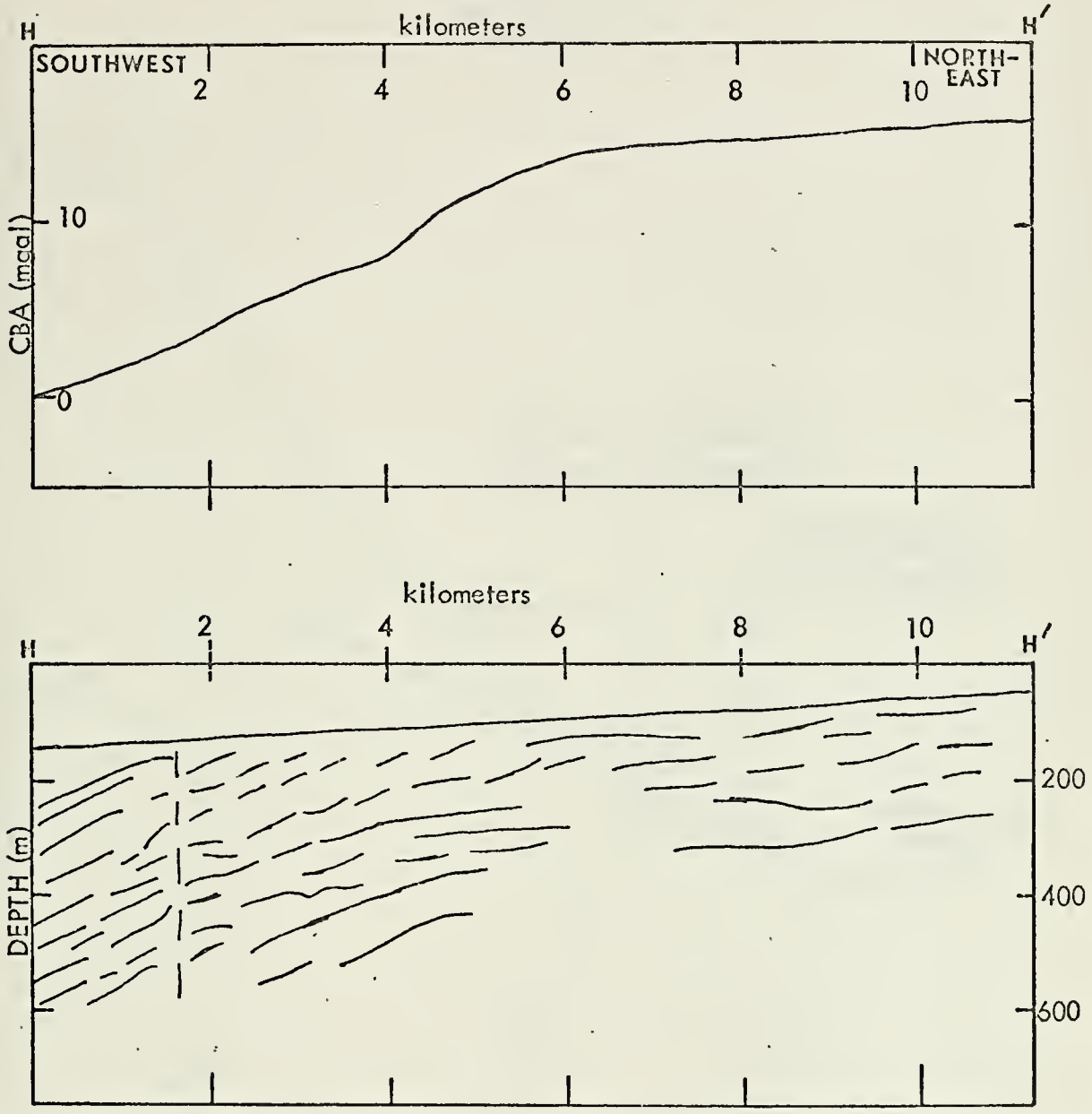

Figure 27. Comparison of CBA and Seismic Profiles for Trackline HH'. (Lower profile after Greene et al., 1973.)

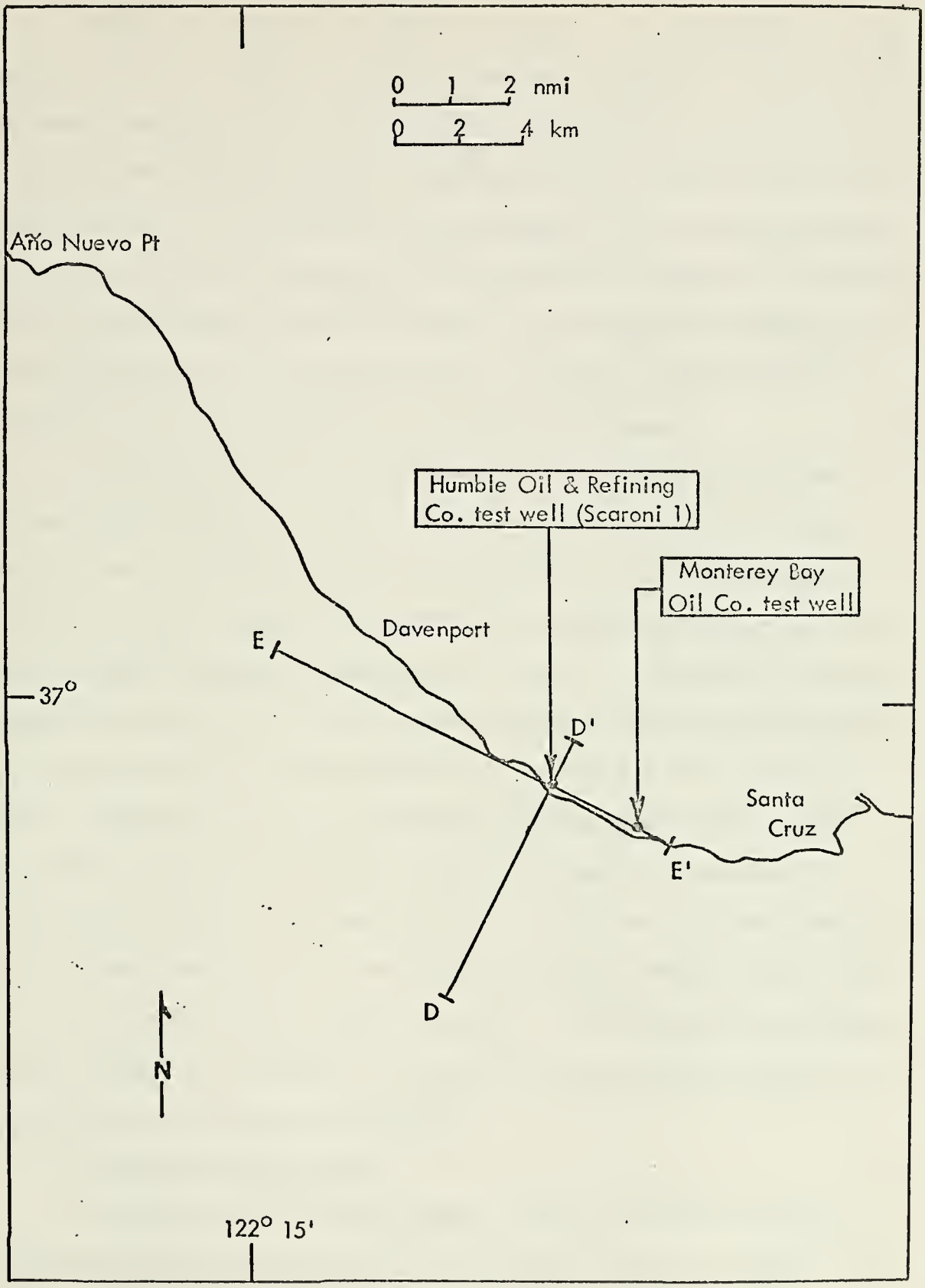

Figure 28. Geographical Location of Profiles for CBA Comparison with Well Core Data.

Figure 29 shows the excellent correlation which exists between the proposed basement location and the corresponding CBA trend. Based on this evidence, verification of Ross and Brabb's predictions of basement depth along line DD' seems legitimate. Although no fault zones are depicted in Ross and Brabb's interpretation of the basement profile, some undoubtedly do exist as DD' cuts across part of the Monterey Bay fault zone. Furthermore, the northernmost end of DD' stops at the theoretical extension of the King City fault. The steep gradient (4 mgal/km) exhibited in the CBA values is usually indicative of subsurface deformation.

The western end of line EE' (Fig. 28) lies at the eastern edge of the Palo Colorado-San Gregorio fault zone; the other end is at the intersection of the forementioned King City fault and the conjectured Santa Cruz fault. Figure 30 illustrates the comparison between Ross and Brabb's proposed basement depths and the author's corresponding CBA cross-section profile for EE'. Good agreement exists for the area removed from the fault zones. The lack of agreement at the western end of line EE' is not significant due to its remoteness from the Humble Well, coupled with the fact that near the Palo Colorado-San Gregorio fault zone, incongruous CBA profiles have been the rule. Due to the fact that faulting is in evidence near point E', the difference between mapped basement depth and the CBA profile there appears realistic. Previous figures have shown sharp increases in CBA values over fault zone areas and this seems to be the case near the Monterey Bay Oil well.

4. Sea Surface Gravity Data

Sea surface gravity measurements, when corrected for horizontal and vertical ship accelerations, cross-coupling effects, instrument drift,

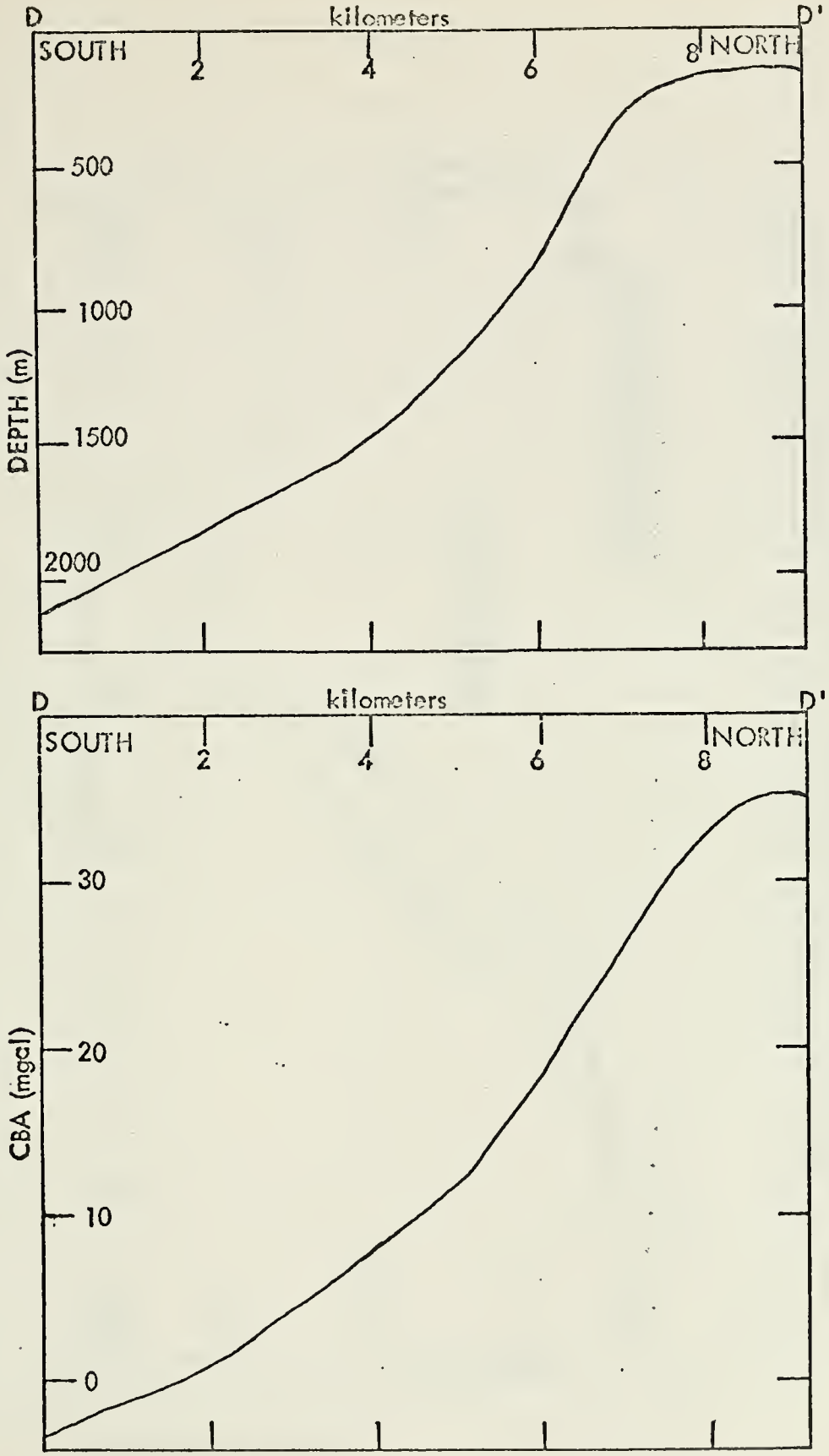

Figure 29. Comparison of CBA Profile with Profile of Proposed Basement Depth from Well Core Data Along Trackline DD'. (Lower profile after Ross and Brabb, 1973.)

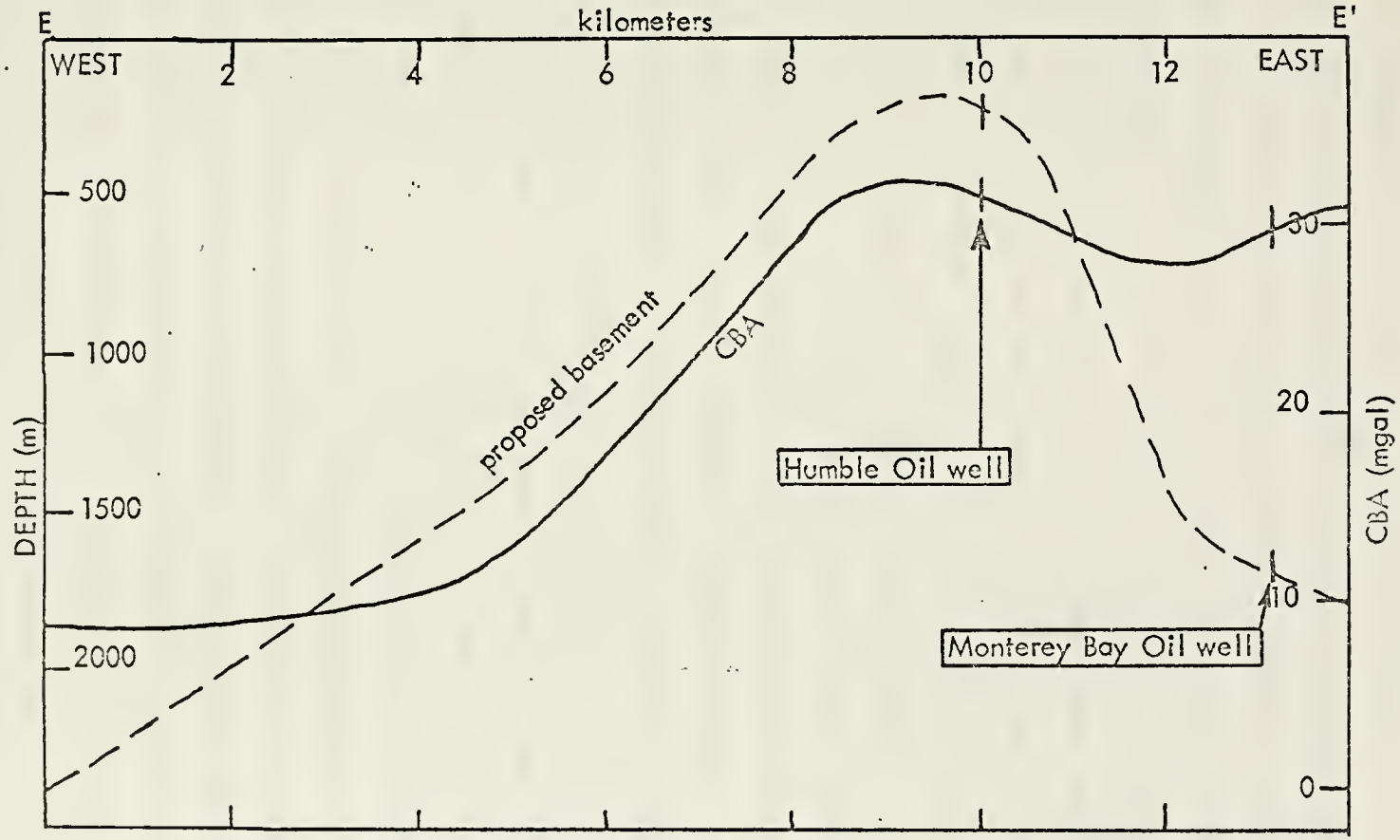

Figure 30. Comparison of CBA Profile With Profile of Proposed Basement Depth from Well Core Data Along Trackline EE'. (Lower profile after Ross and Brabb, 1973.)

earth tides, earth curvature, and the Eotvos effect (due to changes in centripetal acceleration), and with theoretical gravity removed, give the free-air anomaly.

The BARTLETT survey which produced the 160 kJ seismic data previously discussed, also collected sea surface gravimetric data. Gravity values for tracklines BB' and CC' (Fig. 19) are plotted for comparative purposes. As is seen in Figure 31, the sea surface data contains large fluctuations in free-air anomaly values. These can be attributed to the high sea state which was encountered during this portion of the cruise.

The Palo Colorado-San Gregorio fault zone shows up well on the BARTLETT plott and corresponds to the more accurate MFAA profile of the ACANIA data. Between the 5 and 10 km marks the sea surface data is totally unreliable; there is no correlation at all with the seafloor values. The Monterey Bay fault zone is clearly indicated on both profiles. Overall sea surface FAA values were two to three times greater than those for the bottom survey. Acceleration reinforcement between ship and meter oscillations during the surface gravity measurements probably accounts for this.

Figure 32 shows better correlation between sea surface and seafloor measurements but again some of the values obtained from the BARTLETT survey are two to three times greater than the corresponding ACANIA data. The two profiles do illustrate that the horizontal location of the maximum and minimum points are essentially coincidental. The horizontal differences observed at 7 and 15 km probably are due to unreliable navigation during the poor weather on the BARTLETT cruise. The large-scale geological features (Palo Colorado-San Gregorio and Monterey Bay fault zones) are explicitly portrayed on both profiles. The sea surface FAA is in better

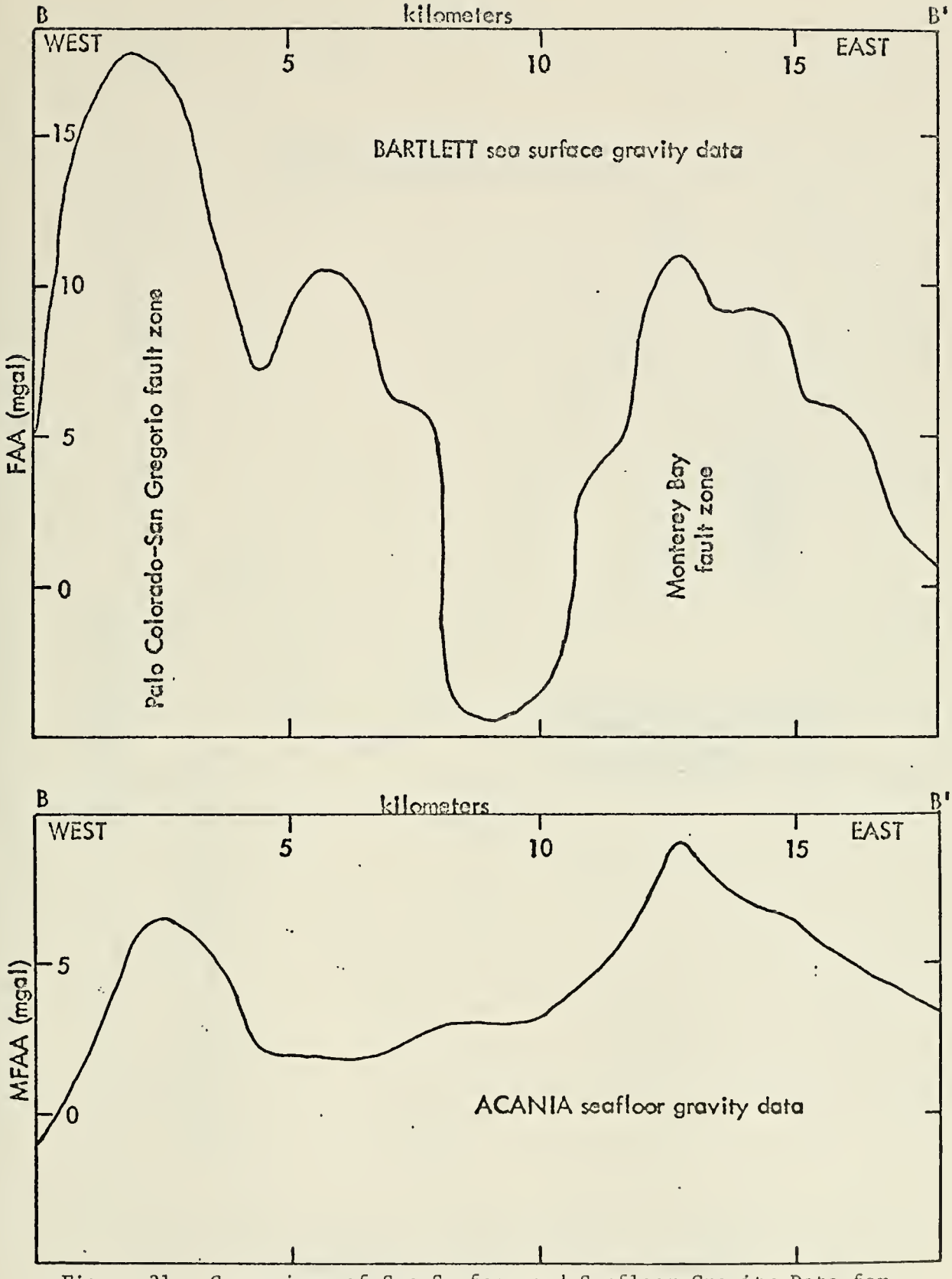

Figure 31. Comparison of Sea Surface and Seafloor Gravity Data for Trackline BB'.

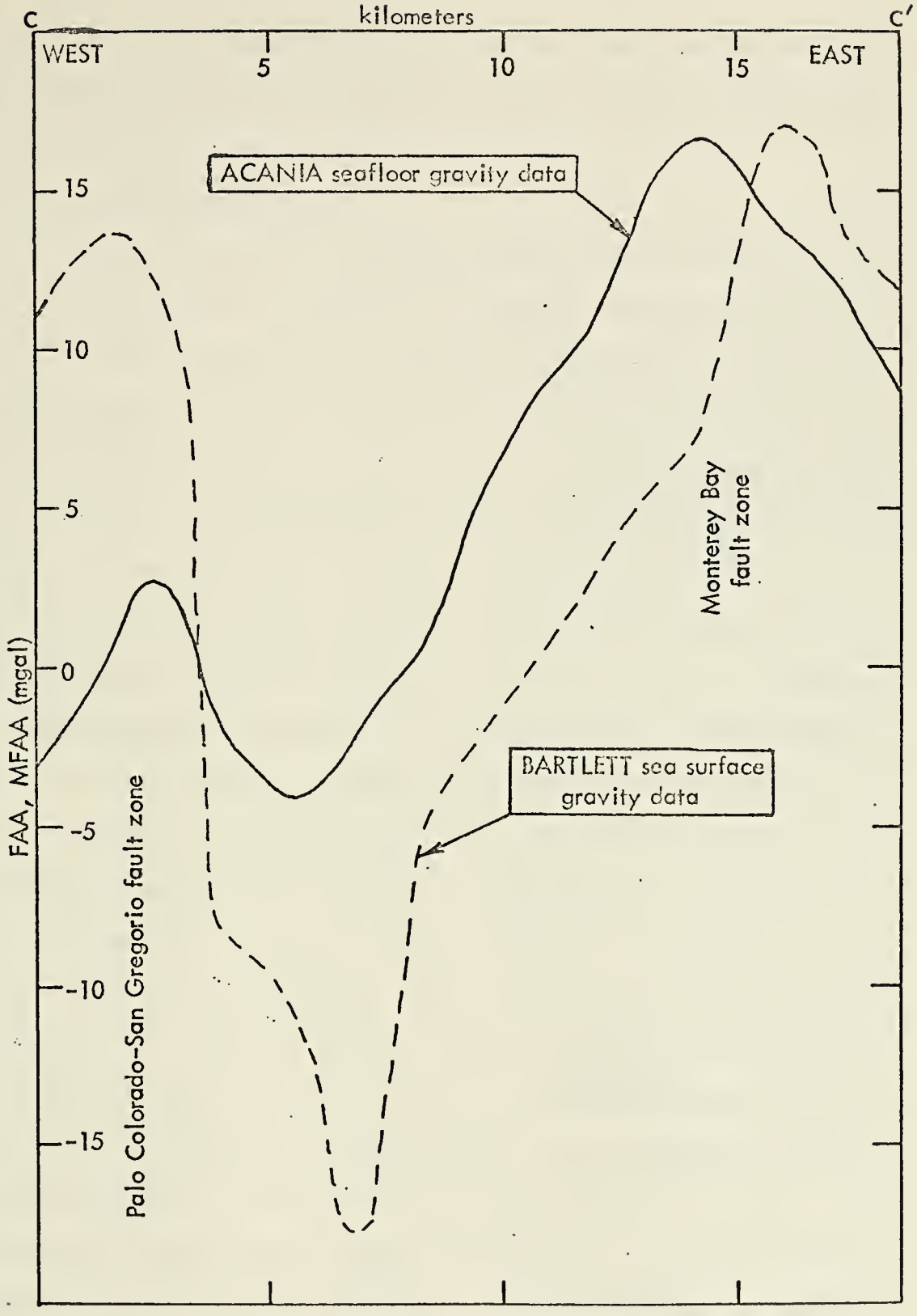

Figure 32. Comparison of Sea Surface and Seafloor Gravity Data for Trackline CC'.

agreement with the corresponding seafloor MFAA for trackline CC' than BB' probably because the former trackline cuts across the crustal deformations at a greater angle than the latter.

5. Sea Surface Magnetic Data

On the same cruise that the forementioned data was obtained, residual magnetism was also measured. The regional magnetic trend was ascertained from the International Geomagnetic Reference Field and the differences between that and the measured quantities were calculated. Since all information reduced to negative values, it can be concluded that the area surveyed by the BARTLETT either had an absence of magnetic materials in the crust or reversed polarity was in evidence (Maxwell, 1971).

Tracks BB' and CC' (Fig. 19) were used in comparing the proposed basement configurations interpreted from the 160 kJ seismic data (referred to the corresponding CBA profiles) and the magnetic data. Approximately 4 km east of point B (Fig. 33) excellent correlation exists between the crustal assymetry of the Palo Colorado-San Gregorio fault zone and the jump in regional magnetism. The gradient of approximately 50 γ/km is indicative of subsurface crustal faulting. Eastward, the magnetic values are fairly constant and apparently do not reflect the small fault zone at 11 km because of its depth and minimal vertical basement displacement.

Figure 34 shows the same high order of correlation between the basement profile (verified to a certain extent by the CBA profile) and the residual magnetism cross-section plotted for trackline CC'. The higher values of magnetism near the westward end of CC' probably reflect the approach to the edge of the continental shelf where negative magnetic values may not be so predominate (Jakosky, 1957). In this case there exists a magnetic gradient of approximately 70 γ/km at the Palo Colorado-

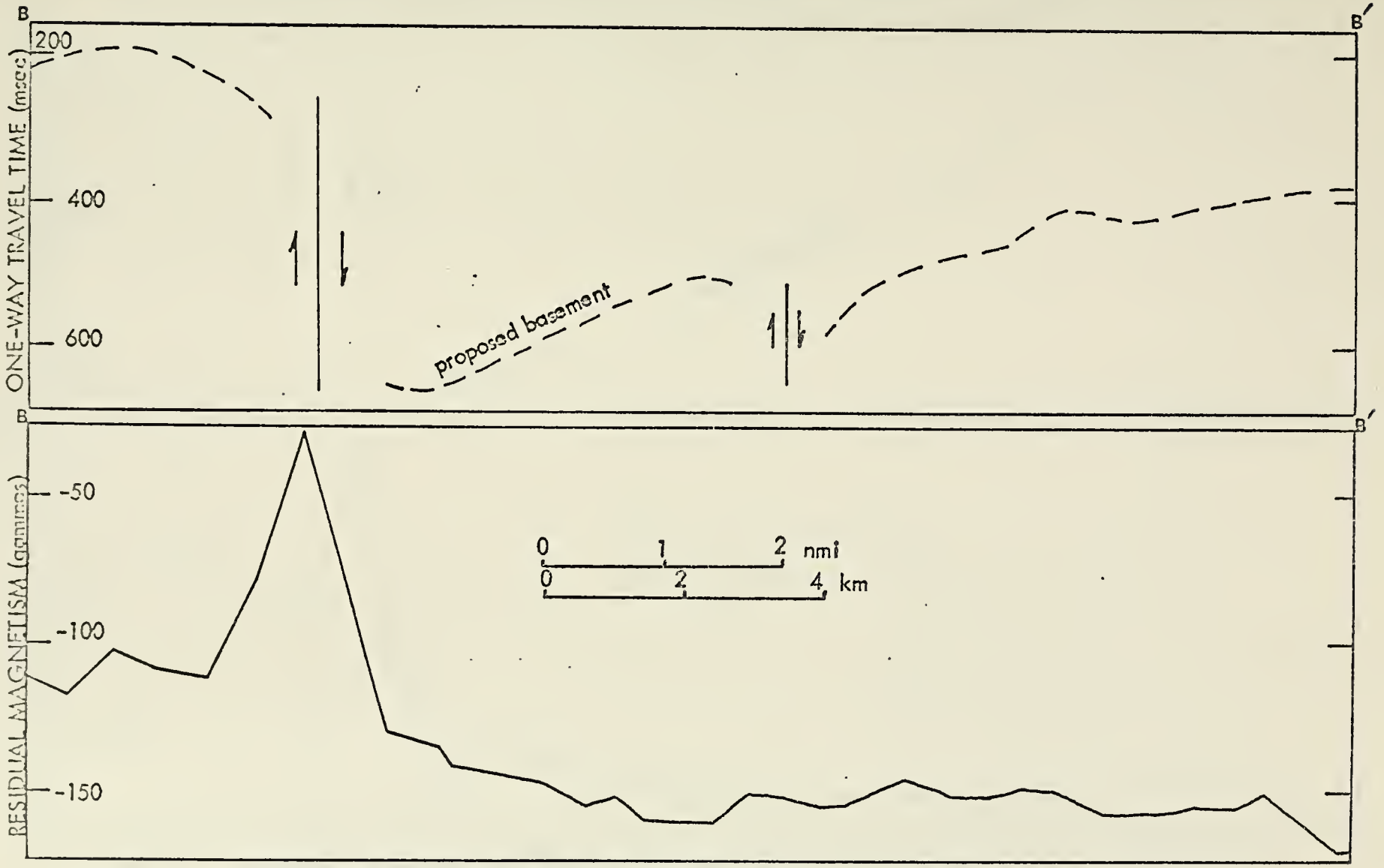

Figure 33. Comparison of Magnetic Data and the Seismic Profile for Trackline BB'. (Upper profile interpretation by H. G. Greene, USGS, oral commun., 1973.)

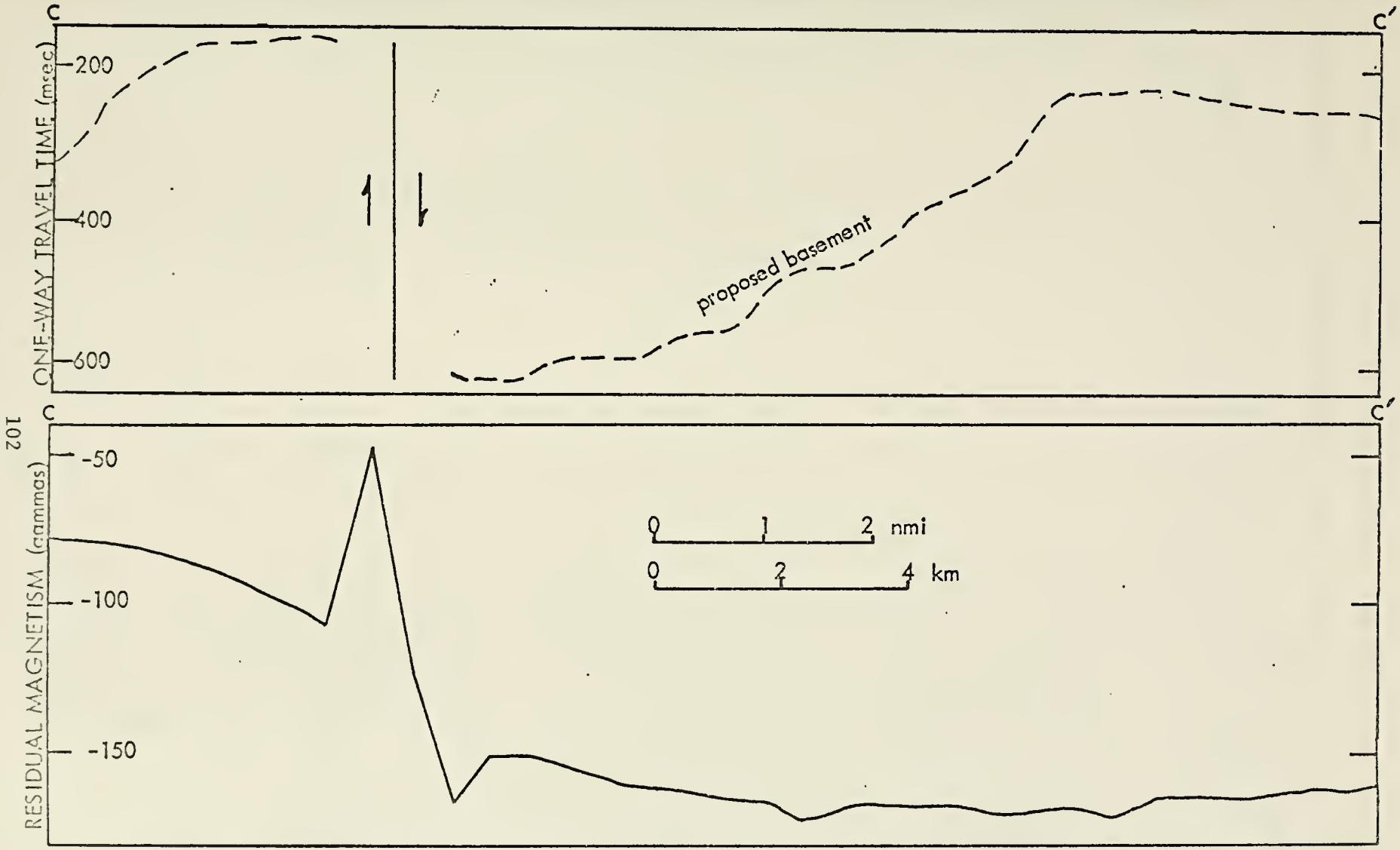

Figure 34. Comparison of Magnetic Data and the Seismic Profile for Trackline CC'. (Upper profile interpretation by H. G. Greene, USGS, oral commun., 1973.)

San Gregorio fault zone. Again, this increase from the values recorded across track BB' can undoubtedly be attributed to the fact that line CC' crosses the Palo Colorado-San Gregorio fault zone almost perpendicularly. The absence of any basement faulting is represented as a fairly constant magnetic trace eastward from the large fault zone.

VI. CONCLUSIONS

There are two major areas of faulting in the area investigated in this report. The most prominent is the Palo Colorado-San Gregorio fault zone: a narrow, northwest-southeast trending zone that joins the San Gregorio fault onland at Año Nuevo Point. Through interpretation of the author's data, there is support for the theory that a fault of this magnitude can be traced from horizontal and vertical plots of CBA values. In fact, it appears that CBA irregularities will almost always become manifest if the granitic structure of the basement is vertically displaced (Fig. 17).

The other zone, the Monterey Bay fault zone, parallels the Salinas Valley and the Sierra de Salinas. It is a wide belt of faults that crosses the southeastern portion of the author's survey area and closely approaches, but does not appear to cross, the Palo Colorado-San Gregorio fault zone. CBA profile analysis aids in verification of seismic data in broad fault regions such as this but CBA data alone is of little use in this case except to trace likely areas of faulting.

Fault displacement along the Palo Colorado-San Gregorio fault zone is similar to that on the San Andreas fault, that is vertical dip-slip and horizontal strike-slip motion, with rocks on the seaward side being displaced to the north. The prediction that an earthquake of magnitude 7.2 to 7.9 could occur on the Palo Colorado-San Gregorio fault zone (Greene et al., 1973) lends much importance to corroborations of seismic profile data through results of gravimetric surveys.

VII. FUTURE WORK

Because gravimetric analysis does not provide a unique model of the earth's crustal structure, corresponding interpretation of seismic and magnetic data is called for. It is recommended that seafloor gravimetry be extended south along the Palo Colorado-San Gregorio fault zone to the maximum attainable depths. This should then be tied in with sea surface gravity and magnetic values to verify or modify existing seismic records.

Since excessive depths and/or slopes in the vicinity of the Monterey Submarine Canyon preclude the possibility of bottom gravimetry in that area, sea surface gravity data and corresponding magnetic information should be correlated with previously interpreted seismic profiles.

The ultimate goal of geophysical investigations in this marine environment is to produce a continuous picture of the off-shore CBA for the entire Monterey Bay area. Incorporation of all available data and maximum utilization of seafloor gravimetry should, in the near future, yield this objective.

CBA COMPUTER PROGRAM FOR BOTTOM GRAVITY SURVEY

```
      IMPLICIT REAL*8 (A-H,O-Z)
      DIMENSION DEG(90),GBA(90),GTH(90),DW(90),DU(90),GOBS(9
     10),DEGR(90),GMG(90),GSTA(90),CC(90),TERC(90),ETID(90),
     1DWC(90),FAA(90),AMFAA(90),SBA(90),LAT(90),LATT(90),LON
     1G(90),LONGG(90),FAC(90),ARGA(90),ARGB(90),EC(90),BC(90)
      NN=68
      DO 80 I=1,NN
      BC(I)=0.0
      EC(I)=0.0
      DEG(I)=0.0
      GBA(I)=0.0
      GTH(I)=0.0
      DW(I)=0.0
      DU(I)=0.0
      GOBS(I)=0.0
      DEGR(I)=0.0
      GMG(I)=0.0
      GSTA(I)=0.0
      CC(I)=0.0
      TERC(I)=0.0
      ETID(I)=0.0
      DWC(I)=0.0
      FAA(I)=0.0
      AMFAA(I)=0.0
      SBA(I)=0.0
      FAC(I)=0.0
      ARGA(I)=0.0
      ARGB(I)=0.0
   80 CONTINUE
      CIRPI=3.14159
      DGDZ=0.09406
      CONST=2.0*CIRPI*6.67*30.48/100000.0
      READ (5,1) (DEG(I),I=1,NN)
    1 FORMAT (8F10.7)
      READ (5,2) (DU(I),I=1,NN)
    2 FORMAT (16F5.1)
      READ (5,3) (GSTA(I),I=1,NN)
    3 FORMAT (8F10.3)
      READ (5,4) (DWC(I),I=1,NN)
    4 FORMAT (8F10.2)
      READ (5,6) (TERC(I),I=1,NN)
    6 FORMAT (8F10.2)
```

```
      READ (5,801) (LONG(I),I=1,NN)
  801 FORMAT (20I3)
      READ (5,802) (LATT(I),I=1,NN)
      READ (5,802) (LONGG(I),I=1,NN)
  802 FORMAT (8F10.2)
      DO 30 I=1,NN
      DEGR(I)=DEG(I)/57.295
   30 CONTINUE
      DO 10 I=1,NN
      DW(I)=DU(I)-DWC(I)
      LAT(I)=36
      ARGA(I)=DSIN(DEGR(I))
      ARGB(I)=DSIN(2.0*DEGR(I))
      GTH(I)=978049.0*(1.0+(0.0052884*((ARGA(I))**2))
     1-0.0000059*((ARGB(I))**2))
      CC(I)=4.462D-04*DW(I)-3.282D-08*DW(I)**2+1.270D-15*DW(I)**3
      GOBS(I)=GSTA(I)-CC(I)
   10 CONTINUE
      DO 50 I=1,NN
      FAC(I)=DGDZ*DW(I)
      BC(I)= CONST*2.67*DW(I)+CONST*1.027*DU(I)
      EC(I)=-FAC(I)+CONST*2.67*DW(I)+CONST*1.027*DU(I)
      FAA(I)=GOBS(I)-GTH(I)-FAC(I)
      AMFAA(I)=FAA(I)+CONST*1.027*DU(I)+CONST*1.027*DW(I)
      SBA(I)=FAA(I)+CONST*2.67*DW(I)+CONST*1.027*DU(I)
      GBA(I)=SBA(I)+TERC(I)
   50 CONTINUE
      DO 90 I=1,NN
      DU(I)=DU(I)*0.3048
      DW(I)=DW(I)*0.3048
      FAC(I)=-FAC(I)
   90 CONTINUE
      WRITE (6,9)
    9 FORMAT ('1',////,2X,'STA #',4X,'GSTA',10X,'DU',10X,'DWC',10X,'DW',
     110X,'CC',10X,'TERC',10X,'LAT',///)
      WRITE (6,99) (I),GSTA(I),DU(I),DWC(I),DW(I),CC(I),TERC(I),DEGR(I)
     1          ,I=1,NN)
   99 FORMAT ('0',T3,I2,T8,F10.3,T25,F8.4,T36,F6.3,T48,F8.4,T63,F4.2,T74
     1,F5.2,T84,F12.6)
      WRITE (6,11)
   11 FORMAT ('1',////,5X,'GTH',15X,'GOBS',15X,'"CBA"',15X,'STATION',//)
      WRITE (6,12)(GTH(I),GOBS(I),GBA(I),(I),I=1,NN)
   12 FORMAT ('0',T2,F10.3,T20,F10.3,T40,F7.2,T60,I2)
      WRITE (6,13)
   13 FORMAT ('1',///  ,5X,'FAA',10X,'AMFAA',10X,'SBA',10X,'STATION',///)
      WRITE (6,14) (FAA(I),AMFAA(I),SBA(I),(I),I=1,NN)
   14 FORMAT ('0',T3,F7.2,T19,F7.2,T3C,F7.2,T47,I2)
      WRITE (6,700)
```

```
  700 FORMAT ('1',///////,14X,'STA',2X,'LATITUDE',2X,'LONGITUDE',2X,
     1'DEPTH',4X,'FAA',4X,'MFAA',4X,'SBA',5X,'CBA',///)
      WRITE (6,701) ((I),LAT(I),LATT(I),LONG(I),LONGG(I),DW(I),FAA(I),AM
     1FAA(I),SBA(I),GBA(I),I=1,29)
  701 FORMAT ('0',T16,I2,T20,I2,T23,F5.2,T30,I3,T34,F5.2,T41,F5.1,T48,F6
     1.2,T56,F5.1,T63,F6.2,T71,F6.2)
      WRITE (6,700)
      WRITE (6,701) ((I),LAT(I),LATT(I),LONG(I),LONGG(I),DW(I),FAA(I),AM
     1FAA(I),SBA(I),GBA(I),I=30,59)
      WRITE (6,700)
      WRITE (6,701) ((I),LAT(I),LATT(I),LONG(I),LONGG(I),DW(I),FAA(I),AM
     1FAA(I),SBA(I),GBA(I),I=60,NN)
      WRITE (6,702)
  702 FORMAT ('1',///////,14X,'STA',2X,'G OBSERVED',2X,'G THEORETICAL',
     13X,'BC',4X,'FAC',5X,'EC',4X,'TC',///)
      WRITE(6,703) ((I),GOBS(I),GTH(I),EC(I),FAC(I),EC(I)
     1,TERC(I),I=1,29)
  703 FORMAT ('0',T15,I2,T20,F10.3,T33,F10.3, T45,F5.2,T51,
     1F6.2,T59,F6.2,T66,F5.2)
      WRITE (6,702)
      WRITE(6,703) ((I),GOBS(I),GTH(I),BC(I),FAC(I),EC(I)
     1,TERC(I),I=30,59)
      WRITE (6,702)
      WRITE(6,703) ((I),GOBS(I),GTH(I),EC(I),FAC(I),EC(I)
     1,TERC(I),I=60,NN)
 9999 STOP
      END
```

REFERENCES CITED

1. Andrews, R. S., 1973. Corrections For Underwater Gravimetry. Naval Postgraduate School, Department of Oceanography, Monterey, California (paper submitted for publication).

2. Beyer, L. A., R. E. Von Huene, T. H. McCulloh, and J. R. Lovett, 1966. Measuring Gravity on the Sea Floor in Deep Water. Journal of Geophysical Research, Vol. 71, No. 8, p. 2091-2100.

3. Bishop, C. C. and R. H. Chapman, 1967. Bouguer Gravity Map of California (Santa Cruz Sheet). California Division of Mines and Geology, San Francisco, California.

4. Brooks, R. B., 1973. A Bottom Gravity Survey of the Shallow Water Regions of Southern Monterey Bay and Its Geological Interpretation. M.S. Thesis, Naval Postgraduate School, Monterey, California (unpublished report).

5. Bullard, E. C., 1936. Gravity Measurements in East Africa. Phil. Trans. Roy. Soc. (London). Ser. A, 235(757): 445-531.

6. Clark, J. C., 1970. Geologic Map of the Southwestern Santa Cruz Mountains Between Año Nuevo Point and Davenport, California. U. S. Geologic Survey Open File Map, Menlo Park, California.

7. Cronyn, B. C., 1973. An Underwater Gravity Survey of Northern Monterey Bay. M.S. Thesis, Naval Postgraduate School, Monterey, California (unpublished report).

8. Dobrin, M. B., 1960. Introduction to Geophysical Prospecting, 2nd Ed. McGraw-Hill Book Co., Inc., New York. 446 p.

9. Greene, H. G., 1970. Geology of Southern Monterey and Its Relationship to the Ground Water Basin and Salt Water Intrusion. Open File Report. USGS, 50 p. (unpublished report).

10. Greene, H. G., W. H. K. Lee, D. S. McCulloch, and E. E. Brabb, 1973. Faults and Earthquakes in the Monterey Bay Region, California. U. S. Geologic Survey Open File Report, Menlo Park, California.

11. Griggs, G. B., 1973. Earthquake Activity Between Monterey and Half Moon Bay, California. California Geology, Vol 26, No. 5, p. 103-110.

12. Hayford, J. F. and W. Bowie, 1912. The Effect of Topography and Isostatic Compensation Upon the Intensity of Gravity (U.S.C. & G.S. Spec. Pub. No. 10). U. S. Govt. Print. Office, Washington, D. C. 132 p.

13. Heiskanen, W. A. and F. A. Vening Meinesz, 1958. The Earth and Its Gravity Field. McGraw-Hill Book Co., Inc., New York. 470 p.

14. Jakosky, J. J., 1957. Exploration Geophysics, 2nd Ed., Trija Pub. Co., Newport Beach, California. 1195 p.

15. LaCoste, L. J. B., 1934. A New Type Long Period Vertical Seismograph. Physics 5: 178-180.

16. LaCoste, L. J. B., 1967. Measurement of Gravity at Sea and in the Air. Rev. Geophys. 5(4): 447-526.

17. LaCoste and Romberg Operating and Repair Manual, Models HD and HG Underwater Gravimeters. LaCoste and Romberg, Inc., Sugartown, Texas (unpublished report).

18. Martin, B. D., 1964. Monterey Submarine Canyon, California: Genesis and Relationship to Continental Geology. PhD Dissertation, University of Southern California, Los Angeles. 249 p. (unpublished report).

19. Maxwell, A. E., 1971. The Sea, Vol 4, Part 1. John Wiley & Sons, Inc., New York. 791 p.

20. Robbins, S. L. and H. W. Oliver, 1970. On Making Inner-Zone Terrain Corrections to Gravity Data. USGS, 13 p.

21. Ross, D. C. and E. E. Brabb, 1973. Petrography and Structural Relations of Granitic Basement Rocks in the Monterey Bay Area, California. Jour. Research, USGS, Vol. 1, No. 3, p. 273-282.

22. Siek, H. C., 1964. A Gravity Investigation of the Monterey-Salinas Area, California. M.S. Thesis, Stanford University, Palo Alto, California. 31 p. (unpublished report).

23. Swick, C. E., 1942. Pendulum Measurements and Isostatic Reductions. Spec. Pub. No. 232. U.S.C. & G.S. 82 p.

24. U. S. Dept. of Commerce, 1973. Tide Tables, High and Low Water Predictions, 1973, West Coast North and South America, incl. Hawaiian Is., U. S. Govt. Print. Office, Washington, D. C.

25. Woodson, W. B., 1973. An Underwater Gravity Survey of the Seafloor Between Point Lobos and Point Sur, California. M.S. Thesis, Naval Postgraduate School, Monterey, California (unpublished report)

26. Woolard, G. P. and J. C. Rose, 1963. International Gravity Measurements. University of Wisconsin Press, Madison, Wisconsin. 518 p.

INITIAL DISTRIBUTION LIST

		No. Copies
1.	Defense Documentation Center Cameron Station Alexandria, Virginia 22314	2
2.	Library, Code 0212 Naval Postgraduate School Monterey, California 93940	2
3.	Professor Robert S. Andrews, Code 58Ad Department of Oceanography Naval Postgraduate School Monterey, California 93940	10
4.	Professor Joseph J. von Schwind, Code 58Vs Department of Oceanography Naval Postgraduate School Monterey, California 93940	3
5.	Lieutenant Brian S. Cronyn, USN USS INDEPENDENCE (CVA-62) Fleet Post Office New York, New York 09501	1
6.	Department of Oceanography Naval Postgraduate School Monterey, California 93940	3
7.	Oceanographer of the Navy Hoffman Building Number 2 2461 Eisenhower Avenue Alexandria, Virginia 22314	1
8.	Office of Naval Research Code 480-D Arlington, Virginia 22217	1
9.	Dr. Robert E. Stevenson Scientific Liaison Office Scripps Institute of Oceanography La Jolla, California 92037	1
10.	Dr. Gary Griggs Division of Natural Sciences Applied Sciences Building University of California, Santa Cruz Santa Cruz, California 95060	1

11. Lieutenant Clayton H. Spikes, USN — 3
3303 Sycamore Place
Carmel, California 93921

12. Dr. Rodger H. Chapman — 1
Division of Mines and Geology
Resources Building, Rm 1341
1416 Ninth Street
Sacramento, California 95814

13. Dr. Howard Oliver — 1
United States Geological Survey
345 Middlefield Road
Menlo Park, California 94025

14. Dr. S. L. Robbins — 1
United States Geological Survey
345 Middlefield Road
Menlo Park, California 94025

15. Mr. H. Gary Greene — 1
United States Geological Survey
345 Middlefield Road
Menlo Park, California 94025

16. Gravity Section — 1
Naval Oceanographic Office
Washington, D. C. 20390

17. Mr. H. B. Parks — 1
LaCoste and Romberg, Inc.
Sugartown, Texas 78752

18. Professor Warren Thompson, Code 58Th — 1
Department of Oceanography
Naval Postgraduate School
Monterey, California 93940

19. Master, R/V ACANIA — 1
Department of Oceanography
Naval Postgraduate School
Monterey, California 93940

20. Lieutenant Walter B. Woodson III — 1
USS GALLANT (MSO-489)
Fleet Post Office
San Francisco, California 96601

21. Captain Nelson P. Watkins, USN (Ret.) — 1
503 West Main Street
Elizabeth City, North Carolina 27909

REPORT DOCUMENTATION PAGE

READ INSTRUCTIONS BEFORE COMPLETING FORM

1. REPORT NUMBER

2. GOVT ACCESSION NO.

3. RECIPIENT'S CATALOG NUMBER

4. TITLE (and Subtitle)

A Gravimetric Survey of the Santa Cruz-Año Nuevo Point Continental Shelf and Adjacent Coastline

5. TYPE OF REPORT & PERIOD COVERED

Masters Degree
September 71 to September 73

6. PERFORMING ORG. REPORT NUMBER

7. AUTHOR(s)

Clayton Henry Spikes

8. CONTRACT OR GRANT NUMBER(s)

9. PERFORMING ORGANIZATION NAME AND ADDRESS

Naval Postgraduate School
Monterey, California 93940

10. PROGRAM ELEMENT, PROJECT, TASK AREA & WORK UNIT NUMBERS

11. CONTROLLING OFFICE NAME AND ADDRESS

Naval Postgraduate School
Monterey, California 93940

12. REPORT DATE

September 1973

13. NUMBER OF PAGES

114

14. MONITORING AGENCY NAME & ADDRESS (if different from Controlling Office)

15. SECURITY CLASS. (of this report)

Unclassified

15a. DECLASSIFICATION/DOWNGRADING SCHEDULE

16. DISTRIBUTION STATEMENT (of this Report)

Approved for public release; distribution unlimited.

17. DISTRIBUTION STATEMENT (of the abstract entered in Block 20, if different from Report)

18. SUPPLEMENTARY NOTES

19. KEY WORDS (Continue on reverse side if necessary and identify by block number)

Bouguer Anomaly
Geology
Geophysics
Gravimetric Survey
Gravity
Marine Geology
Monterey Bay Fault Zone
Palo Colorado-San Gregorio Fault Zone
Seismic Activity

20. ABSTRACT (Continue on reverse side if necessary and identify by block number)

Gravity data was collected from 82 seafloor and 41 land stations in a 334 sq km area between Santa Cruz and Año Nuevo Point, California.

The methods of data collection and reduction are discussed, with the introduction of a unique sequence pertaining to application of gravity data corrections. A complete Bouguer anomaly map is depicted and subsequently tied in with a previous survey of northern Monterey Bay. Isoline gradient analysis supports the concept that complete Bouguer

anomaly profiles can be utilized to map granitic basement displacements.

Complete Bouguer Anomaly cross-sections are compared with corresponding profiles of seismic, well core, sea surface gravity, and magnetic data. Excellent correlation is exhibited between these profiles and the Palo Colorado-San Gregorio fault zone. Faulting within the Monterey Bay fault zone can be traced from analysis of related profiles. Supporting evidence of the purported dip-slip and strike-slip motion along the Palo Colorado-San Gregorio fault zone is presented.